

**Intercellular Communication between Fibroblast Phenotypes,  
Macrophages and Myoblasts during Cellular Migration**

**By**

**Dhamini S.H. Ramklowan**

**Submitted in fulfilment of the academic requirements of Master of Science**

In Biochemistry

School of Life Sciences

College of Agriculture, Engineering and Science

University of KwaZulu-Natal

Pietermaritzburg

South Africa

February 2022

## **PREFACE**

---

The research contained in this thesis was completed by the candidate while based in the Discipline of Biochemistry, School of Life Sciences of the College of Agriculture, Engineering and Science, University of KwaZulu-Natal, Pietermaritzburg, South Africa. The research was financially supported by the National Research Foundation.

The contents of this work have not been submitted in any form to another university and, except where the work of others is acknowledged in the text, the results reported are due to investigations by the candidate.



---

Signed: Prof C.U. Niesler

Date: 2022/02/10

## DECLARATION 1: PLAGIARISM

---

I, Dhamini S.H. Ramklowan declare that:

- (i) the research reported in this thesis, except where otherwise stated or acknowledged, is my original work;
- (ii) this thesis has not been submitted in full or in part for any other degree or examination to any other university;
- (iii) this thesis does not contain any other persons' data, pictures, graphs or other information, unless specifically acknowledged as being sourced from other persons';
- (iv) this thesis does not contain other persons' writing, unless specifically acknowledged as being sourced from other researchers. Where other sources have been quoted then:
  - their words have been rewritten but the general information attributed to them has been referenced;
  - Where their exact words have been used, their writing has been placed inside quotation marks, and referenced;
- (v) This thesis does not contain text, graphics or tables copied and pasted from the Internet, unless specifically acknowledged, and the source being detailed in the thesis and in the References section.

  
Signed: Dnamini Ramklowan

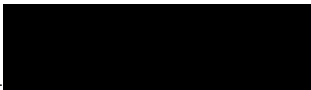
Date: 2022/02/10

## DECLARATION 2: PUBLICATIONS

---

Details of contributions to publications/conferences that form part and/or include research presented in this thesis.

**Ramklowan, D.S.H., van de Vyver, M. & Niesler, C. (2020).** *A co-culture model to investigate the effect of a pro-inflammatory diabetic microenvironment on fibroblast differentiation and wound healing in vitro.* Society for Advanced Cell Culture Modelling for African Conference 2020, North-West University, Potchefstroom, South Africa; 21 - 24 March 2020 **Cancelled due to Covid**



---

Signed: Dhamini Ramklowan

Date: 2022/02/10

## ABSTRACT

---

There are various cell types that are crucial for wound healing to proceed successfully, which includes the stages of haemostasis, followed by inflammation, proliferation and finally remodelling. Haemostasis is characterised by the formation of a clot which serves to prevent the loss of blood and provides a scaffold for incoming cells. Inflammation involves the phagocytosis of pathogenic organisms by neutrophils, which, thereafter, apoptose and itself is phagocytosed by macrophages. The inflammatory stage contains both M1 macrophages, which are pro-inflammatory, and M2 macrophages, which are anti-inflammatory. The transition from the inflammatory stage to the proliferative stage is marked by the secretion of growth factors such as TGF- $\beta$ , released by M2 macrophages, that signals for the migration of fibroblasts into the wounded area. Once at the wound site, fibroblasts proliferate and secrete ECM factors such as hyaluronan and collagen type III. Fibroblasts differentiate to myofibroblasts, with an intermediate phase referred to as proto-myofibroblasts, in response to mechanical stress and factors released by macrophages. Myofibroblasts can be distinguished from fibroblasts, as they express  $\alpha$ -SMA. During the remodelling phase, ongoing collagen synthesis allows for strengthening and maturation of the tissue.

The current study focused on understanding how the presence of these different cellular role players, specifically fibroblasts, myofibroblasts, M1 macrophages and M2 macrophages, influences myoblast wound closure using an *in vitro* wound closure assay. To achieve this, the first aim was to establish distinct populations of fibroblasts, myofibroblasts, M1 and M2 macrophages. Thereafter, double and triple co-culture assays were used to investigate the effect of these phenotypes on cellular wound closure.

A fibroblast population was established by de-differentiating L929 murine cell lines in the absence of serum for six days. To maintain the fibroblast phenotype upon the re-introduction of serum (which would otherwise stimulate their differentiation back to myofibroblasts), cells were subsequently incubated with sodium orthovanadate, which is known to inhibit the expression of alpha-smooth muscle actin, and thereby the differentiation of fibroblasts to myofibroblasts. With this approach, fibroblasts and myofibroblasts, as well as the intermediate proto-myofibroblasts, were established for further co-culture investigations. M1 macrophage polarization was achieved through incubation for 24 hours with LPS, while M2 macrophage polarisation, attempted through the use of IL-4, was unsuccessful. Subsequent double co-

culture experiments revealed firstly that the presence of myoblasts modified myofibroblast wound closure to be significantly faster than that of either fibroblasts or proto-myofibroblasts; this was not observed in the absence of myoblasts. Conversely, myoblasts wound closure was significantly faster when co-cultured in the presence of proto-myofibroblasts, but not fibroblasts and myofibroblasts, compared with myoblast wound closure alone. Furthermore, double co-cultures containing myoblasts and/or M1-LPS<sup>-</sup> and M1-LPS<sup>+</sup> macrophages revealed that, myoblasts wound closure was significantly faster when co-cultured with macrophages not previously exposed to LPS compared with those LPS-treated. From these results it can be concluded that the presence of distinct cellular phenotypes plays differential roles in influencing the cellular wound closure required for wound healing.

## ACKNOWLEDGMENTS

---

I would like to give thanks to and show my utmost gratitude and appreciation to a few important people, without whom this tumultuous journey wouldn't have been complete:

Prof. Niesler, thank you for your guidance and motivation throughout this study. Your enthusiasm and driven nature during these 2 long years dominated by covid have been an inspiration to me to always strive to do my best. Thank you for always being so accommodating and insightful.

Dr. Celia Snyman, I am ever grateful for your insightful out-of-the-box thinking and your ability to always look at things from a different perspective. Thank you for being such a warm and welcoming person to which I can always ask for help.

To my parents, thank you for encouraging and supporting all my dreams. I would be nothing without you. Mum, there are no words to describe how grateful I am for you. For staying up late with me, packing me the best lunches, stressing about my work more than I do and always pushing me to be the best version of myself and realise my highest potential. All my love.

To my wonderful grandparents, Nana and Nani, it is a blessing to still have you along on this journey with me. Your love, support and care through these years have motivated me to keep pushing to reach the finish line.

To my nieces and nephews (Samishca, Zo, Ridhav and Yahvi), Your little playful and joyous hearts have kept me sane through this degree. Thank you for a safe space to let put my inner child and be carefree. You keep me free-spirited and young at heart. Your little hugs and infectious smiles are the best stress-relievers.

To my extended family, uncles, and aunts, I am ever so grateful that you all support my life's decisions. Your unparalleled support and unconditional love is appreciated.

To Suhavna and Akira, I am so grateful and appreciative that I got to share this journey with you and have you by my side. Thank you for all the laughs, car therapy sessions, adventures, encouragement, breakdowns and breakthroughs. May we always grow from strength to strength with each other.

Thank you to the NRF for the financial support and UKZN for providing the platform for me to do this degree.

And lastly to me, because self-love is the greatest love. Thank you for always preserving in the face of adversity. You have come to know your heart and realising your goals and staying true to yourself regardless of what life might throw you. Keep reaching for everything you set your mind to. Let this manuscript serve to remind you that everything is within your grasp, you just have to put your hand out and reach for it.



# TABLE OF CONTENTS

---

	<b><u>Page</u></b>
PREFACE.....	II
DECLARATION 1: PLAGIARISM .....	III
DECLARATION 2: PUBLICATIONS .....	IV
ABSTRACT.....	V
ACKNOWLEDGMENTS .....	VII
TABLE OF CONTENTS.....	IX
LIST OF FIGURES .....	XII
LIST OF TABLES.....	XIV
ABBREVIATIONS .....	XV
1. INTRODUCTION .....	1
1.1. Wound healing .....	3
1.1.1. Haemostasis .....	4
1.1.2. Inflammation.....	7
1.1.3. Proliferation .....	7
1.1.4. Remodelling .....	8
1.2. Skeletal muscle injury.....	9
1.3. Macrophages .....	10
1.4.1. Fibroblast.....	12
1.4.2. Differentiation of fibroblast to myofibroblast .....	13
1.4.3. Myofibroblasts.....	14
1.5. Satellite cells to myoblasts.....	15
1.6.1. Diabetes Mellitus.....	16
1.6.2. Diabetic foot ulcers (DFUs) .....	16
1.6.3. Prevalence of diabetes in South Africa .....	17
1.7. Studies understanding the role of fibroblasts and myofibroblasts in diabetic wound healing .....	17
1.8. Summary .....	18

1.9. Aims and objectives .....	19
2.MATERIALS AND METHODS .....	21
2.1. General Reagents and Lab Procedures .....	21
2.1.1. Reagents .....	21
2.1.2. Standard Cell Culture. ....	21
2.1.3. Crystal Violet Staining. ....	22
2.1.4. Analysis of cell number. ....	22
2.1.5. Analysis of cell circularity. ....	23
2.1.6. Immunocytochemistry and fluorescence microscopy. ....	24
2.1.6.1. Detection of $\alpha$ -SMA. ....	24
2.1.6.2. Detection of CD86. ....	24
2.1.6.3. Detection of Arginase. ....	25
2.1.6.4. Staining of nuclei, mounting of coverslips and fluorescent viewing. ....	25
2.1.7. Determining fluorescence intensity. ....	25
2.1.8. In vitro wound healing assay. ....	26
2.2. Dedifferentiation of myofibroblasts to fibroblasts .....	26
2.2.1. Effect of sodium orthovanadate on expression of $\alpha$ -SMA in fibroblasts. ....	27
2.3. Using LPS and Il-4 to establish M1 and M2 phenotypes, respectively: .....	28
2.3.1. M1 phenotype .....	28
2.3.2. M2 phenotype .....	29
2.4. Double and Triple Co-cultures .....	30
2.4.1. Double Co-Culture. ....	30
2.4.2. Triple Co-Culture. ....	31
2.5. Statistical analysis. ....	32
3.RESULTS .....	33
3.1. Establishment of Phenotypes .....	33
3.1.1. Establishment of dedifferentiated fibroblast cultures. ....	33
3.1.2. Vanadate suppresses the expression of $\alpha$ -SMA. ....	36
3.1.3. Polarisation to the M1 macrophage phenotype. ....	44
3.1.4. Polarisation to the M2 macrophage phenotype. ....	46
3.2. Effect of Different Cellular Phenotypes on Wound Closure .....	49
3.2.1. Fibroblasts and Myofibroblasts decrease myoblast wound closure. ....	49

3.2.2. Myoblasts differentially affect myofibroblast vs fibroblast migration. ....	53
3.2.3. Effect of M1-LPS <sup>-</sup> and M1-LPS <sup>+</sup> macrophages on myoblast wound closure. ...	55
3.2.4. Effect of fibroblasts and myofibroblasts on myoblast wound closure when cultured in the presence of M1-LPS <sup>-</sup> and M1-LPS <sup>+</sup> macrophages. ....	56
4. DISCUSSION .....	60
5. LIMITATIONS AND FUTURE PERSPECTIVES .....	63
6. CONCLUSION .....	64
7. CONFERENCE .....	66
8. REFERENCES .....	69

# LIST OF FIGURES

---

<b>Figure</b>	<b>Page</b>
Figure 1: Overall schematic diagram of wound healing.....	2
Figure 2: Schematic representation of the stages of cutaneous wound healing: (A) haemostasis, (B) inflammation, (C) proliferation, and (D) remodelling.....	6
Figure 3: Schematic representation of the polarisation of macrophages..	10
Figure 4: Schematic illustration of the differentiation of fibroblasts to myofibroblasts during wound healing.....	14
Figure 5: Schematic representation of Activation of satellite cells to produce differentiate myoblasts. .	15
Figure 6: Standard curve representing increasing numbers of cells stained with crystal violet. (A) Myofibroblasts, (B) Fibroblasts, (C) Macrophages and (D) Myoblasts.).	23
Figure 7: Image of (A) Crystal violet stained L929 cells whose (B) cell morphology.	24
Figure 8: Schematic representation of scratch assay within a well..	26
Figure 9: Schematic representation of L929 dedifferentiation in SFM..	27
Figure 10: Schematic representation for fibroblasts treated with vanadate.....	28
Figure 11: Schematic representation of Macrophages treated with LPS (0.1 µg/ml) and IL-4 (0.1 µg/ml).....	30
Figure 12: Schematic representation of plating double co-cultures containing either fibroblasts or myofibroblasts with myoblasts.....	31
Figure 13: Schematic representation of plating triple co-cultures containing M1 macrophages and either fibroblasts or myofibroblasts and myoblasts.....	32
Figure 14: Dedifferentiation of myofibroblasts to fibroblasts when cultured in SFM for either 3 or 6 days showing the change in expression of $\alpha$ -SMA.....	34
Figure 15: Dedifferentiation of myofibroblasts to fibroblasts when cultured in SFM for either 3 or 6 days showing the shift in cell circularity.....	35
Figure 16: L292 cells were incubated for (A) 3 days in SCM, or (B) 6 days in SFM followed by incubation for (C) 16 hours in SCM, (D) 24 hours SCM, (E) 16 hours in vanadate, and (F) 16 hours in vanadate and 7 hours in SCM..	38
Figure 17: Shift in fibroblast circularity when cultured with (A) vanadate and (B) SCM at the start and end of the wound closure assays..	40

Figure 18: Effect of vanadate on the cell proliferation of myofibroblasts, fibroblasts, macrophages and myoblasts.....	43
Figure 19: J774A.1 macrophages incubated in LPS .....	45
Figure 20: J774A.1 macrophages incubated with IL-4.....	48
Figure 21: Myoblast wound closure alone and when co-cultured with the different fibroblast phenotypes.. .....	50
Figure 22: Bright Field Light Microscopy Images of Myoblast Wound Closure over 7 hours. ....	52
Figure 23: Fibroblast, protomyofibroblast and myofibroblast migration.. .....	54
Figure 24: Myoblast wound closure in the presence of M1-LPS <sup>-</sup> and M1-LPS <sup>+</sup> macrophages.. .....	56
Figure 25: The effect of the presence of fibroblasts, protomyofibroblasts and myofibroblasts during myoblasts wound healing in the presence of (B) M1-LPS <sup>-</sup> macrophages and (C) M1-LPS <sup>+</sup> macrophages.....	58
Figure 26: Summary of study. ....	65

## LIST OF TABLES

---

Table	Page
Table 1: Interquartile data ranges for the circularity data for the dedifferentiation of myofibroblasts to fibroblasts.....	36
Table 2: Interquartile data ranges for the shift in fibroblast circularity when cultured with 10 $\mu$ M sodium orthovanadate and SCM at the start and end of the wound closure assays. ....	41
Table 3: Summary of mean data showing differential significant effect of fibroblast and myofibroblast phenotypes on myoblast wound closure. ....	51
Table 4: Summary of mean data showing differential significant effect of myoblasts on fibroblasts, protomyofibroblast and myofibroblast migration .....	55

## ABBREVIATIONS

---

<b><math>\alpha</math>-SMA</b>	<b><math>\alpha</math>-Smooth Muscle Actin</b>
<b>CD</b>	Chow Diet
<b>CTCF</b>	Corrected Total Cell Fluorescence
<b>DFUs</b>	Diabetic Foot Ulcers
<b>ECM</b>	Extracellular Matrix
<b>EGF</b>	Epidermal Growth Factor
<b>FGF</b>	Fibroblast Growth Factor
<b>HFD</b>	High Fat Diet
<b>IFN-<math>\gamma</math></b>	Interferon- $\gamma$
<b>IGF</b>	Insulin-like Growth Factor
<b>IL-1/4/6/10/13</b>	Interleukin-1/4/6/10/13
<b>IL-1RA</b>	Interleukin-1 receptor antagonist
<b>LPS</b>	Lipopolysaccharide
<b>MMPs</b>	Matrix Metalloproteinases
<b>NO</b>	Nitric oxide
<b>PBS</b>	Phosphate buffer saline
<b>PDGF</b>	Platelet Derived Growth Factor
<b>SCM</b>	Serum Containing Medium
<b>SFM</b>	Serum Free Medium
<b>T2DM</b>	Type 2 Diabetes Mellitus
<b>TGF-<math>\alpha/\beta</math></b>	Transforming Growth Factor- $\alpha/\beta$
<b>TIMPs</b>	Tissue Inhibitor of Metalloproteinases
<b>TNF-<math>\alpha</math></b>	Tumour Necrosis Factor- $\alpha$
<b>VEGF</b>	Vascular Endothelial Growth Factor

## 1. Introduction

Successful wound repair requires the completion of four stages of wound healing, namely haemostasis, inflammation, proliferation and lastly remodelling (Figure 1) (Velnar, *et al.*, 2009; Guo & DiPietro, 2010). Vasoconstriction and clot formation are distinguishable features of haemostasis (Monaco & Lawrence, 2003). The clot serves to prevent further loss of blood and provides a foundation for cells migrating to the site of injury (Monaco & Lawrence, 2003). During inflammation, an immune barrier is established where neutrophils phagocytose foreign microbes, apoptose and are then phagocytosed by neighbouring macrophages (Velnar, *et al.*, 2009). Macrophages are an important component required for the progression from the inflammatory to the proliferative phase (Velnar, *et al.*, 2009). It secretes potent growth factors such as vascular endothelial growth factor (VEGF) and transforming growth factor- $\beta$  (TGF- $\beta$ ), that activate cells such as fibroblasts (Velnar, *et al.*, 2009). Proliferation can be identified by the migration of active fibroblasts, its' synthesis of extracellular matrix (ECM) components such as collagen I-IV, and finally its' differentiation into myofibroblasts, which aids in the contraction of the wound; angiogenesis is also particularly active during this phase (Velnar, *et al.*, 2009). During remodelling, weaker collagen III, laid down previously by fibroblasts, is replaced with stronger collagen I, produced by myofibroblasts, which is important for scar formation and the strength and integrity of the healed wound (Velnar, *et al.*, 2009; Alhajj, *et al.*, 2021).



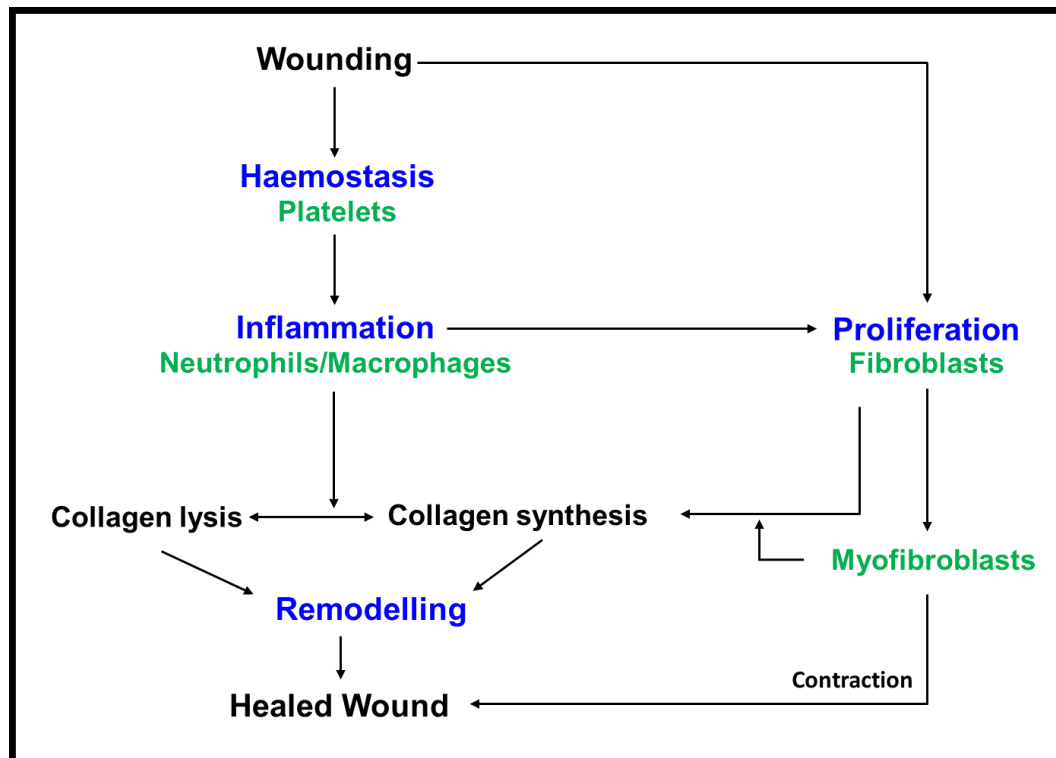


**Figure 1: Overall schematic diagram of wound healing.** (Modified, based of diagram from Robson, *et al.*, 2001). Wound healing (indicated in blue) proceeds from haemostasis and inflammation through to proliferation and finally remodelling. Platelets aid in clot formation during haemostasis. Neutrophils and macrophages are important cells that phagocytose pathogens during inflammation. Fibroblasts proliferate and produce ECM factors such as collagen during the proliferative phase. It then differentiates into myofibroblasts, which facilitates wound contraction. The healed wound is strengthened and enhanced during the remodelling phase.

Hyperglycaemia, hypothyroidism, pathogenic infections and ischemia are characteristic clinical disorders that promote impaired wound healing (Broughton & Janis, 2006). Diabetes mellitus is a metabolic disease characterised by hyperglycaemia (high blood sugar) as a result of a dysregulated insulin signalling system. A common complication of diabetes is impaired wound healing, particularly in the form of foot ulcers; if not resolved, this may result in lower limb amputations. During wound healing, macrophages can polarise into two distinguishable phenotypes (Hesketh, *et al.*, 2017). The pro-inflammatory M1 phenotype becomes prevalent at the start of the inflammatory phase, followed by the anti-inflammatory M2 phenotype (Hesketh, *et al.*, 2017). However, in diabetics, a persistent M1 pro-inflammatory phenotype exists; this is thought to contribute to the impairment in wound repair (Salazar, *et al.*, 2016). In pro-inflammatory conditions such as diabetes, the persistence of the M1 macrophage phenotype causes the newly laid ECM to be cleaved by matrix metalloproteinases (MMPs), such as MMP9 (Aitchison, *et al.*, 2021). The damage to the ECM hinders the migration of

cells, such fibroblasts, into the wounded area (Aitcheson, *et al.*, 2021). Moreover, high glucose levels reduce the macrophages' phagocytic activity making it more susceptible to infection and also leads to an increase in the secretion of pro-inflammatory cytokines (Aitcheson, *et al.*, 2021).

As mentioned earlier, fibroblasts are vital cells that coordinate tissue repair (Darby, *et al.*, 2014). Fibroblasts act as synthetic cells, secreting ECM factors such as collagen (Lerman, *et al.*, 2003). They also secrete growth factors that signal to other cells within the wound; whether this intercellular communication is phenotype-dependent (e.g., fibroblasts versus myofibroblast) is not clear (Lerman, *et al.*, 2003). Hinderances of fibroblast function can lead to  $\alpha$ -SMA and desmin to non-healing or chronic wounds (Lerman, *et al.*, 2003). Fibroblasts differentiate into myofibroblasts which are distinguishable from fibroblasts as they contain stress fibres which express  $\alpha$ -smooth muscle, but do not express vimentin (Darby, *et al.*, 2014). Myofibroblasts have a principal role in the closure of wounds as they produce the contractile forces which pull the wound edges together (Li & Wang, 2011). The diabetic environment has been shown to negatively impact fibroblast proliferation and dysregulate differentiation to myofibroblasts (Liu, *et al.*, 2004; Wan, *et al.*, 2021). This occurs as the polarisation of M1 to M2 macrophages (which would normally promote the proliferation of fibroblasts and their differentiation to myofibroblasts) is hindered (van Linthout, *et al.*, 2014). Moreover, a decrease in fibroblast number via apoptosis has also been observed under this pathological condition (Liu, *et al.*, 2004).

This review expands on the stages, cells and growth factors involved in normal and pathological wound healing, with specific emphasis on the role of macrophages and fibroblasts as well as the context of diabetes mellitus.

### **1.1. Wound healing**

A wound is characterised by the destruction of tissue structure and a resulting disturbance in function of that tissue (Robson, *et al.*, 2001). A wound can extend from breaks in epithelia to injuries deep into subcutaneous tissue affecting structures such as nerves, muscles, tendons, organs, and bone (Velnar, *et al.*, 2009). Wounds can be classified as either acute or chronic (Monaco & Lawrence, 2003). Acute wounds undergo a series of overlapping, sequential phases that necessitate the coordination of several cell types (such as platelets, monocytes,

macrophages, fibroblasts, keratinocytes, and endothelial cells) as well as multiple signalling networks consisting of various cytokines, growth factors and chemokines resulting in a healed wound (Monaco & Lawrence, 2003; Barrientos, *et al.*, 2008). In contrast, in the case of a chronic wound, the injury does not heal within the presumed time (such as that of an acute wound) due to abnormal wound healing phases (Al-Shaibani, *et al.*, 2016).

Wound healing is an evolutionary conserved, multicellular, complex process consisting of four fundamental phases that occur at varying degrees depending on the type of tissue affected (Barrientos, *et al.*, 2008; Guo & DiPietro, 2010; Monaco & Lawrence, 2003). These stages of wound healing are haemostasis, inflammation, proliferation, and remodelling (Velnar, *et al.* 2009). For the sake of simplicity, the well characterised and extensively studied, cutaneous wound healing model will be used to describe the interactions of cells with each other as well as with growth factors, chemokines and cytokines released during the healing process. This description of wound healing is broadly applicable to all tissues.

#### **1.1.1. Haemostasis**

Disturbances to the epidermal barrier due to injury allows for the secretion of previously stored interleukin-1 (IL-1) by keratinocytes found at the wound site (Barrientos, *et al.*, 2008). The secreted IL-1 signals to the surrounding cells of the cutaneous injury that has occurred (Barrientos, *et al.*, 2008). Haemostasis is the immediate response to injury (Figure 2A) (Velnar, *et al.*, 2009). Molecular and cellular responses are initiated following vascular injury due to significant wounding (Monaco & Lawrence, 2003). Haemostasis includes three consecutive steps: vasoconstriction, platelet aggregation and blood coagulation (Al-Shaibani, *et al.*, 2016). Vasoconstriction is characterised by the release of vasoactive amines, such as thrombin and prostaglandins, which cause blood vessels to constrict, thereby stopping bleeding (Wallace & Zito, 2021). Platelets aggregate and adhere to each other as well as to the sub-endothelium and release  $\alpha$ -granules, dense bodies (which contain compounds such as serotonin and ATP) and lysosomes (Monaco & Lawrence, 2003). Alpha granules release immunomodulatory and proteinaceous factors, such as fibroblast growth factor-2 (FGF-2), fibronectin, platelet derived growth factor (PDGF), coagulation factors V and VIII, fibrinogen, transforming growth factors  $\alpha$  and  $\beta$  (TGF- $\alpha$  and TGF- $\beta$ ) and epidermal growth factors (EGF), that are utilised throughout the healing process to stimulate cellular functions such as angiogenesis and fibroblasts differentiation (Velnar, *et al.*, 2009).

Blood coagulation (clotting) is brought about by platelets and factors such as fibronectin, collagen and thrombin form the clot (Broughton & Janis, 2006). The clot limits contamination by pathogens and prevents further fluid and electrolyte loss, (Monaco & Lawrence, 2003). It concentrates the secreted growth factors and cytokines that initiate the inflammation stage and provides a provisional matrix that supports infiltrating cells such as monocytes, neutrophils, macrophages and fibroblasts (Broughton & Janis, 2006).

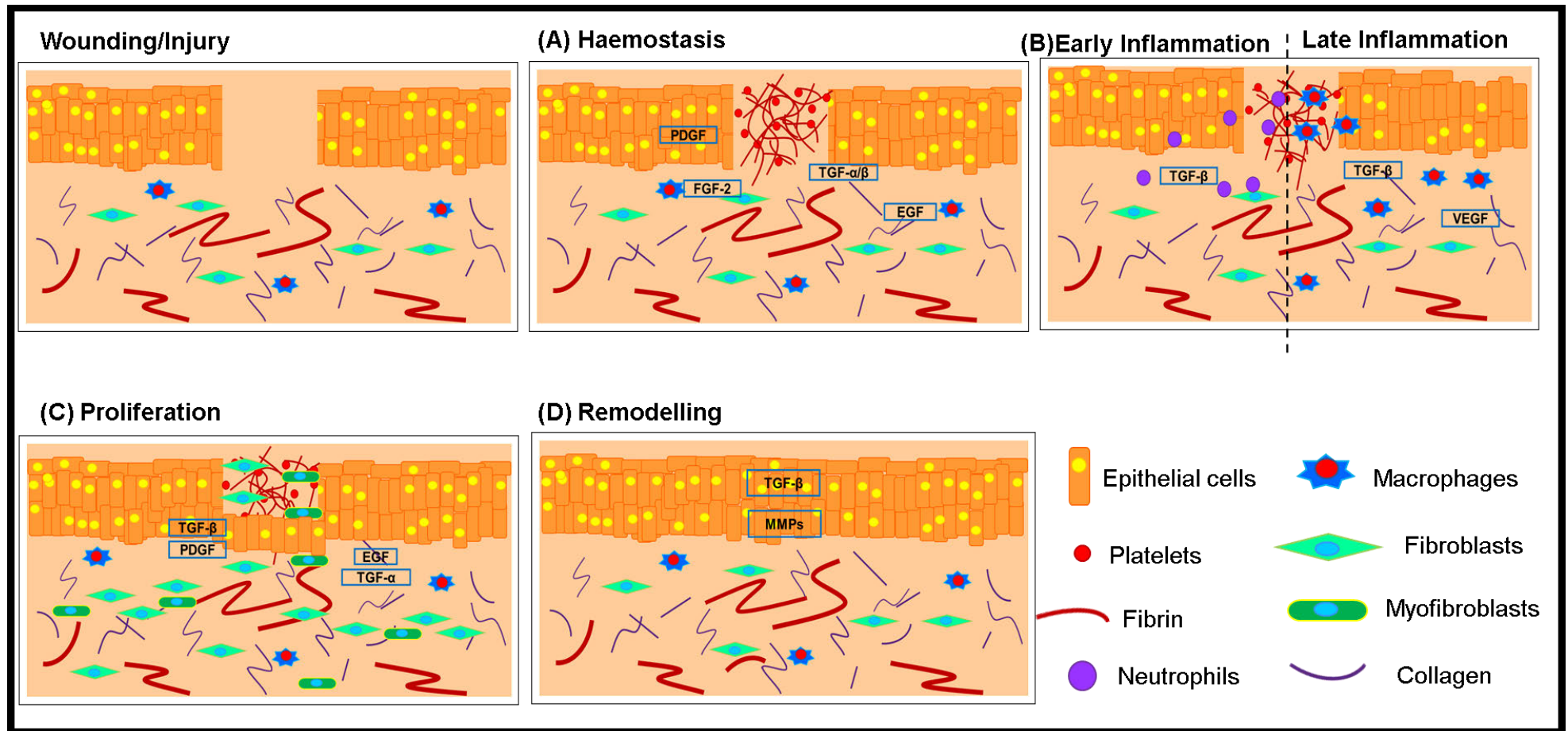


**Figure 2: Schematic representation of the stages of cutaneous wound healing: (A) haemostasis, (B) inflammation, (C) proliferation, and (D) remodelling.** Specific molecular and cellular events are used to identify each stage. The stages are co-ordinated by many factors that cells recognise or release during wound-healing. (Adapted from Jackson, et al., 2012).

### **1.1.2. Inflammation**

During inflammation, blood vessels vasodilate which serves to aid in the migration of lymphocytes, leukocytes, neutrophils and macrophages to the wound site (Figure 2B) (Monaco and Lawrence, 2003). Inflammation is characterised by an early and late stage (Hart, 2002; Velnar, *et al.*, 2009). Both the early and late stages promote the establishment of an immune barrier against invading microbes (Velnar, *et al.*, 2009). Early inflammation marks the initiation of the complement cascade and molecular events which results in the migration of neutrophils into the wound (Broughton, *et al.*, 2006; Velnar, *et al.*, 2009). Neutrophils are attracted to the wound site by chemo-attractive agents, such as TGF- $\beta$  (Broughton & Janis, 2006). Within the wound area, neutrophils secrete oxygen-derived free radicals and proteolytic enzymes that destroy foreign microbes and materials which it then phagocytoses (Richardson, 2004; Broughton & Janis, 2006; Velnar, *et al.*, 2009). Once the contaminants have been destroyed, the neutrophils apoptose (Hunt, *et al.*, 2000; Velnar, *et al.*, 2009).

During late inflammation, the apoptotic bodies and any other cellular remains are phagocytosed by macrophages via a process known as efferocytosis (Velnar, *et al.*, 2009). These macrophages are predominantly monocyte-derived macrophages; however, some tissues (such as the skin) do have resident tissue macrophages (Brancato & Albina, 2011). The tissue-resident macrophages are thought to be the first responders following injury (Kim & Nair, 2019). The tissue-resident macrophages are capable of self-renewing, whereas the monocyte-derived macrophages apoptose once the inflammation phase has resolved (Kim & Nair, 2019; Hashimoto, *et al.*, 2013). Macrophages also secrete potent growth factors, (such as VEGF and TGF-  $\beta$ ), which activate keratinocytes, fibroblasts, and endothelial cells (Velnar, *et al.*, 2009). Macrophages assist in the transition from the inflammatory phase to the proliferative phase of wound repair (Broughton & Janis, 2006).

### **1.1.3. Proliferation**

New ECM is synthesized, deposited, and organised at the wound site during the proliferation (Figure 2C) (Barrientos, *et al.*, 2008). The proliferative stage is also distinguished by the migration of fibroblasts into the wound site, synthesis of collagen, angiogenesis and beginning of re-epithelization (Velnar, *et al.*, 2009). Factors such as PDGF (released by platelets) and TGF- $\beta$  (produced by macrophages) attract fibroblasts to the wound area (Velnar, *et al.*, 2009).

At the injured site, fibroblasts proliferate in response to growth factors such as insulin-like growth factor (IGF), PDGF and TGF- $\beta$ , and produce matrix proteins such as hyaluronan, fibronectin, proteoglycans, glycosaminoglycans and collagen (types III) (Monaco & Lawrence, 2003; Velnar, *et al.*, 2009). Fibroblasts differentiate into myofibroblasts that express  $\alpha$ -SMA and produce lamellipodia that assist in wound contraction (Velnar, *et al.*, 2009).

Collagen is synthesized and secreted by fibroblasts in response to stimuli from growth factors such as EGF, TGF- $\beta$  and PDGF; it provides strength and integrity to the tissue (Monaco & Lawrence, 2003; Velnar, *et al.*, 2009). Collagen, glycosaminoglycans and proteoglycans are vital components of the ECM of the granulation tissue, which provides a scaffold over which epithelial cells migrate for re-epithelialisation to occur (Robson, *et al.*, 2001).

#### **1.1.4. Remodelling**

Completion of re-epithelialisation and potential scar formation occurs during the remodelling phase (Figure 2D) (Velnar, *et al.*, 2009). Collagen III, the main component of the granulation tissue, is degraded by MMP enzymes (such as MMP-8 and MMP-13) and replaced with the stronger collagen I (Robson, *et al.*, 2001; Suda, *et al.*, 2015; Caley, *et al.*, 2015). Collagen I is the main structural component of the dermis and is synthesized by myofibroblasts in response to TGF- $\beta$  (Barrientos, *et al.*, 2008, Velnar, *et al.*, 2009; Darby, *et al.*, 2014). Tissue inhibitors of metalloproteinases (TIMPs) regulate the activity of MMPs (Monaco & Lawrence, 2003). During the remodelling phase, a state of equilibrium is reached between the rate of collagen synthesis and breakdown as well as the remodelling of the ECM (Monaco and Lawrence, 2003). However, the tissue strength of the remodelled tissue is never as good as the original uninjured tissue (Monaco and Lawrence, 2003). This is because the collagen within the granulation tissue of the wound environment is orientated differently and is also biochemically different to collagen in uninjured skin (Robson, *et al.*, 2001). The collagen within repaired skin is arranged in overlapping parallel fibres which decreases the tensile strength of the skin, whereas in uninjured skin, collagen is arranged in a stronger basket-weave pattern (Robson, *et al.*, 2001). The lysine residues within the collagen found in granulation tissue display increased hydroxylation and glycosylation, which correlates with the thinner fibres as compared to uninjured skin (Robson, *et al.*, 2001).

## 1.2. Skeletal muscle injury

Daily activities and exercises can cause muscles fibres to undergo mechanical damage, however more serious injuries such as contusions, strains and lacerations may cause loss of functional capacity (Järvinen, *et al.*, 2005; Nguyen, *et al.*, 2019). Severe muscle injury can be classified as either a contusion (caused by a non-penetrating, blunt force that ruptures blood vessels under the skin causing a hematoma), strain (when muscles or tendons are stretched too far or partially torn which damages the structure or interconnections between muscles and tendons or muscles and bone) or laceration (crushing or deep penetrative force that causes tissue loss and may lead to scar formation) (Garrett Jr., *et al.*, 1984; Nikolau, *et al.*, 1987; Crisco, *et al.*, 1994; Järvinen, *et al.*, 2005).

Skeletal muscle healing, as with cutaneous wound repair, is a dynamic process that requires the synchronized actions of multiple cell types (Laumonier & Menetrey, 2016; Mackey, *et al.*, 2017; Martins, *et al.*, 2020). Following injury, myofibers rupture and undergo necrosis, which causes the unharmed myofibers to contract leaving a gap between the blood vessels which allows for the formation of a haematoma (Järvinen, *et al.*, 2005; Laumonier & Menetrey, 2016). Growth factors and cytokines are released from the damaged blood vessels which attract M1 macrophages to the injury site (Mann, *et al.*, 2011). M1 macrophages are pro-inflammatory cells that aid in lysis of cells, phagocytose cell debris and stimulation of myoblast differentiation (Laumonier & Menetrey, 2016). Later, there is a transition to M2 macrophages, which are more anti-inflammatory and promote the formation of myotubes (Laumonier & Menetrey, 2016).

For the regeneration phase to proceed, inflammatory cytokines and growth factors within the wounded area must activate satellite cells; these are quiescent skeletal muscle stem cells found between the plasma membrane and basal lamina of the myofibers (Cossu & Biressi, 2005; Danna, *et al.*, 2014; Laumonier & Menetrey, 2016). Some activated satellite cells differentiate and fuse together to form myofibers that replace the injured muscle, whilst the rest replenish the satellite-cell pool through self-renewal (Mann, *et al.*, 2011). The migration and proliferation of fibroblasts within the injured muscle site is essential for efficient muscle repair as they produce ECM components such as fibronectin, laminin, proteoglycans, collagen types I and III and elastin which acts as a scaffold to the new myofibers and stabilises the tissue (Mann, *et al.*, 2011). Studies by Mackey and colleagues (2017) indicate that the activity of satellite cells during the regeneration of muscles is promoted by fibroblasts in a contact-dependent manner.



The study showed that when a permeable membrane separated the fibroblast from the myoblast populations, the fibroblasts had no effect on any stages of myogenesis (Mackey, *et al.*, 2017).

### 1.3. Macrophages

During wound healing, macrophages have two distinguishable phenotypes, M1 and M2 (Hesketh, *et al.*, 2017) (Figure 3). The pro-inflammatory M1 macrophages are the first to appear; this is followed by a transition to an anti-inflammatory M2 phenotype during later parts of the inflammatory phase (Hesketh, *et al.*, 2017). M1 and M2 macrophage subsets can both be derived from monocytes in response to either *classical activation* (induced via lipopolysaccharide (LPS), interferon- $\gamma$  (IFN- $\gamma$ ) or tumour necrosis factor- $\alpha$  (TNF- $\alpha$ ) or via *alternative activation* (induced via IL-4 or IL-13), respectively (Hesketh, *et al.*, 2017). In addition, an existing M1 macrophage can polarise to an M2 phenotype within the wound environment (Hesketh, *et al.*, 2017).

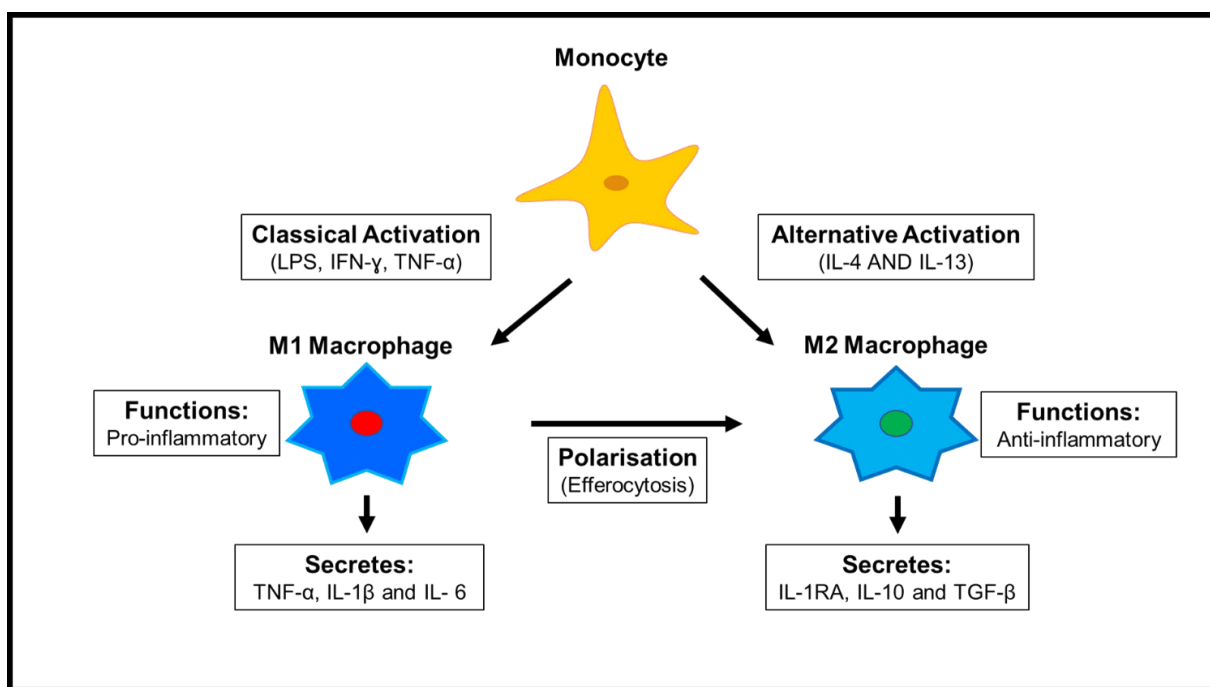


**Figure 3: Schematic representation of the polarisation of macrophages.** Monocytes can be activated to M1 macrophages via classical activation, or to M2 macrophages via alternative activation. M1 macrophages may polarise to M2 macrophages due to efferocytosis, (i.e. the phagocytosis of the neutrophilic apoptotic bodies by the macrophages). M1 macrophages are pro-inflammatory and secrete TNF- $\alpha$ , IL-1 $\beta$  and IL-6 among other factors, whereas M2 macrophages are anti-inflammatory and secrete IL-1RA, IL-10 and TGF- $\beta$  among other factors. (Adapted from Hesketh, *et al.*, 2017).

M1 macrophages express surface markers including CD40, CD80 and CD86 and secrete factors such as TNF- $\alpha$ , IL-1 $\beta$  and IL-6 (Schliefsteiner, *et al.*, 2020). Antigen-presenting cells, such as macrophages, express CD40 which is a co-stimulatory molecule that is part of the TNF family (Kawabe, *et al.*, 2011). The CD40 on macrophages prompts the production of pro-inflammatory cytokines and, in the presence of IFN- $\gamma$ , allows for the production of nitric oxide (NO) which aids in an effective immune response against microbial pathogens (Suttles & Stout, 2009). CD80 and CD86 belong to the Immunoglobulin superfamily that have costimulatory roles in the initial activation of T-cells (Yun & Clark, 1998). Tumour necrosis factor- $\alpha$  (TNF- $\alpha$ ) induces the generation of fibronectin and proteoglycan by fibroblasts which stimulates the formation of ECM within the wound (Ritsu, *et al.*, 2017). Interleukin-1 $\beta$  (IL-1 $\beta$ ) is part of a positive feedback loop that promotes the pro-inflammatory macrophage phenotype, and thereby induces its' own production (Mirza, *et al.*, 2013). Interleukin-6 (IL-6) upregulates the expression of IL-1 as well the infiltration of leukocytes into the wound site (Lin, *et al.*, 2003).

In comparison, M2 macrophages express surface markers CD163 and CD206, secrete factors such as IL-1 receptor antagonist (IL-1RA), IL-10 and TGF- $\beta$  and expresses arginase-1 (Orecchioni, *et al.*, 2019; Schliefsteiner, *et al.*, 2020). CD163 belongs to the scavenger cysteine-rich superfamily class B that has multiple functions including homeostatic functions; it also acts as a receptor for haemoglobin-haptoglobin complexes (Fabriek, *et al.*, 2009). CD206 is a mannose receptor and C-type lectin that functions in the immune recognition of pathogens by interacting with surface glycolipids and glycoproteins on the surface of pathogens (Suzuki, *et al.*, 2018). Interleukin-1RA (IL-1RA) counteracts the signalling mediated by IL-1 $\alpha/\beta$  and TNF- $\alpha$  (Ishida, *et al.*, 2006). Interleukin-10, an immunoregulatory cytokine, regulates innate and adaptive responses by down-regulating pro-inflammatory mediators such as TNF- $\alpha$  and IL-6 and up-regulating anti-inflammatory mediators such as IL-1RA and soluble TNF-receptor (Eming, *et al.*, 2007). Transforming growth factor- $\beta$ 1 (TGF- $\beta$ 1) aids in the proliferation of fibroblasts and their differentiation to myofibroblasts, which then leads to an increased production of collagen which aids in strengthening of the wound (Hesketh, *et al.*, 2017). The enzyme arginase-1 hydrolyses arginine to ornithine during the urea cycle (Orecchioni, *et al.*, 2019).

The polarization of M1 to M2 macrophages is paramount for TGF- $\beta$  production, which contributes to the progression of wound healing from the inflammatory to the proliferation phase; it stimulates the migration, proliferation, and differentiation of fibroblasts in the wound site, thereby enabling wound contraction, angiogenesis, and re-epithelization (Valluru, *et al.*,

2011). Hence, if there is a decrease in the production of TGF- $\beta$ , due to M1 macrophages not polarising to M2 macrophages, this inevitably hinders fibroblast functionality within the wound site. Moreover, the number of macrophages decrease within the wound site during the remodelling phase. If M2 macrophages persist within the wound site, the prolonged stated would result in excess wound healing resulting in fibrosis (Kim & Nair, 2019).

#### **1.4.1. Fibroblast**

Fibroblasts are non-terminally differentiated mesenchymal cells that are spindle-shaped, which are obtained from the embryonic mesoderm (Kendall & Feghali-Bostwick, 2014; Li & Wang, 2011). Fibroblasts, characteristically express vimentin (an intermediate filament protein) but does not express  $\alpha$ -SMA (a contractile protein) or desmin (an intermediate filament protein) (Li & Wang, 2011). Throughout the whole body, fibroblasts can be found within connective tissue (Kendall & Feghali-Bostwick, 2014). Fibroblasts regulate the amount ECM present within a tissue under normal conditions (Kendall & Feghali-Bostwick, 2014). They contribute to tissue fibrosis, angiogenesis, and wound healing (Li & Wang, 2011). Fibroblasts produce and release VEGF, which acts on the VEGF-receptor on endothelial cells to promote angiogenesis (Kendall & Feghali-Bostwick, 2014). During wound healing, fibroblasts can produce contractile forces which are thought to facilitate wound closure by bringing the edges of the wound together (Li & Wang, 2011).

As part of the inflammatory response, macrophages and platelets produce and release chemoattracts such as IL-1 $\beta$ , TNF- $\alpha$  and PDGF that bind to specific receptors on the cell surface which direct fibroblasts to the site of injury (Bainbridge, 2013). Once at the site, fibroblasts produce various MMPs that degrade the fibrin clot and replace it with ECM components such as collagen types I-IV, laminin, fibronectin, proteoglycans, and elastin that act as a scaffold for the new fibres, stabilizes the tissue and function as a signal and support for granulation-tissue generation, angiogenesis, and epithelisation (Porter, 2007; Rozario & DeSimone, 2010; Mann, *et al.*, 2011; Li & Wang, 2011 Bainbridge, 2013). Fibroblasts function as both synthetic and signalling cells as they produce a collagen-rich ECM and secrete growth factors that are vital for cell-to-cell communication during wound healing, respectively (Lerman, *et al.*, 2003).

#### 1.4.2. Differentiation of fibroblast to myofibroblast

Fibroblasts differentiate to myofibroblasts in response to factors such as TGF- $\beta$ 1, TGF- $\beta$ 2 and TGF- $\beta$ 3 secreted by M2 macrophages; this occurs towards the end of the inflammation phase and start of the proliferation phase (Kim, *et al.*, 1999; Velnar, *et al.*, 2009; Bainbridge, 2013). During the differentiation of fibroblasts to myofibroblasts, there is a transient cell called the protomyofibroblast (Hinz, 2007).

Fibroblasts are stimulated by TGF- $\beta$ 1 and TGF- $\beta$ 2 to attach to fibrous proteins in the ECM across integrin containing adhesions (Hinz, *et al.*, 2007; Bainbridge, 2013). The cross-linked structure of the ECM in uninjured tissue stress shields fibroblasts, however during injury the microenvironment changes owing to this stress shield no longer being present (Tomasek, *et al.*, 2002). Following mechanical stress in the microenvironment of the wound site as well as the binding to fibrous proteins, fibroblasts express actin filaments and stress fibres and are called protomyofibroblasts (Figure 3) (Tomasek, *et al.*, 2002; Gabbiani, 2003; Hinz, *et al.*, 2007). Protomyofibroblasts are characterised by the formation of stress fibres that express cytoplasmic  $\beta$  and  $\gamma$  actins (Gabbiani, 2003). Transforming growth factor  $\beta$ 1 (TGF- $\beta$ 1) increases the expression of cellular fibronectin (ED-A splice variant isoform) expressed at the surface of protomyofibroblasts, (Hinz, 2007). The proto-myofibroblasts can generate some contractile force (Gabbiani, 2003). Protomyofibroblasts have stress fibres (from *de novo* contractile bundles) that sufficiently generate a force that pulls cells forward, populating tissue spaces during the pre-remodelling of the ECM and migration process (Kwan, *et al.*, 2012). These cells can also function as an independent cell type in some adult tissues without differentiating to myofibroblasts (Tomasek, *et al.*, 2002). The presence of the ED-A fibronectin and TGF- $\beta$ 1 during mechanical stress further stimulates the differentiation of myofibroblasts from protomyofibroblasts (Gabbiani, 2003). Myofibroblasts are thought to be pivotal for the wound healing process; under physiological wound repair, myofibroblast either dedifferentiate to fibroblasts or apoptose (Figure 4) (Li & Wang, 2011; Ko, *et al.*, 2019).

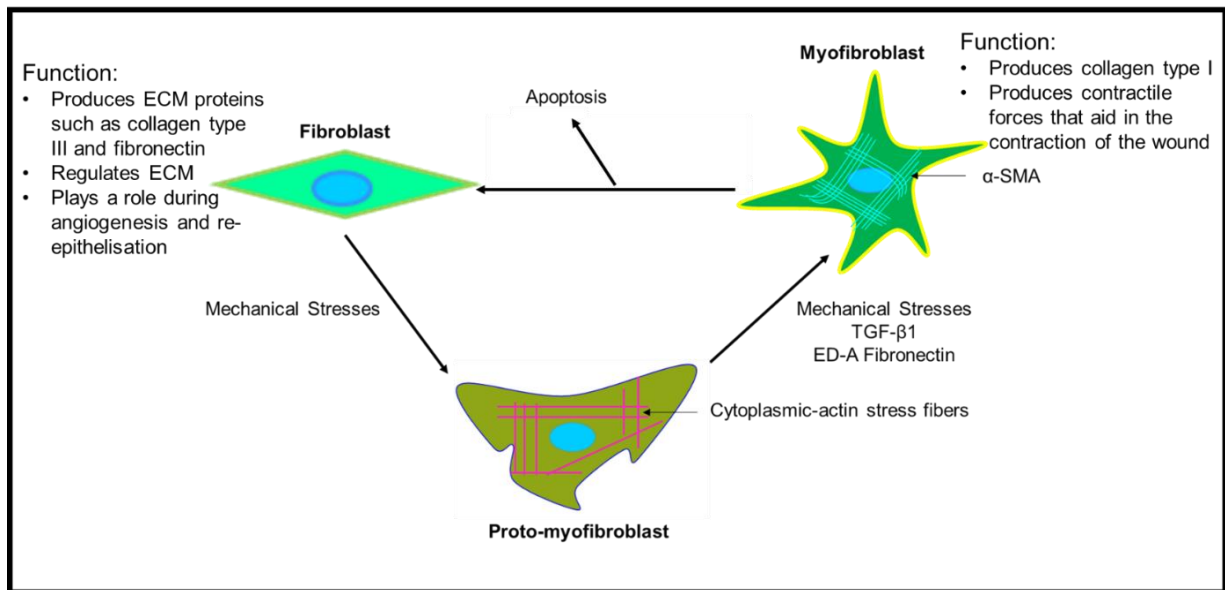


**Figure 4: Schematic illustration of the differentiation of fibroblasts to myofibroblasts during wound healing.** Mechanical stresses within the microenvironment results in the differentiation of fibroblasts to protomyofibroblasts. Thereafter, the mechanical stress within the microenvironment coupled with the presence of ED-A fibronectin and TGF- $\beta$ 1 allows for the transition from the protomyofibroblast to the myofibroblast. Myofibroblasts aid in wound contraction. The protomyofibroblasts express cytoplasmic-actin stress fibres, whereas myofibroblasts express  $\alpha$ -SMA. Following wound closure, myofibroblasts either dedifferentiate to fibroblasts or are removed from the wound site by apoptosis. (Adapted from Gabbiani, 2003).

### 1.4.3. Myofibroblasts

Myofibroblasts contain stress fibres made up of smooth muscle-related contractile proteins, such as smooth muscle myosin heavy chain, desmin and  $\alpha$ -SMA (which identifies it from fibroblasts) (Darby, *et al.*, 2014). Myofibroblasts function to produce ECM proteins, such as glycoproteins, collagen type I and proteoglycans, which stimulate normal growth of tissues and organs, differentiation of epithelial cells, and wound healing (Powell, *et al.*, 1999; Li & Wang, 2011). The contractile fibres of the myofibroblast are arranged in microfilament bundles; fibroblasts lack these microfilament bundles (Gabbiani, 2003). The contractile microfilament bundles function as a mechano-transduction system that transmits the force generated by the stress fibres to the ECM, as well as transduces ECM signals into intracellular signals (Tomasek, *et al.*, 2002). In the wound environment, excessive contraction by myofibroblasts may lead to scarring or undesirable contraction (Chitturi, *et al.*, 2015).

### 1.5. Satellite cells to myoblasts

In adult muscle, myogenic precursors referred to as satellite cells reside in a quiescent state between the plasma membrane and basal lamina of myofibers (Cossu & Biressi, 2005). The satellite cell progression through the myogenic program is said to be reliant on the ratio of expression of markers Pax7 and MyoD (Dumont, *et al.*, 2015; Snijders, *et al.*, 2015). Quiescence is favoured by a high Pax7: MyoD ratio, whereas an intermediate ratio promotes proliferation of the satellite cells, and a low ratio stimulates differentiation (Dumont, *et al.*, 2005). During proliferation, if Pax7 expression is elevated, these cells do not differentiate, but stimulate self-renewal by returning to the quiescent state and maintaining the satellite cell pool (Snijders, *et al.*, 2015).

When muscle injury occurs, satellite cells relocate to the wounded area and enter the cell cycle (Dumont, *et al.*, 2005) (Figure 5). During the inflammation phase of wound healing, an increase in TNF- $\alpha$ , IL-1 $\beta$  and IL-6 (pro-inflammatory cytokines) stimulates the initiation of myoblast proliferation (Dumont, *et al.*, 2005). Myoblasts exit from the cell cycle after several rounds of proliferation and differentiate into myocytes (Dumont, *et al.*, 2005). Following differentiation, myocytes need to recognize and adhere to each other in-order to fuse into myotubes (Dumont, *et al.*, 2005). The fusion comprises of an early and late phase during which the cells first adhere to one another, then fuse to nascent multinucleated myotubes, respectively (Dumont, *et al.*, 2005). These multinucleated myotubes then mature and become highly specialized and functional myofibers (Dumont, *et al.*, 2005).

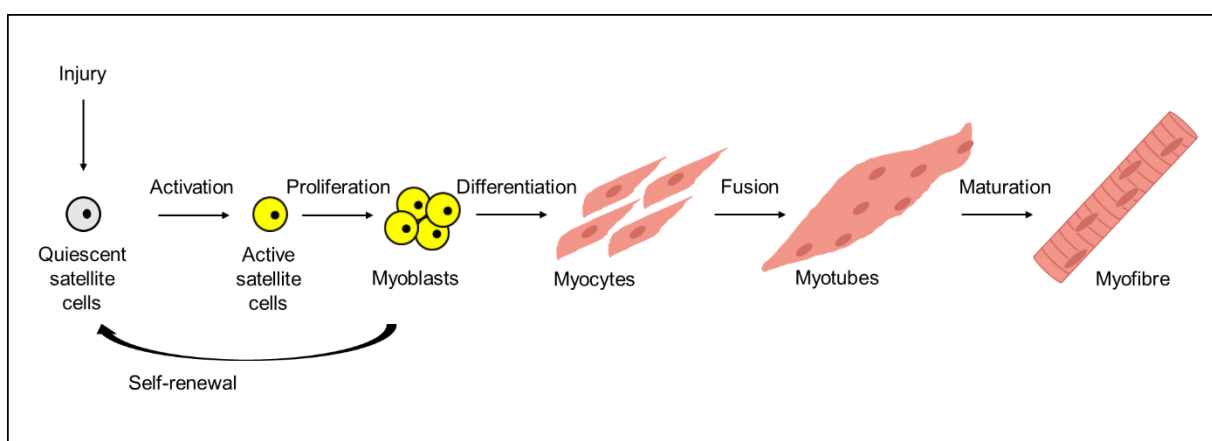


**Figure 5: Schematic representation of Activation of satellite cells to produce differentiated myoblasts.** Following injury, quiescent satellite cells proliferate, where some differentiate into myoblasts whilst others self-renew to regenerate the quiescent satellite cell pool. Myoblasts differentiate into myocytes that fuse to form myotubes followed by maturation into myofibers (new muscle fibres) that replace the damaged muscle tissue. (Adapted from Nguyen, *et al.*, 2019).

### **1.6.1. Diabetes Mellitus**

Type 2 diabetes mellitus (T2DM) is a metabolic disease that is characterised by high glucose levels (Pheiffer, *et al.*, 2018). The hyperglycaemic environment of T2DM causes a pro-inflammatory microenvironment due to increased release of cytokines by leukocytes (which adhere increasingly to the endothelial surface near the wound) (Shakya, *et al.*, 2015). Abnormal glucose levels and increased cytokine levels result in the malfunction of epidermal cells, macrophages, and fibroblasts cells, including the dysfunction of leukocyte phagocytosis, bactericidal capacity and chemotaxis, which ultimately leads to the impairment of wound healing (Loots, *et al.*, 1998; Sibbald & Woo, 2008).

Biopsies of the epidermis from diabetic patients have revealed pathogenic markers that relate to a delay in wound healing (Stojadinovic, *et al.*, 2005). Stojadinovic and colleagues (2005) observed that at the edge of non-healing wounds, c-Myc was expressed in excess and  $\beta$ -catenin present in the nucleus. The activated  $\beta$ -catenin and c-Myc inhibits keratinocyte migration, therefore impairing wound healing (Stojadinovic, *et al.*, 2005). Stojadinovic and colleagues (2005) stated that the nuclear localisation of the  $\beta$ -catenin and the overexpression of c-Myc may serve as a molecular marker within the epidermis of chronic wounds. Diabetic skin has a decreased skin barrier prior to wounding and is identified as being thinner than normal skin (Du, 2018).

Due to high glucose levels, diabetic patients suffer from neuropathy (damage to the nerves) (Greene, *et al.*, 1990; Brem & Tomic-Canic, 2007). This causes a decrease in signals sent from wounded area to the brain and to other tissues within the body (Brem & Tomic-Canic, 2007; Said, 2007). Hence, following injury, fibroblasts may not receive relevant pro-migratory signals and therefore do not move to the wound site towards the end of the inflammatory stage; this could contribute to the non-healing nature of these wounds (Brem & Tomic-Canic, 2007). Moreover, in a hyperglycaemic environment, as seen in diabetics', the synthetic, secreting and proliferative abilities of fibroblasts are also diminished (Berlanga-Acosta, *et al.*, 2013).

### **1.6.2. Diabetic foot ulcers (DFUs)**

Diabetic foot ulcers (DFUs) can be described as cracks, ulcers or fissures that may arise on the feet (Abbas, *et al.*, 2002). Diabetic foot ulcers (DFUs) are exacerbated due to conditions such as neuropathy and hypoxia that occur in patients; these hinder sensation in the limbs and reduce

the amount of oxygen reaching cells and tissues, thereby contributing to wound healing impairment (Guo & DiPietro, 2010). Evidence from experimental and clinical studies suggests that the impaired wound healing within DFUs often leads to sepsis and consequently gangrene, ultimately ending in lower limb amputations (Loots, *et al.*, 1998; Goie & Naidoo, 2016).

### **1.6.3. Prevalence of diabetes in South Africa**

Globally, there are considerable healthcare costs, and increased mortality, and morbidity due to diabetes mellitus (Sahadew, *et al.*, 2016). South Africa is one of the sub-Saharan African countries with the highest rate of T2DM (Goie & Naidoo, 2016; Sahadew, *et al.*, 2016). The International Diabetes Federation has estimated that 7% (3.85 million people) of the South African population, between the ages of 21-79 have T2DM (International Diabetes Federation, 2015). Africa at large has a high percentage of diabetic patients with DFUs that have progressed to infection and gangrene due to the lack of education on proper medical care as well as the lack of proper health-care systems, particularly within rural areas (Pillay, *et al.*, 2019).

During normal, acute wound healing, the M1 macrophage phase is usually comparatively shorter than the M2 macrophage phase (Delavary, *et al.*, 2011). However, in diabetics, the hyperglycaemic environment leads to a persistent M1 pro-inflammatory phenotype; this contributes to an increase in the production of pro-inflammatory cytokines such as IL-1 $\beta$  and IL-6, hindering progression of wound healing from the inflammation stage to the proliferation stage (Salazar, *et al.*, 2016; Wen, *et al.*, 2006). A hyperglycaemic environment can cause the preprogramming of haematopoietic cells, generating monocytes (which differentiate to macrophages) that are predisposed to a pro-inflammatory phenotype (Hesketh, *et al.*, 2017). Hence, the ability of the altered macrophages to phagocytose the apoptotic neutrophils is hindered (Hesketh, *et al.*, 2017).

### **1.7. Studies understanding the role of fibroblasts and myofibroblasts in diabetic wound healing**

A study by Ehrlich and colleagues (1999) hypothesized that wound contraction can be produced by fibroblasts, hence myofibroblasts were not required. He treated rats with vanadate, which is a protein tyrosine phosphatase inhibitor, to inhibit the expression of  $\alpha$ -SMA in rats. The inhibition of  $\alpha$ -SMA, inhibits the differentiation of fibroblasts to myofibroblasts (Ehrlich, *et al.*, 1999). He made full-excisional wounds on the backs of the rats and had observed that



the absence of myofibroblasts did not hinder the rate of wound healing. He concluded that myofibroblasts were not vital for wound contraction to occur. Surprisingly, he had also observed that the deposition of collagen within the rats treated with vanadate (did not express  $\alpha$ -SMA, hence myofibroblasts were absent) was more orderly than the control rats (expressed  $\alpha$ -SMA, hence myofibroblasts were present). This suggests that vanadate may play a role in matrix deposition and possibly scar formation (Ehrlich, *et al.*, 1999).

Contrastingly, a study by Seitz and colleagues (2010) assessed the difference in wound healing in high-fat diet-induced (HFD) obese diabetic mice and genetically obese diabetic mice (*ob/ob*) and compared it to normal, non-diabetic, lean mice on a chow diet (CD). They observed a decrease in the performance of keratinocytes, endothelial cells and fibroblasts which decreased the formation of granulation tissue and re-epithelisation. Compared to the normal lean mice, there was a delay in the closure of the wounds in the HFD-mice and *ob/ob* mice. Five days post wounding, the diameter of the wounds on the HFD-mice and *ob/ob* mice increased. This was confirmed as analysis of cross-sections of the wound site showed an enlarged distance between the wound margin neo-epithelia and a decrease in the size of neo-epithelia. Seven days post-wounding, re-epithelialisation was incomplete in the HFD-mice and significantly impaired in genetically obese mice, whereas the wounds in control mice were completely re-epithelialized.

Myofibroblasts within the wound sites of HFD mice and *ob/ob* mice were analysed due to the delayed wound healing (Seitz, *et al.*, 2010). The expression of  $\alpha$ -SMA mRNA was used as a marker to detect the presence of myofibroblasts (Seitz, *et al.*, 2010). At day five, there was an expected increase in  $\alpha$ -SMA mRNA in the CD mice and HFD mice, which decrease at day 11. However, the *ob/ob* mice, did not show any expression of  $\alpha$ -SMA mRNA during the healing period. This suggested a lack of differentiated myofibroblasts, which may be related to the delayed wound repair observed (Seitz, *et al.*, 2010).

## 1.8. Summary

During the wound healing process, it is vital that each stage; haemostasis, inflammation, proliferation, and remodelling; occurs in a timely and sequential manner for proper closure of the wound. Failure to follow this sequence of events, may result in non-healing chronic wounds, which leads to further complications and may ultimately result in limb amputation. There are a multitude of different cells, growth factors and cytokines that are required to aid

the healing process. During the wound healing process, it is vital that the M1 pro-inflammatory macrophage transits into the M2 anti-inflammatory macrophage for successful wound healing. M2 macrophages stimulates the production of TGF- $\beta$ , which stimulates the migration and functioning of fibroblasts in the wound site. Fibroblasts actively aid wound healing by producing collagen and differentiating to myofibroblasts during the proliferative phase. Myofibroblasts are known to produce contractional forces that aid in the closure of the wound. Beyond this, the role of fibroblasts and myofibroblasts in wound healing is unclear; a greater understanding could benefit our approach to wound repair under pathological conditions.

### **1.9. Aims and objectives**

Data on the effect of different fibroblast and macrophage phenotypes on myoblast wound closure would offer a better understanding of these cell types on each other during wound closure, which could provide new approaches to enhance wound repair under pathological conditions.

The current study aimed to understand the effect of different cellular role players, specifically fibroblasts (both undifferentiated and differentiated) and macrophage phenotypes, on *in vitro* wound healing using myoblasts as the wounding model.

To achieve this aim, the first set of objectives were:

1. To establish *in vitro* methods for generating different fibroblast and macrophage phenotypes. More specifically:
  - a. Using the effect of the presence and absence of serum in cell culture media on L929 cells to generate fibroblast, protomyofibroblast and myofibroblast phenotypes *in vitro*.
  - b. Polarising J774A.1 macrophages to M1 and M2 phenotypes using LPS and IL-4, respectively.
2. Subsequently, the second set of objectives used double co-culture models to determine the effect of:
  - a. Fibroblasts, protomyofibroblasts and myofibroblasts on myoblast wound closure.

- b. Myoblasts on fibroblast, protomyofibroblast and myofibroblast wound closure.
  - c. Polarised macrophages on myoblast wound closure.
- 3. Finally, the third set of objectives used the triple co-culture model to determine the effect of:
  - a) Each of the fibroblast phenotypes (fibroblasts, protomyofibroblasts and myofibroblasts) in the presence of M1 polarised macrophages on myoblast wound closure.
  - b) Each of the fibroblast phenotypes (fibroblasts, protomyofibroblasts and myofibroblasts) in the presence of M2 polarised macrophages on myoblast wound closure.

## **2. Materials and Methods**

### **2.1. General Reagents and Lab Procedures**

#### **2.1.1. Reagents**

Phosphate buffer saline (or PBS, 2.67 mM KCl (EMSURE, Cat. 7447-40-7), 1.47 mM  $\text{KH}_2\text{PO}_4$  (Analytical Reagent), 136.9 mM NaCl (MERCK, Cat. 1038129) and 8.10 mM  $\text{Na}_2\text{HPO}_4$  (EMSURE, Cat. 7558794), pH 7.2) was prepared and autoclaved where necessary. Sodium orthovanadate (or vanadate;  $\text{Na}_3\text{VO}_4$ ; 200 mM; Lot. SLBZ8763, Sigma) was prepared in double distilled water, adjusted to pH 10 with HCl and then boiled till clear, thereafter filtered and stored in the freezer ( $-20^\circ\text{C}$ ). Lipopolysaccharide (or LPS; 1 mg/ml; a gift from Prof. Anil Chuturgoon, College of Health Sciences, UKZN) was prepared in distilled water and stored at  $-20^\circ\text{C}$ . Interleukin-4 (or IL-4, 20  $\mu\text{g}$ ; Peprotech, Cat. 214-14, Cranbury, NJ, USA) was diluted to 20  $\mu\text{g}/\text{ml}$  in PBS-0.1% BSA and stored at  $-20^\circ\text{C}$ .

#### **2.1.2. Standard Cell Culture.**

Mouse J774A.1 macrophage (ATCC, Cat. TIB-67<sup>TM</sup>), L929 myofibroblasts (ATCC, Cat. CRL-6364<sup>TM</sup>) and C2C12 myoblasts (ATCC, Cat. CRL-1772<sup>TM</sup>, Manassas, VA, USA) were maintained in growth medium (serum-containing medium or SCM) containing Dulbecco's Modified Eagles Medium (DMEM, HyClone, Cat. SH30243.01, USA) with added 10% (v/v) fetal bovine serum (FBS, Gibco, Cat. 10499-044, Waltham, MA, USA) and 2% (v/v) penicillin-streptomycin (Lonza, Cat. DE17-602E, Basel, Switzerland). Culture medium was changed every 48-72 hours. When cells reached confluence, they were passaged into different flasks. The old SCM from L929 myofibroblasts and C2C12 myoblasts was discarded, followed by washing twice with PBS to remove any remaining SCM; thereafter the cells were trypsinized to detach cells from the flask, and lastly SCM was added to neutralise the trypsin. For J774A.1 macrophages, the old SCM was first discarded, and cells washed twice with PBS followed by the addition of SCM, after which a cell scraper was used to detach the cells from the bottom of the flask. Lastly the cell cultures were split (1:3) into different flasks and topped up with 10 ml SCM. All cell types are incubated at  $37^\circ\text{C}$  with 5%  $\text{CO}_2$ . Serum-free medium (SFM) consisted of DMEM with added 2% (v/v) penicillin-streptomycin.

### **2.1.3. Crystal Violet Staining.**

Cells were stained with crystal violet to determine a) cell number changes and b) to analyse morphology. Prior to staining, the culture medium was removed, and cells washed with distilled water followed by incubation with 0.2% crystal violet (0.2g crystal violet in 100 ml methanol) for 20 minutes. Excess crystal violet was washed off with distilled water and the plate allowed to air dry overnight. This was followed by solubilisation of crystal violet with 1% sodium dodecyl sulfate (SDS) for one hour. The absorbance of the solubilised crystal violet was measured at 595 nm using the Versmax Microplate Reader.

### **2.1.4. Analysis of cell number.**

To establish a standard curve for analysis of cell number, 10, 20, 40, and 80 x10<sup>3</sup> myoblast cells or 25, 50, 100 and 200 x10<sup>3</sup> fibroblasts, myofibroblasts and macrophages were plated in 24-well plates in SCM (carried out in triplicates) (Feoktistova, *et al.*, 2016; Venter and Niesler, 2019). The cells were incubated for 4 hours to allow adherence to the culture plate followed by staining with crystal violet as described above. Resulting standard curves are shown in Figure 6. (Fewer cells were used in the construction of the myoblast standard curve as myoblasts are larger in size than fibroblasts and macrophages as well as have a shorter doubling time. Hence, a plateau was reached faster when more cells were used, which produced an inaccurate standard curve.)

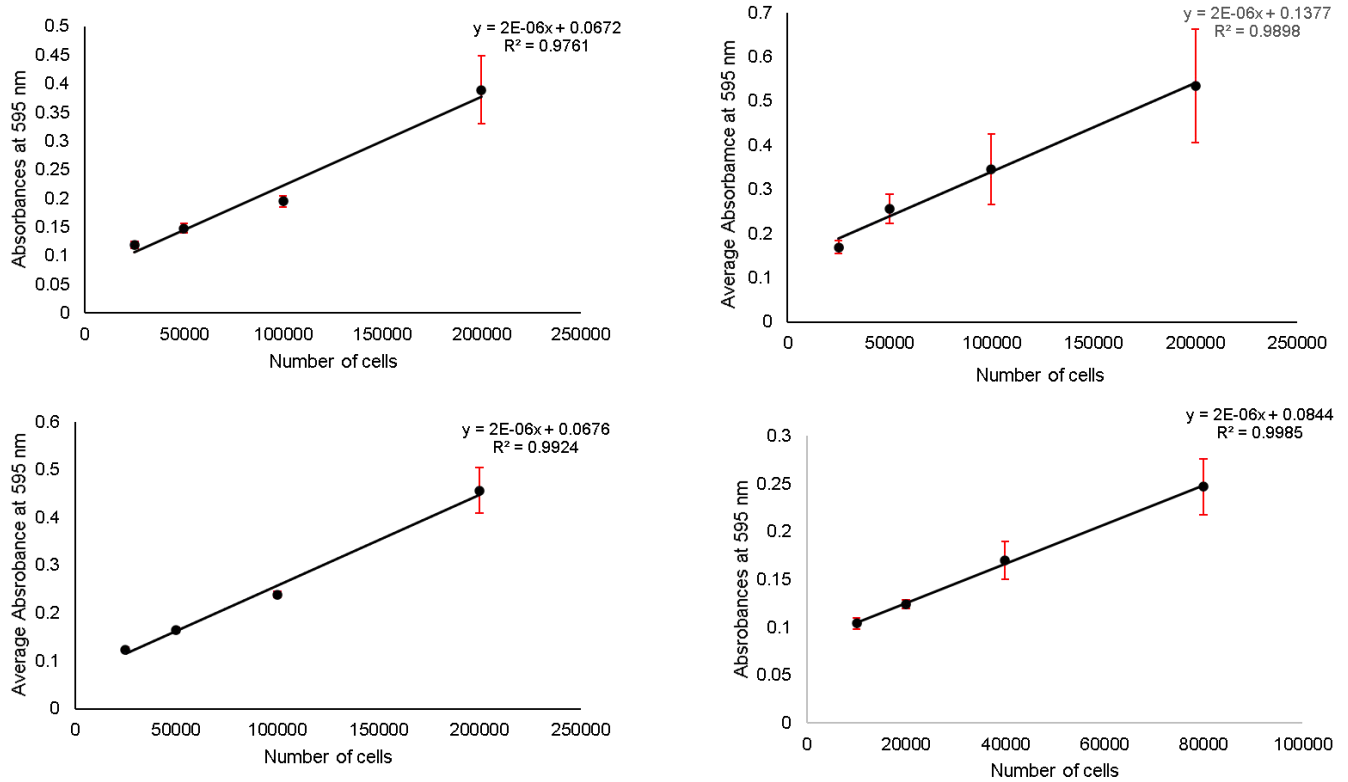


**Figure 6: Standard curve representing increasing numbers of cells stained with crystal violet. (A) Myofibroblasts, (B) Fibroblasts, (C) Macrophages and (D) Myoblasts.** All standard curves show a linear relationship between number of cells and absorbance at 595 nm. The standard curve equations and correlation coefficients for each graph are: (A)  $y=2*10^{-06}x+0.0672$  and  $R^2=0.992$ , respectively, (B)  $y=2*10^{-06}x+0.1377$  and  $R^2=0.9898$ , respectively, (C)  $y=2*10^{-06}x+0.0676$  and  $R^2=0.976$ , respectively and (D)  $y=2*10^{-06}x+0.0844$  and  $R^2=0.999$ , respectively. Data are represented as Mean  $\pm$  Standard Error of the Mean (SEM). Data for standard curves represents triplicates. A blank (zero) was not used for the absorbance readings, hence the graph does not intersect at the origin (0;0).

### 2.1.5. Analysis of cell circularity.

After cells were stained with crystal violet, images were visualized and captured with an Olympus CKX41 microscope (Olympus Corporation, Tokyo, Japan) and a Motic 3.0-megapixel camera (10x objective lens; three fields of view per replicate; four replicates per experiment) (Motic, Kowloon, Hong Kong). Morphology was quantitatively analysed by assessing cell circularity using ImageJ software and a macro created by Venter *et al.* (2021) to determine the circularity of the cells, where a value between 0 and 1 were assigned to indicate cells that are irregularly shaped or perfectly circular, respectively (Figure 7).

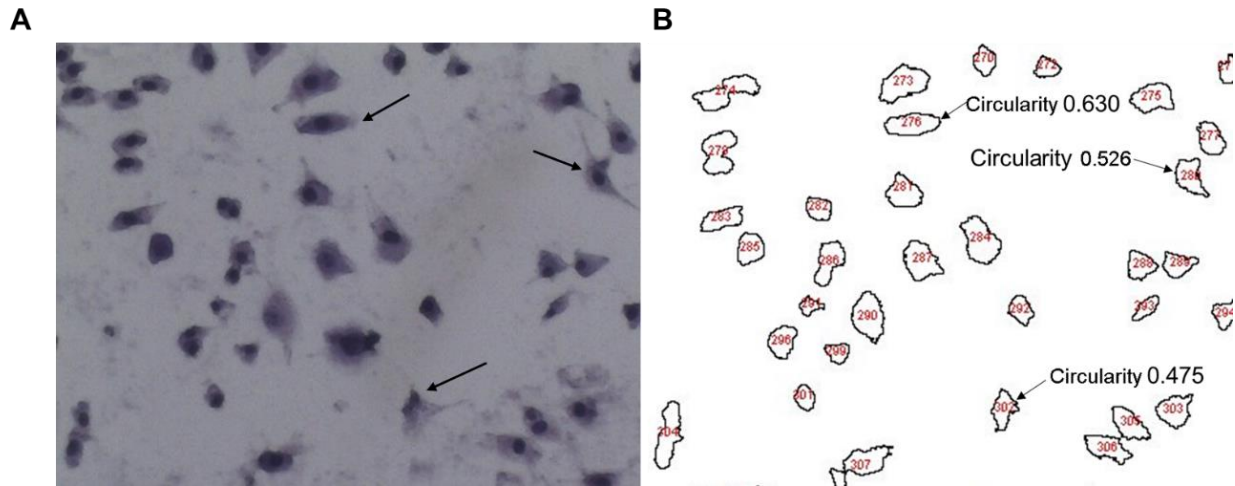


**Figure 7:** Image of (A) Crystal violet stained L929 cells whose (B) cell morphology was assessed using ImageJ. Cell circularity is indicated for three cells. The rounder the cell, the higher the circularity value (i.e., closer to 1).

## 2.1.6. Immunocytochemistry and fluorescence microscopy.

### 2.1.6.1. Detection of $\alpha$ -SMA.

Cells were washed once with PBS and then fixed using a 4% (v/v) paraformaldehyde solution for 10 minutes. Subsequently, cells were washed once with PBS and then permeabilised with 0.3% (v/v) Triton X-100 for 10 minutes. Donkey serum (5% (v/v), Sigma, Cat. D9663) was added as a blocking agent for 30 minutes, followed by incubation with the primary antibody (monoclonal mouse anti- $\alpha$ -smooth muscle actin;  $\alpha$ -SMA; 1:1000; Sigma, Cat. A 2547) for 2 hours at room temperature thereafter incubated with the secondary antibody (Dylight 594-conjugated donkey anti-mouse antibody; 1:1000; Jackson ImmunoResearch, Cat. 715-515-151, Newmarket, Suffolk, UK) for 2 hours at room temperature in the dark, washing cells twice with PBS between each step. Cells were then processed as described in 2.1.6.4. below.

### 2.1.6.2. Detection of CD86.

Cells were washed once with PBS and then fixed with a 4% (v/v) paraformaldehyde solution for 30 minutes. Thereafter cells were washed with PBS followed by incubation with the primary antibody (PE-conjugated rat anti-CD86; 1:200; BioLegend, Cat. 105008) overnight at 4°C. Cells were then processed as described in 2.1.6.4. below.

### **2.1.6.3. Detection of Arginase.**

Cells were washed once with PBS and then fixed with a 4% (v/v) paraformaldehyde solution for 10 minutes. Subsequently, cells were washed once with PBS and then permeabilised with 0.3% (v/v) Triton X-100 for 10 minutes. Donkey serum was added as a blocking agent for 30 minutes, followed by incubation with the primary antibody (mouse anti-arginase-1 E-2; 1:500, Santa Cruz Biotechnology Inc, Cat. Sc-271430, Dallas, TX, USA) for 2 hours at room temperature. Cells were incubated with the secondary antibody (Dylight 488-conjugated donkey anti-mouse antibody; 1:2000; Jackson ImmunoResearch, Cat. 715-485- 151) overnight at 4°C. Cells were then processed as described in 2.1.6.4. below.

### **2.1.6.4. Staining of nuclei, mounting of coverslips and fluorescent viewing.**

The nuclei were stained with Hoechst 33342 (1:100, stock 10 mg/ml; Sigma, Cat. B2261) for 10 minutes and then washed three times with PBS before being mounted on glass slides with 10% Mowiol (Sigma, Cat. 81381). The cells were viewed, and images captured with the Olympus Florescence Microscope (20x objective). PBS was used as a diluent throughout.

### **2.1.7. Determining fluorescence intensity.**

The intensity of the fluorescence was measured by using ImageJ in which the corrected total cell fluorescence (CTCF) was then calculated for 10 cells in each image and averaged (El-Sharkawey, 2016). Using the selection/drawing tools in ImageJ, the perimeter of the cell of interest was selected as follows: from the set measurements menu, select area, integrated density and mean gray value option (*Analyse → Set Measurements → Select Area/Integrated density/Mean gray value*). Thereafter, quantify (*Analyse → Measure*) and insert values into the equation used to calculate CTCF (to get the mean gray value, select an area around the cell that has no fluorescence, this will be the mean background fluorescence):

$$\text{CTCF} = \text{Integrated Density of cell} - (\text{area of cell} * \text{mean background fluorescence}).$$



### 2.1.8. *In vitro* wound healing assay.

The scratch assay was performed as described by Louis *et al.* (2008) and Goetsch *et al.* (2011) with changes, in which a gel loading tip was used to physically remove cells from the centre of the confluent monolayer in the centre of the well, thus, creating a “wound” (Figure 8); 500 µl SCM was then added. The cultures were incubated for 7 hours, and images were taken at 0, 3, 5 and 7 hours using the Olympus CKX41 microscope and a Motic 3.0-megapixel camera (4x objective). The wound edges were manually selected, and wound area automatically calculated using the Motic Images Plus 2.0 ML software. Percent wound closure was calculated using the equation:

$$\%Wound\ closure = \frac{(Area\ of\ wound\ at\ 0\ hour - Area\ of\ wound\ at\ x\ hour)}{Area\ of\ Wound\ at\ 0\ hour} \times 100$$

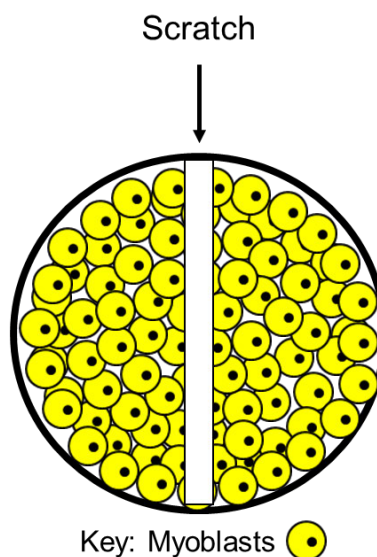


**Figure 8: Schematic representation of scratch assay within a well.** A “wound” is created in the center of the well using gel loading tips to physically remove a monolayer of the confluent cells.

### 2.2. Dedifferentiation of myofibroblasts to fibroblasts

To establish both fibroblast and myofibroblast cultures *in vitro*, L929 cells were plated (in quadruplicate, n=1) and cultured in SFM or SCM as described below (Figure 9).

- SCM:  $10 \times 10^3$  myofibroblasts cells were cultured in the presence of SCM for three days.

- SFM:  $20 \times 10^3$  and  $40 \times 10^3$  myofibroblasts cells were cultured in the presence of SCM and allowed to adhere for four hours. After four hours, the SCM medium was changed to SFM. The wells containing  $40 \times 10^3$  cells were incubated for three days, whereas those containing  $20 \times 10^3$  cells were incubated for six days.

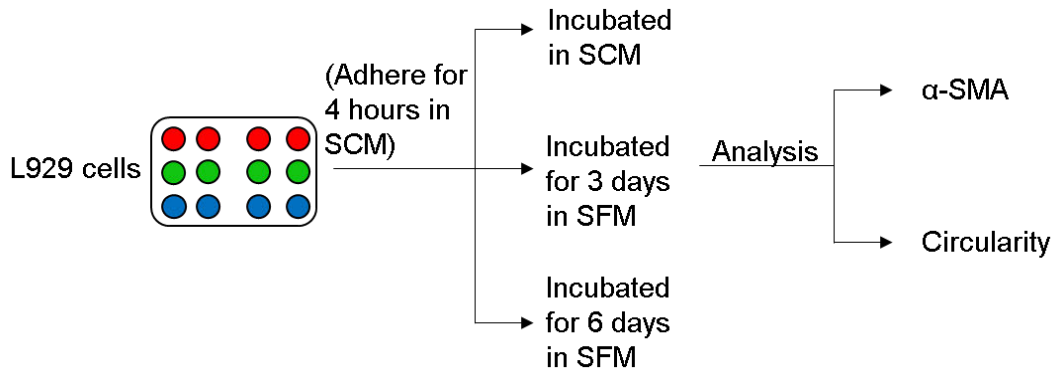


**Figure 9: Schematic representation of L929 dedifferentiation in SFM.** Using 12-well plates, L929 cells were plated out in quadruplicate. The cells adhered for 4 hours, followed by change in medium to serum-free medium (SFM) in two plates and were incubated for either 3 days or 6 days. The results were then analysed by either detection of  $\alpha$ -SMA or analysis of cell circularity. (NB: Red =  $10 \times 10^3$  cells in serum-containing medium (SCM), Green =  $40 \times 10^3$  cells in SFM for 3 days, and Blue =  $20 \times 10^3$  cells in SFM for 6 days).

Different cell numbers were plated for the SCM and SFM treated cells to account for absence of growth promoting serum in SFM and ensure that the cells became equally confluent. Detection of  $\alpha$ -SMA (expressed in myofibroblasts) by immunocytochemistry and fluorescence microscopy as well as the analysis of the circularity of the cell was used to confirm the change from a myofibroblast to a fibroblast phenotype.

### 2.2.1. Effect of sodium orthovanadate on expression of $\alpha$ -SMA in fibroblasts.

When fibroblasts are cultured in SCM for 24 hours or longer, they differentiate to myofibroblasts. To assess whether vanadate hinders this differentiation, fibroblasts were incubated with and without vanadate ( $10 \mu\text{M}$ ) for 16 hours and then in SCM for 7 hours, after which immunocytochemistry and fluorescence microscopy and cell circularity was used to determine the resulting phenotype (Figure 10). These different time frames and culture conditions are used as they emulate the culture conditions during the co-culture assays. These

were important to ascertain which phenotype was present at the start and finish of the wound healing assays. The assays were carried out in triplicates (n=1)

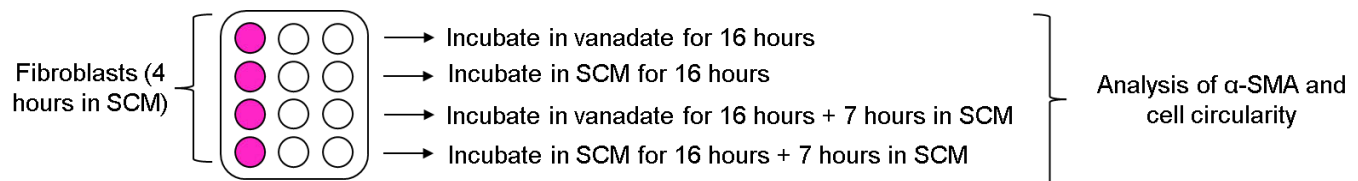


**Figure 10: Schematic representation for fibroblasts treated with vanadate.** Fibroblasts were plated out. Cells were either treated with 10  $\mu$ M sodium orthovanadate (in SCM) or just SCM for 16 hours, followed by incubation in serum-containing medium (SCM) for 7 hours.

### 2.3. Using LPS and IL-4 to establish M1 and M2 phenotypes, respectively:

#### 2.3.1.M1 phenotype

J774A.1 macrophages ( $50 \times 10^3$  cells) were plated in SCM into 12-well plates and treated as follows with LPS (0.1  $\mu$ g/ml) to polarise cells to the M1 phenotype (Venter, *et al.*, 2021) (Figure 11A):

- 24 hours in LPS
- 24 hours in LPS followed by 24 hours in SCM alone
- 24 hours in LPS followed by 4 hours in SCM alone and then 16 hours in vanadate + SCM
- 24 hours in LPS followed by 4 hours in SCM alone, 16 hours in vanadate and 24 hours in SCM alone

Thereafter, the presence of CD86 (M1 macrophage cell surface marker) was detected by immunocytochemistry and fluorescence microscopy.

### **2.3.2. M2 phenotype**

J774A.1 macrophages ( $50 \times 10^3$  cells) were plated in SCM into 12-well plates and treated as follows with IL-4 (0.1  $\mu\text{g/ml}$ ) to polarise cells to the M2 phenotype (Lin and Hu, 2017):

- 48 hours in IL-4
- 48 hours in IL4 and 24 hours in SCM alone
- 48 hours in IL4, 4 hours in SCM alone and 16 hours in vanadate
- 48 hours in IL4, 4 hours in SCM alone, 16 hours in vanadate and 24 hours in SCM alone

Thereafter, the presence of arginase (M2 macrophage marker) (Figure 11B) was detected by immunocytochemistry and fluorescence microscopy. The presence of CD86 (Figure 11C) was also determined on the cells treated with IL-4 to determine whether the M1 macrophage phenotype persists.

A range of culture conditions were used to mimic the environment of the cells during co-culture and wound healing assays. These serve to determine whether macrophages remain in the polarised states during different assay conditions.

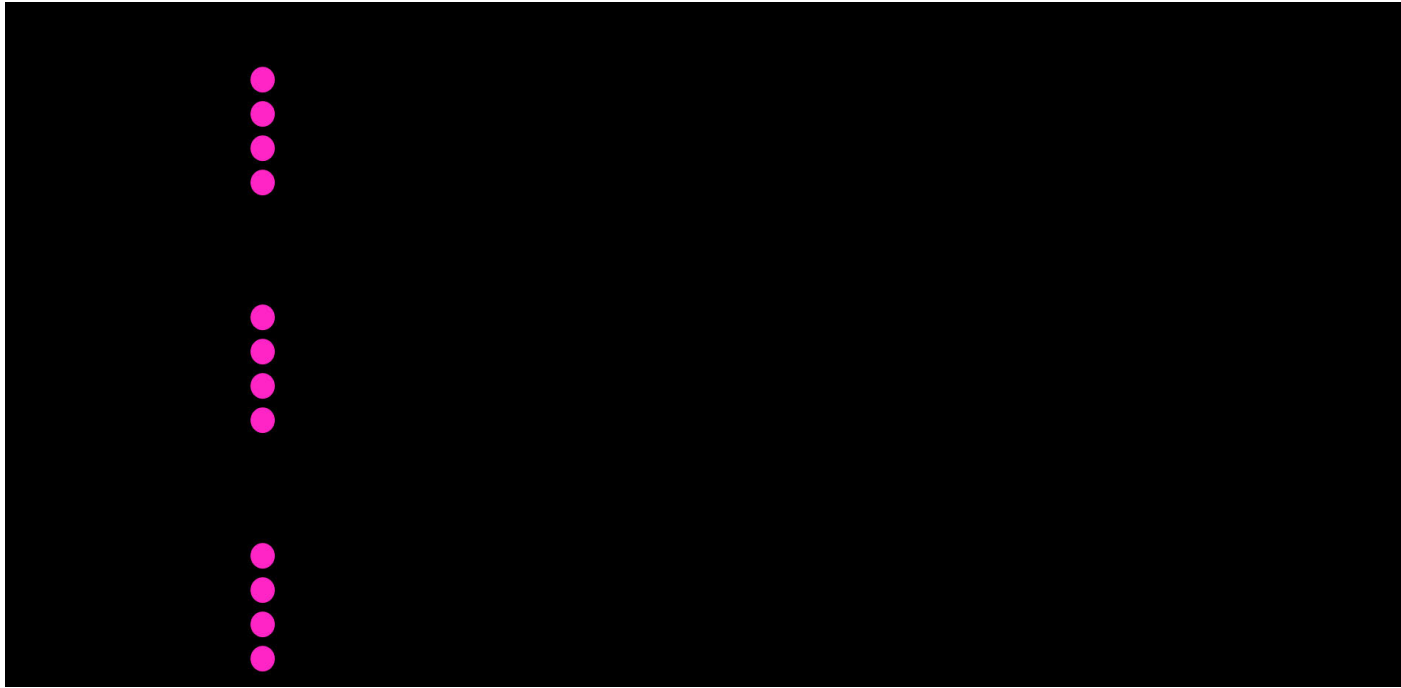


**Figure 11: Schematic representation of macrophages treated with LPS (0.1 µg/ml) and IL-4 (0.1 µg/ml) in serum-containing medium (SCM).** Macrophages were plated out on 12-well plates and treated with either LPS (0.1 µg/ml) for 24 hours or IL-4 (0.1 µg/ml) for 48 hours, followed by treatments in either 24 hours in SCM, 4 hours in SCM and 16 hours in vanadate or 4 hours in SCM, 16 hours in vanadate and 24 hours in SCM. Cells were then treated with anti-CD86 or/and anti-arginase antibodies to detect CD86 (M1 macrophages) and Arginase (M2 macrophages).

## 2.4. Double and Triple Co-cultures

### 2.4.1. Double Co-Culture.

Co-cultures were carried out (in triplicate and each experiment repeated six times) as described by Venter, *et al.* (2018) with amendments (Figure 12). J774A.1/L929/C2C12 cells ( $40 \times 10^3$  cells) were plated at the edge of a well in a 24 well plate in a volume of SCM that did not exceed 100 µl. A centrifugal force was applied to the plate by rotating the plate in a circular motion to allow for the distribution and attachment of the cells to the outer edge of the wells. The cells were allowed to adhere by incubation for one hour. Subsequently, C2C12/L929 cells ( $160 \times 10^3$  cells) were plated in the centre of the well in a volume of SCM not exceeding 500 µl (Figure 12). Cells were allowed to adhere for 4 hours, followed by incubation with either vanadate (10 µM) for 16 hours in the presence of fibroblasts or LPS (0.1 µg/ml) for 24 hours in the presence of M1 macrophages. This is followed by *in vitro* wound healing assay.

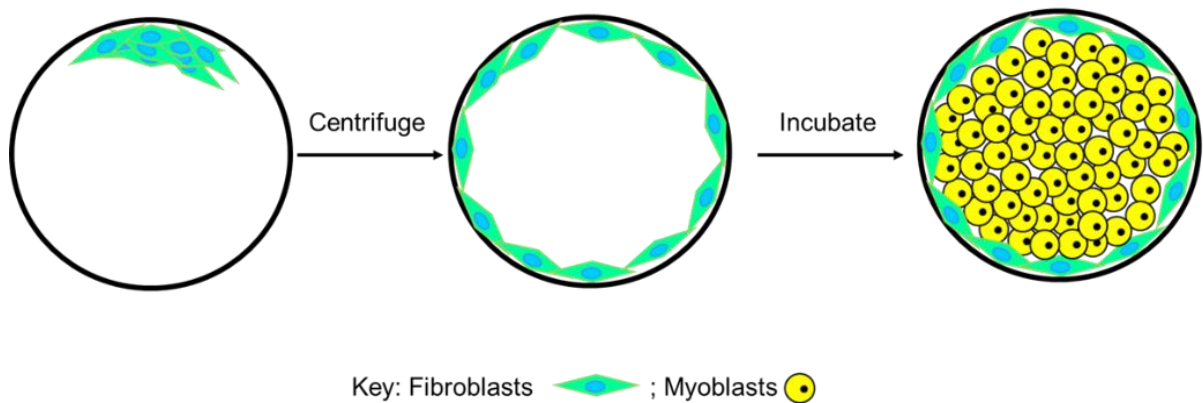


**Figure 12: Schematic representation of plating double co-cultures containing either fibroblasts or myofibroblasts with myoblasts.** The fibroblast or myofibroblast populations were plated on the edge of a well in a 24-well plate and plate briefly swirled to allow cells to adhere to edge of the well. Myoblast cells were plated in the centre of the well. Cells were incubated for 16 hours to allow myoblast cells to reach confluence, thereafter, followed by a scratch assay to analyse the cell migration.

#### 2.4.2. Triple Co-Culture.

Triple co-cultures were performed (in triplicate and each experiment repeated six times) as described by Venter, *et al.* (2018) with amendments (Figure 13). L929 cells ( $40 \times 10^3$  cells) and J774A.1 cells ( $40 \times 10^3$  cells) were plated at the edge of a well in a 24 well plate in a volume of SCM that did not exceed  $100 \mu\text{l}$ . A centrifugal force was applied to the plate by rotating the plate in a circular motion to allow for the distribution and attachment of the cells to the outer edge of the wells. The cells were allowed to adhere by incubation for one hour. Subsequently, myoblasts ( $90 \times 10^3$  cells) were plated in the centre of the well in a volume of SCM not exceeding. Cells were allowed to adhere for 4 hours, followed by incubation with vanadate ( $10 \mu\text{M}$ ) for 16 hours in the presence of fibroblasts. This was followed by *in vitro* wound healing assay.

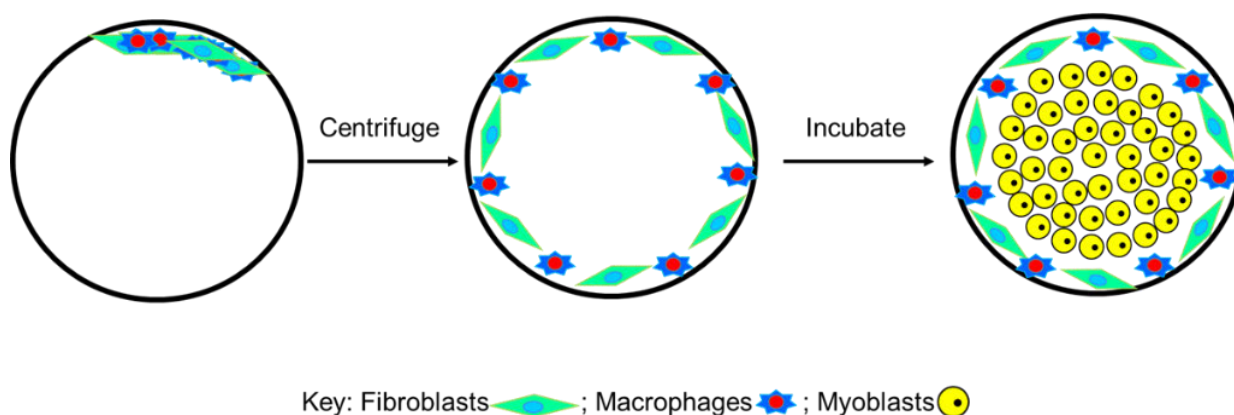


**Figure 13: Schematic representation of plating triple co-cultures containing M1 macrophages and either fibroblasts or myofibroblasts and myoblasts.** Fibroblasts and macrophages were plated on the edge of a well in a 24-well plate in a volume of SCM not exceeding 100  $\mu$ l. The plate was briefly swirled to allow cells to adhere to edge of the well. Myoblast cells were plated in the centre of the well. Cells were incubated for 16 hours to allow myoblast cells to reach confluence, thereafter, followed by a scratch assay to analyse the cell migration.

## 2.5. Statistical analysis.

Results were analysed using either/or one-Way ANOVA, two-Way ANOVA or three-Way ANOVA test using GraphPad Prism (developed by GraphPad Software Inc., version 9.3.1.). Data with values of  $p < 0.05$  were deemed to be statistically significant. All data was represented as Mean  $\pm$  SEM.

### **3. Results**

#### **3.1. Establishment of Phenotypes**

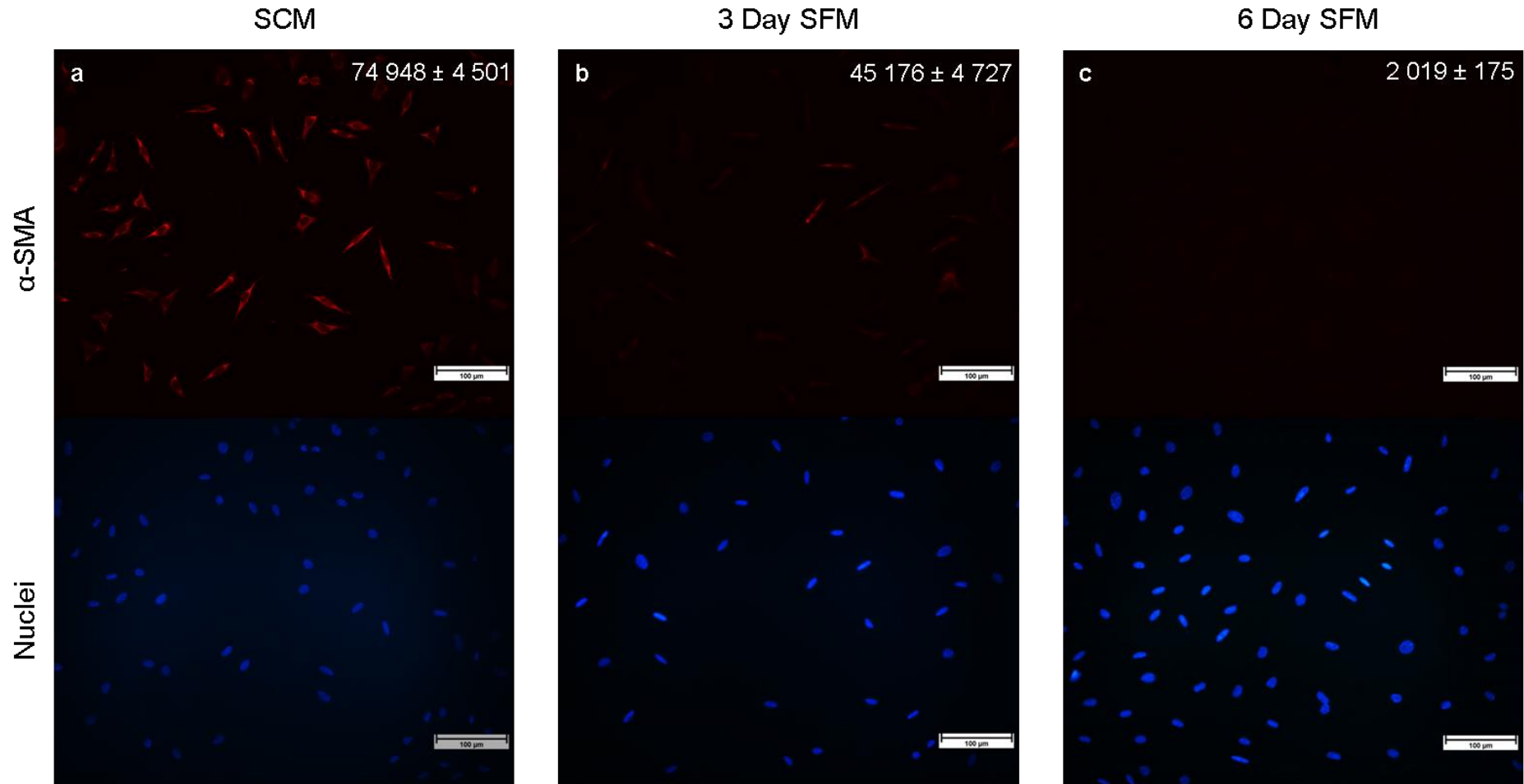
##### **3.1.1. Establishment of dedifferentiated fibroblast cultures.**

When fibroblasts are cultured in SCM, it differentiates into myofibroblasts, hence under standard culture conditions, there are predominantly myofibroblasts present. Given our interest in analysing the effect of fibroblasts versus myofibroblasts on myoblast wound closure, we sought to first establish a method to dedifferentiate myofibroblasts in culture and thereby establish distinct populations of fibroblasts and myofibroblasts.

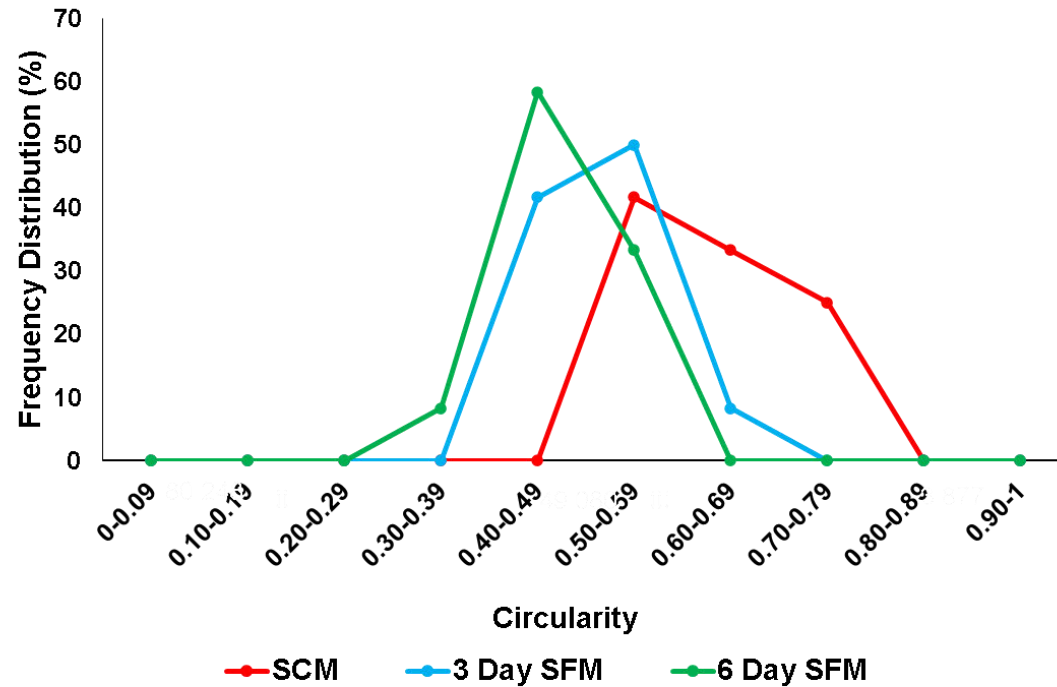
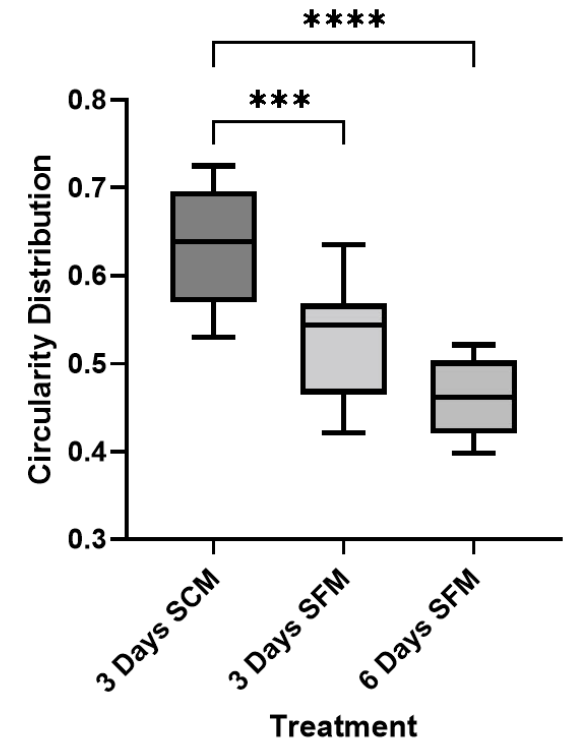
The use of immunocytochemistry and fluorescence microscopy, to evaluate the expression of  $\alpha$ -SMA, indicated that when the myofibroblasts were incubated in the absence of serum, there was a time-dependent loss of expression of  $\alpha$ -SMA (Figure 14). L929 cells cultured in SCM had the brightest fluorescence with a mean CTCF value of  $74\,948 \pm 4\,501$  per cell; the abundant expression of  $\alpha$ -SMA indicated the presence of myofibroblasts (Figure 14a). Thereafter, fluorescence got progressively weaker having a mean CTCF value of  $45\,176 \pm 4\,727$  per cell at day 3 (Figure 14b), which suggests that the cells are transitioning through the transient protomyofibroblast stage. Cells cultured for six days in SFM, showed little to no fluorescence with a mean CTCF value of  $2\,019 \pm 175$  per cell, which indicates that cells have dedifferentiated from myofibroblasts to fibroblasts, hence no longer express  $\alpha$ -SMA (Figure 14c).

Cells cultured in SCM or SFM for either 3 days or 6 days were then further characterised via analysis of morphology to determine circularity during dedifferentiation (Figure 15). A shift in the circularity was observed (Figure 15A), such that the median circularity changed from 0.639 to 0.544 to 0.462 (Figure 15B, Table 1). The interquartile range for each phenotype shows that the distribution of cell circularity for cells cultured for 3 days in SFM and 6 days in SFM is significantly distinct from those cultured for 3 days in SCM. Fifty percent of the myofibroblast population displays a cell circularity distribution of 0.570-0.696, whereas 50% of the protomyofibroblast population displays a cell circularity distribution of 0.465-0.569 and 50% of the fibroblast population displays a cell circularity distribution of 0.420-0.504 (Figure 15B, Table 1). Therefore, the cells cultured for 3 days in SCM (myofibroblasts) which have a rounder shape, significantly changed to a more elongated shape when cultured in SFM for 6 days (fibroblasts).





**Figure 14: Dedifferentiation of myofibroblasts to fibroblasts when cultured in serum-containing medium (SCM) or serum-free medium (SFM) for either 3 or 6 days showing the change in expression of  $\alpha$ -SMA.** Cells were immunostained with monoclonal mouse anti- $\alpha$ -SMA followed by Dylight 594-conjugated donkey anti-mouse antibody (red). The nuclei were stained with Hoechst 33342 (blue). The images were captured using the Olympus Fluorescence Microscope at 20x objective (scale bar: 100  $\mu$ m). CTCF values were calculated and averaged for 10 cells. The mean CTCF value per cell  $\pm$  SEM is indicated in the top right corner.

**A****B**

**Figure 15: Dedifferentiation of myofibroblasts to fibroblasts when cultured in SFM for either 3 or 6 days showing the shift in cell circularity. (A)** To establish a population of fibroblasts, myofibroblasts were cultured in SFM for either 3 or 6 days followed by staining with crystal violet and images were captured with an Olympus CKX41 microscope coupled to a Motic 3.0-megapixel camera (10x objective) thereafter ImageJ was used to analyse the cell circularity. **(B)** Box and Whisker diagram showing the interquartile range for the distribution of cell circularity. \*\*\* $p=0.0003$ . \*\*\*\* $p<0.0001$

**Table 1: Interquartile data ranges for the circularity data for the dedifferentiation of myofibroblasts to fibroblasts**

	3 Days SCM	3 Days SFM	6 Days SFM
<b>Q1</b>	0.570	0.465	0.420
<b>Q2 (Median)</b>	0.639 Myofibroblast	0.544 Protomyofibroblasts	0.462 Fibroblast
<b>Q3</b>	0.670	0.569	0.504

Circularity for cells cultured for 3 days in SCM were calculated over 890 cells and have a median circularity of 0.639 (red) and a cell circularity distribution of 0.570-0.670, can be referred to as myofibroblasts. Circularity of cells cultured for 3 days in SFM were calculated over 730 cells have a median circularity of 0.544 (blue) and a cell circularity distribution of 0.465-0.569, can be referred to as protomyofibroblasts. Circularity of cells cultured for 6 days in SFM were calculated over 708 cells and have a median circularity of 0.462 (green) and a cell circularity distribution of 0.420-0.504, can be referred to as fibroblasts. Difference in cell numbers is attributed to different culture conditions, i.e.: cells grow faster in the presence of serum. (n=1, used 4 pictures each from 3 wells).

### 3.1.2. Vanadate suppresses the expression of $\alpha$ -SMA.

Given that many subsequent assays were to be carried out in the presence of serum, it was important to determine how long fibroblasts would maintain an undifferentiated phenotype in the presence of SCM. Fibroblasts were therefore cultured in SCM for 16 hours and 23 hours, followed by analysis of  $\alpha$ -SMA expression. The difference in cell numbers analysed from one panel to the next is due to pictures being taken from different areas within the wells for each treatment and is not an indication of cell death. It was observed that  $\alpha$ -SMA re-expression was underway following 16 hours incubation in SCM suggesting that the fibroblasts begin to differentiate back to the myofibroblast phenotype between 16 – 24 hours once exposed to SCM (Figure 16). As expected, myofibroblasts (incubated in SCM alone) abundantly express  $\alpha$ -SMA (Figure 16a) with a mean CTCF value of  $95\,919 \pm 7\,630$  per cell. Fibroblasts, incubated in SFM for 6 days, (Figure 16b) demonstrated little expression of  $\alpha$ -SMA with a mean CTCF value of  $2\,577 \pm 306$  per cell. When fibroblasts were incubated in SCM for 16 hours (Figure 16c), an increase in mean CTCF value  $19\,762 \pm 1\,217$  per cell, was recorded, suggesting an increase in  $\alpha$ -SMA expression. The mean CTCF value increased further to  $29\,788 \pm 3\,974$  per cell by 23 hours in SCM (Figure 16d), but had not reached levels seen in myofibroblasts, suggesting that the transitory protomyofibroblast phase was underway.

Vanadate was then introduced to delay  $\alpha$ -SMA expression and maintain the fibroblast phenotype in the presence of SCM. Cells incubated for 16 hours in SCM + vanadate

demonstrated a decreased mean CTCF value ( $5\,961 \pm 850$  per cell) as compared to cells that were incubated in SCM alone for 16 hours (mean CTCF value of  $19\,762 \pm 1\,217$  per cell). Cells that were incubated in SCM + vanadate for 16 hours followed by SCM alone for 7 hours (to mimic the conditions of the scratch assay during wound healing) had a mean CTCF value of  $17\,143 \pm 1\,201$  per cell. Vanadate was therefore able to restrict the re-expression of  $\alpha$ -SMA in the presence of SCM, suggesting retention of the fibroblast phenotype at the start of the scratch assay (16 hours in SCM + vanadate). However, after cells were returned to SCM alone, by 7 hours (which would coincide with the end of the scratch assay) the transition to protomyofibroblasts was underway.

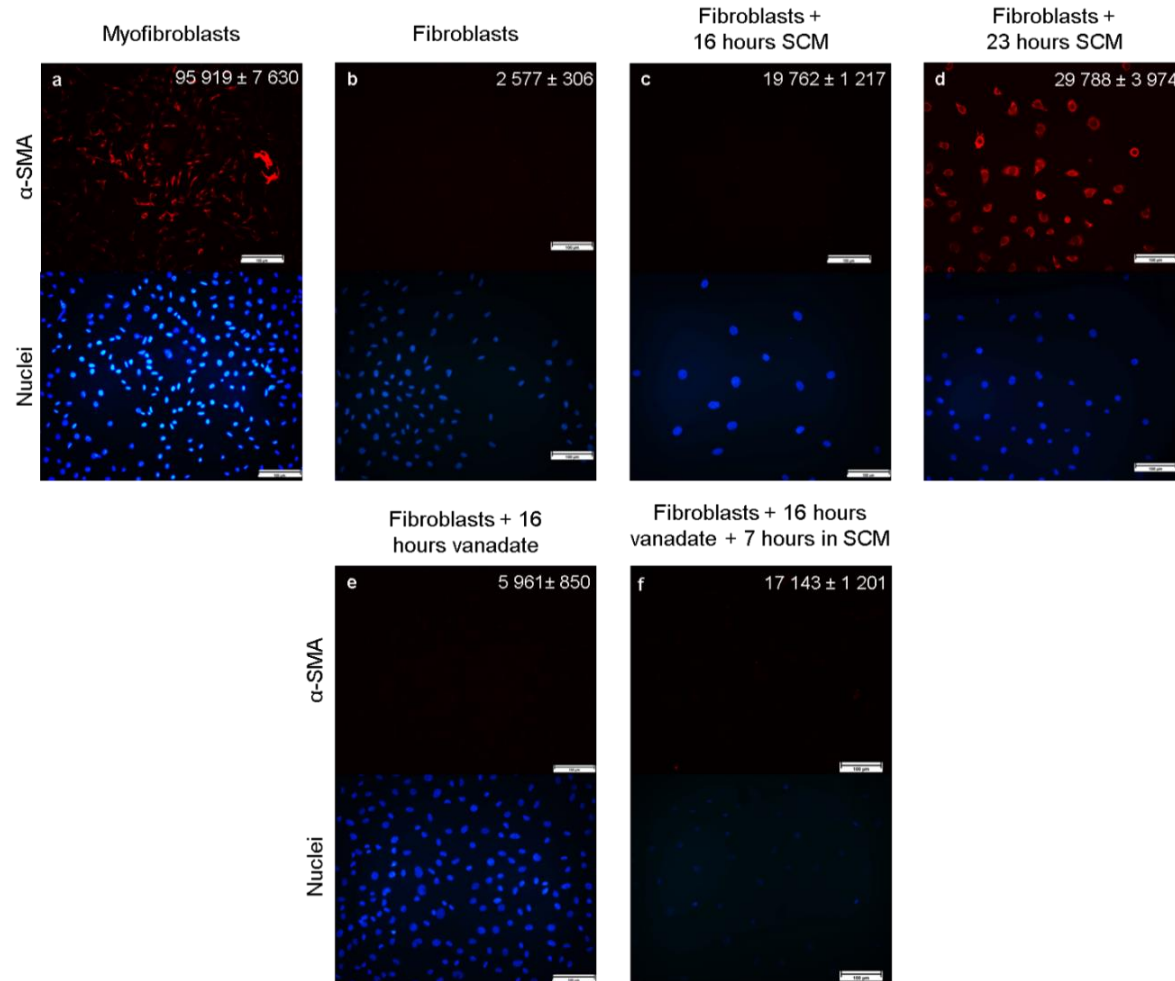


**Figure 16:** L292 cells were incubated for (A) 3 days in SCM, or (B) 6 days in SFM followed by incubation for (C) 16 hours in SCM, (D) 24 hours SCM, (E) 16 hours in vanadate, and (F) 16 hours in vanadate and 7 hours in SCM. Cells were immunostained with monoclonal mouse anti- $\alpha$ -SMA followed by Dylight 594-conjugated donkey anti-mouse antibody (red). The nuclei were stained with Hoechst 33342 (blue). The images were captured using the Olympus Fluorescence Microscope at 20x objective (scale bar: 100  $\mu$ m). CTCTF values were calculated and averaged for 10 cells. The mean CTCTF value  $\pm$  SEM per cell is indicated in the top right corner.

The circularity of the fibroblasts cultured in vanadate and SCM during the start and end of the wound closure assays were also assessed to determine whether they were still fibroblasts or had begun to differentiate. Fibroblasts cultured for 16 hours in SCM + vanadate, 16 hours in SCM + vanadate followed by 7 hours SCM, 16 hours SCM alone and 24 hours in SCM alone all showed a wide distribution of cell circularity. When fibroblasts were cultured for 16 hours in SCM + vanadate a peak frequency of 33.82% was seen at 0.40-0.49 (Figure 17A) with a median circularity of 0.4 (Figure 17C; Table 2). This indicates that the cells were maintained in the fibroblast phenotype (refer to Table 1). Fibroblasts cultured for 16 hours in SCM + vanadate followed by 7 hours in SCM had a peak frequency of 26.14% at 0.50-0.59 (Figure 17A) with a higher median circularity of 0.489 (Figure 17C; Table 2), indicating that cells had begun to transition through the protomyofibroblast phenotype. By 16 hours in SCM alone, the cells had a peak frequency of 33.08% at 0.50-0.59 (Figure 17B) with a median circularity of 0.480 (Figure 17C; Table 2), whereas those cultured for 23 hours in SCM alone showed a peak frequency of 33.76% at 0.60-0.69 (Figure 17B) with a median circularity of 0.553 (Figure 17C; Table 2). This suggests an increasing shift to the myofibroblast phenotype. This indicates that when fibroblasts are cultured in SCM with vanadate (as they would have been at the start of the wound closure assay) they remain as fibroblasts. Our data also suggests that subsequent exposure to SCM initiated a slow transition via the protomyofibroblast phenotype to the myofibroblast stage.

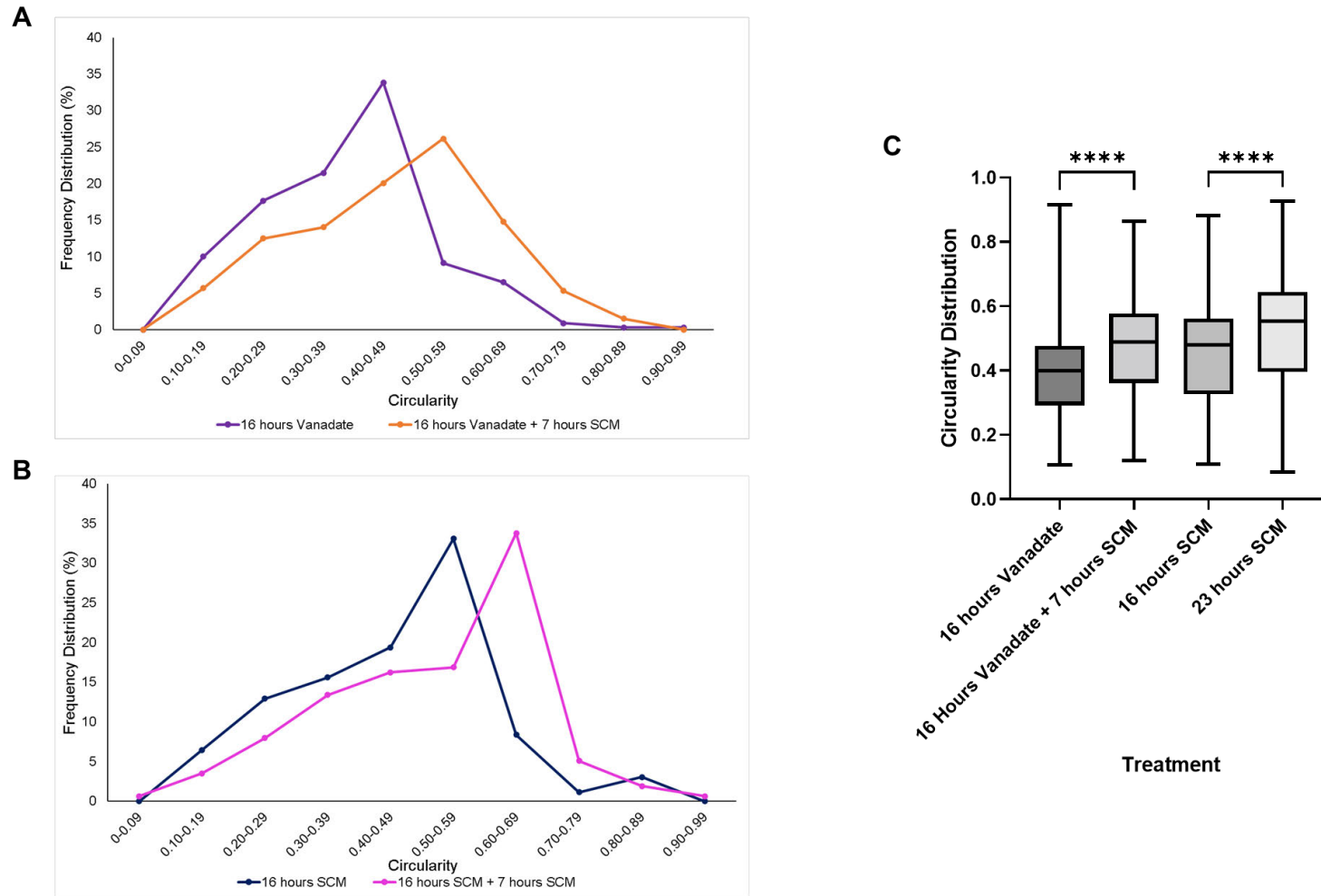


**Figure 17: Shift in fibroblast circularity when cultured with (A) 10  $\mu$ M sodium orthovanadate and (B) SCM at the start and end of the wound closure assays.** Fibroblasts were cultured as per the conditions set during the start and end of the wound closure assays, i.e., cultured for 16 hours in vanadate, 16 hours in vanadate + 7 hours in SCM, 16 hours in SCM, and 23h SCM. This was followed by staining with crystal violet and images were captured with an Olympus CKX41 microscope coupled to a Motic 3.0-megapixel camera (10x objective) thereafter ImageJ was used to analyse the cell circularity. (n=1, 3 wells, 1x picture each) (C) Using ImageJ an average circularity was calculated for each time point. \*\*\*\*p<0.0001.

Comparing the distribution data from Tables 1 and 2, the distribution of fibroblasts (3 days SFM; 0.420-0.504) and fibroblasts cultured for 16 hours in SCM + vanadate (0.292-0.477) have a similar range, hence at the start of the wound closure analysis the cells are in the fibroblast phenotype. The cell circularity distribution between the protomyofibroblasts (3 days SFM; 0.465-0.569) and the fibroblasts cultured for 16 hours in SCM + vanadate and 7 hours in SCM and those cultured for 16 hours in SCM alone, having similar ranges of 0.361-0.577 and 0.327-0.562, respectively. This indicates that these cells are in the protomyofibroblast phenotype. Myofibroblasts cultured for 3 days in SCM, and fibroblasts cultured for 23 hours in SCM only have a similar cell circularity distribution of 0.570-0.670 and 0.396-0.645, respectively, which indicates that fibroblasts cultured for 23 hours in SCM alone are differentiating to the myofibroblast phenotype.

We can therefore consider the cells at the start of the wound assay as undifferentiated fibroblasts (as they are cultured in the presence of vanadate prior to the start of the assay). On the other hand, fibroblasts cultured in SCM for 7-16 hours (in the absence of vanadate) are protomyofibroblasts, while cells cultured in SCM for 23 hours have differentiated to myofibroblasts (Table 2).

**Table 2: Interquartile data ranges for the shift in fibroblast circularity when cultured with 10  $\mu$ M sodium orthovanadate and SCM at the start and end of the wound closure assays.**

	16 hours SCM+ Na <sub>3</sub> VO <sub>4</sub> (Fibroblasts)	16 hours SCM + Na <sub>3</sub> VO <sub>4</sub> + 7 hours SCM alone (Protomyofibroblasts)	16 hours SCM alone (Protomyofibroblasts)	23 hours SCM alone (Myofibroblasts)	
<b>Q1</b>	0.292	0.361	0.327	0.396	<b>Median</b>
<b>Q2</b>	0.400	0.489	0.480	0.553	←
<b>Q3</b>	0.477	0.577	0.562	0.645	

Cell circularity for cells cultured for 16 hours in SCM + Na<sub>3</sub>VO<sub>4</sub> were done using 342 cells and 16 hours in SCM + Na<sub>3</sub>VO<sub>4</sub> + 7 hours in SCM were done using 265 cells, respectively. These indicate the cells at the start and end of wound closure, having a median circularity of 0.400 (purple) and 0.489 (orange), respectively. Cell circularity for cells cultured for 16 hours in SCM and 23 hours in SCM, indicate the cells at the start and end of wound healing analysis, respectively. The median circularity for cells incubated for 16 hours in SCM was 0.480 (blue) by analysing 266 cells, whereas for cells incubated for 23 hours was 0.553 (pink) for 316 cells. The difference in cell numbers is due to the cell culture conditions, i.e.: cells grow faster in SCM with no added reagents.



Sodium orthovanadate is known to affect cell proliferation; as this may affect cell numbers plated during the assay, it was important to determine effects on the relevant cell types (macrophages, myoblasts, myofibroblasts, fibroblasts). Cells (40 000) were incubated with vanadate for 24 hours, followed by analysis of cell number using crystal violet staining. The presence of vanadate positively impacted myofibroblast proliferation whereby the cell number increased to  $247\,400 \pm 63\,382$  cells when in the presence of vanadate as compared to  $185\,233 \pm 85\,333$  cells in the absence of vanadate, however this effect was not significant (Figure 18). Proliferation of fibroblasts was mildly, but not significantly, slower in the presence of vanadate with numbers reaching  $71\,818 \pm 29\,046$  over 24 hours, as opposed to  $89\,150 \pm 17\,898$  cells in the absence of vanadate. When macrophages were cultured in the presence of vanadate, cell numbers were not markedly different at  $50\,867 \pm 7\,259$  in the presence of vanadate compared to  $52\,033 \pm 10\,833$  in the absence of vanadate (Figure 18). Finally, myoblasts cultured in the presence of vanadate showed a decrease in cell number from the 40 000 cells originally plated to  $24\,467 \pm 8\,248$  cells, whilst when in the absence of vanadate cell numbers increased from 40 000 cells to  $41\,800 \pm 7\,024$  cells (Figure 18). This indicates that vanadate has a negative influence on the myoblast cell number, most likely causing death of these cells.

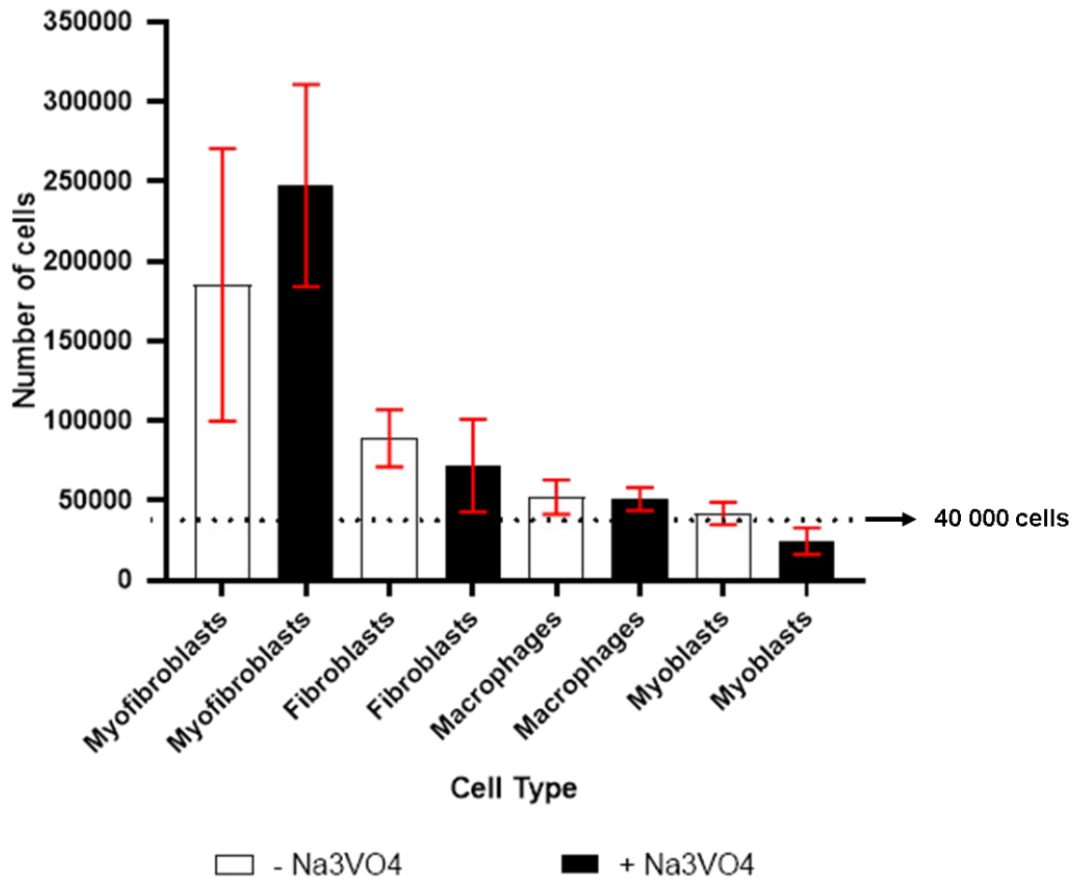


**Figure 18: Effect of 10  $\mu$ M sodium orthovanadate on the cell proliferation of myofibroblasts, fibroblasts, macrophages and myoblasts.** Forty thousand cells were plated out (as indicated on the graph by the dotted line) and were cultured in the presence and absence of vanadate for 24 hours, after which cell proliferation was analysed. Cells were stained with crystal violet followed by solubilisation with 1% SDS. Absorbance was read at 595 nm. The equations of the cell standards for each cell type in Figure 10 were used to calculate the cell numbers after treatment with/without vanadate. Data is represented as Mean  $\pm$  Standard Error of the Mean (SEM); n= 3 (each n in triplicates)

Throughout the wound closure assay, the fibroblasts will therefore begin to differentiate once exposed to SCM in the absence of vanadate. It was unfeasible to continue with the treatment of vanadate throughout the wound healing assays, as the addition of vanadate hindered the growth of myoblasts and negatively affects its' viability. Given the data on  $\alpha$ -SMA expression and circularity, we are confident that at the start of the wound closure assay, fibroblasts (cultured in SCM + vanadate for 16 hours) have retained their phenotype, while those treated subsequently with SCM alone (16 hours) will be referred to as protomyofibroblasts. This labelling convention is used in section 3.2

### 3.1.3. Polarisation to the M1 macrophage phenotype.

J774 macrophages were polarised to the M1 phenotype using LPS. Immunocytochemistry and fluorescence microscopy was used to detect the presence of CD86, a cell surface marker of M1 macrophages. Firstly, it was important to establish whether the cells expressed CD86 prior to incubation with LPS. Cells were observed to display bright fluorescence (mean CTCF value  $68\,288 \pm 5\,131$  per cell; Figure 18a) in the absence of LPS. This suggested that the cells have been polarised to the M1 phenotype. Thereafter cells were incubated with LPS ( $0.1\ \mu\text{g/ml}$ ) and then incubated under the various culture conditions of the assays to discern whether the M1 macrophage phenotype persisted. When the cells are cultured under the following conditions an intensely bright fluorescence was seen: 24 hours in LPS (mean CTCF value of  $81\,039 \pm 5\,970$  per cell; Figure 19b), 24 hours in LPS, 4 hours in SCM and 16 hours in vanadate (mean CTCF value of  $90\,751 \pm 7\,224$  per cell ; Figure 19c), 24 hours in LPS, 4 hours in SCM, 16 hours in vanadate and 24 hours in SCM (mean CTCF value of  $113\,929 \pm 5\,000$  per cell ; Figure 19d), as well as when cultured for 24 hours in LPS and 24 hours in SCM (mean CTCF value of  $95\,522 \pm 6\,571$  per cell; Figure 19e). A control, in which the cells were treated with LPS for 24 hours and then immunostained with arginase 1 (E-2) showed little to no fluorescence, indicating the absence of the M2 phenotype with a mean CTCF value of  $8\,423 \pm 749$  per cell (Figure 19f). The data indicated that the M1 macrophage phenotype was already present prior to LPS incubation and persisted, *potentially to a greater extent* following LPS incubation, and during each of the various culture conditions that will be experienced during the co-culture and wound healing assays. . When the J774A.1 cells were treated with LPS, vs no LPS it can be seen that there is an increase in the CTCF value which is an indication that the LPS activated the macrophages to the M1 phenotype.

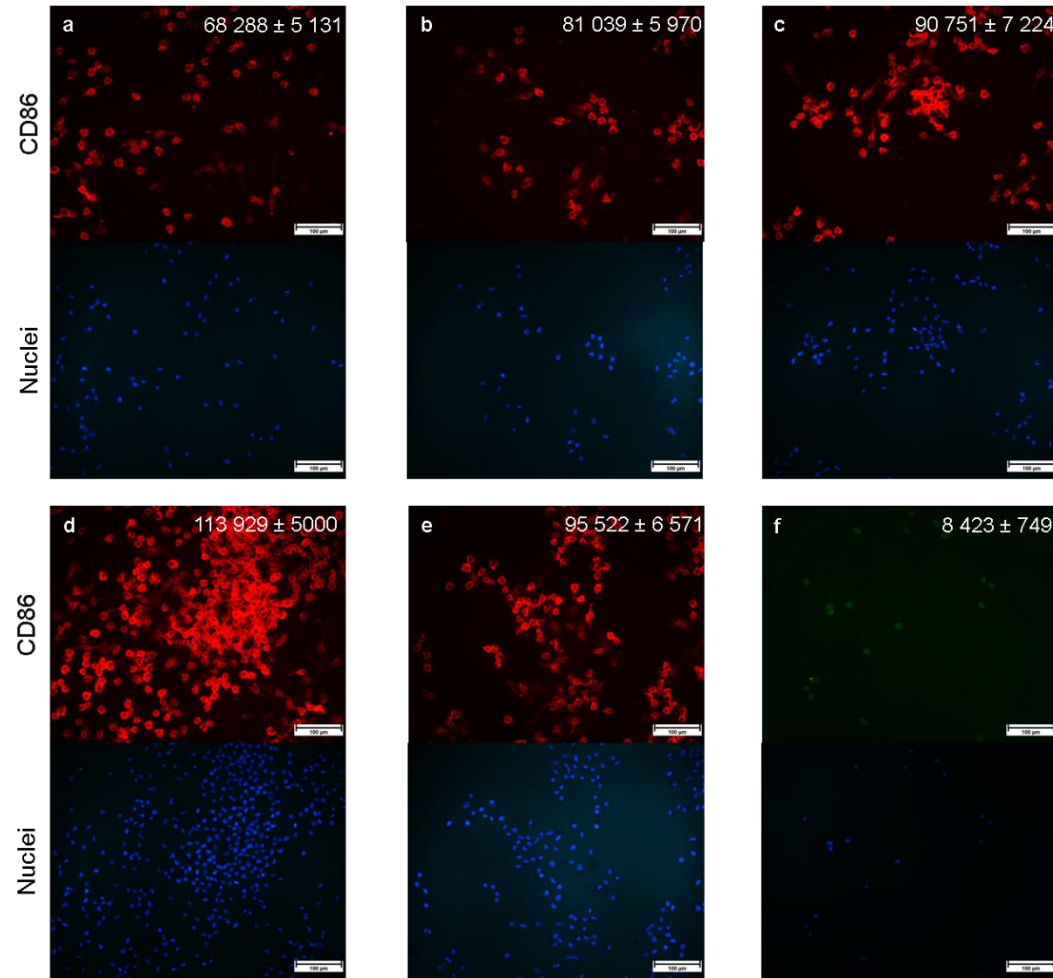


**Figure 19:** J774A.1 macrophages incubated in (A) SCM and (B) 0.1 µg/ml LPS for 24 hours, (C) LPS for 24 hours and 16 hours in vanadate, (D) LPS for 24 hours, 4 hours in SCM and 16 hours in vanadate and 24 hours in SCI(E) LPS for 24 hours, 24 hours in SCM, and immunostained with PE-conjugated rat anti-CD86 (red). (F) J774A.1 macrophages were incubated with LPS for 24 hours and immunostained with arginase 1 (E-2) (green; included to prove lack of M2 polarisation). The nuclei were stained with Hoechst 33342 (blue). The images were captured using the Olympus Fluorescence Microscope at 20x objective (scale bar: 100 µm). CTCF values were calculated and averaged for 10 cells. The mean CTCF value ± SEM per cell is indicated in the top right corner.

### 3.1.4. Polarisation to the M2 macrophage phenotype.

IL-4 has been reported to stimulate the polarisation of macrophages to the M2 phenotype (Lin and Hu, 2017). Therefore, the J774A.1 cells were incubated with IL-4 to stimulate polarisation to the M2 phenotype. Immunocytochemistry and fluorescence microscopy was used to detect the presence of arginase, an enzyme expressed by the M2 phenotype (Orecchioni, *et al.*, 2019). In the absence of IL-4, J774A.1 cells, after being immunostained for arginase, only demonstrated a slight fluorescence, having a mean CTCF value of  $5\,036 \pm 455$  per cell (Figure 20Av). Following a 48 hour incubation with IL-4 (0.1  $\mu\text{g/ml}$ ), J774A.1 macrophages showed very little fluorescence when cultured as follows: (i) 48 hours in IL-4 (mean CTCF value of  $4\,951 \pm 286$  per cell ; Figure 20Ai), (ii) 48 hours in IL-4, 4 hours in GM and 16 hours in vanadate (mean CTCF value of  $8\,683 \pm 898$  per cell ; Figure 20Aii), (iii) 48 hours in IL-4, 4 hours in GM, 16 hours in vanadate and 24 hours in GM (mean CTCF value of  $3\,171 \pm 481$  per cell ; Figure 20Aiii), as well as when cultured for (iv) 48 hours in IL-4 and 24 hours in GM (mean CTCF value of  $7\,673 \pm 705$  per cell; Figure 20Aiv), and stained with mouse anti-arginase 1 (E-2). We therefore concluded that we were not able to successfully establish the M2 phenotype.

Under the same conditions, cells were analysed for expression of CD86 (Fig 20, panel B): cells cultured for (i) 48 hours in IL-4 (mean CTCF value of  $61\,381 \pm 10\,231$  per cell ; Figure 19Bi), (ii) 48 hours in IL-4, 4 hours in GM and 16 hours in vanadate (mean CTCF value of  $12\,110 \pm 1\,073$  per cell ; Figure 19Bii), (iii) 48 hours in IL-4, 4 hours in GM, 16 hours in vanadate and 24 hours in GM (mean CTCF value of  $46\,200 \pm 6\,003$  per cell ; Figure 19Biii), as well as when cultured for (iv) 48 hours in IL-4 and 24 hours in SCM (mean CTCF value of  $87\,852 \pm 8\,931$  per cell ; Figure 19Biv) showed intense fluorescence for the M1 marker. It should also be noted, that when the cells are cultured in IL-4 for 48 hours, 4 hours in GM and then 16 hours in vanadate, the CD86 staining decreased (Figure 19Bii) having a mean CTCF value of  $12\,110 \pm 1\,073$  per cell. This decrease in CD86 expression could be due to the presence of vanadate, however the way in which vanadate suppresses the expression of CD86 is unknown. These cells did not show a noticeable increase in arginase expression (under the same culture conditions) (Figure 19Aii). We concluded that these cells had not been polarised to the M2 phenotype, rather, they remained in an M1 polarised state as indicated by the CD86 fluorescence intensity (Figure 20Biii). The polarisation of the M1 macrophages to the M2 phenotype was therefore unsuccessful, henceforth only the effect of the M1 phenotype on

myoblast wound closure was analysed. Polarisation of M1 macrophage phenotype to the M2 macrophage phenotype proved to be difficult.

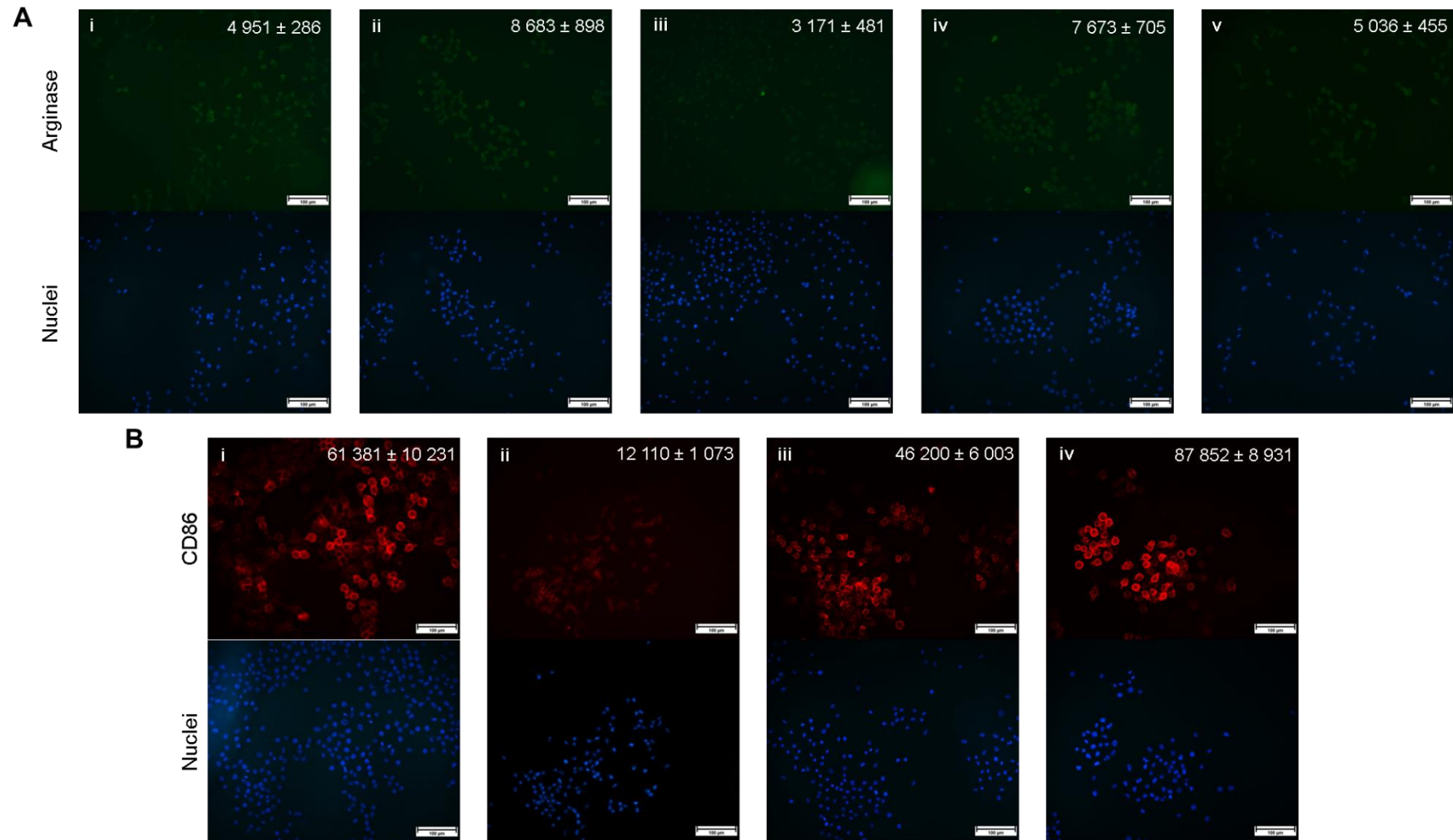


**Figure 20:** J774A.1 macrophages incubated with 0.1 µg/ml IL-4 for (i) 48 hours, (ii) 48 hours, 4 hours in GM and 16 hours in vanadate, (iii) 48 hours, 4 hours in GM, 16 hours in vanadate and 24 hours in GM, (iv) 48 hours and 24 hours in GM and (v) J774A.1 macrophages were in SCM. J774A.1 macrophages were immunostained with (A) anti- arginase 1 (E-2) (green) and (B) PE-conjugated rat anti-CD86 (red). The nuclei were stained with Hoechst 33342 (blue). The images were captured using the Olympus Fluorescence Microscope at 20x objective (scale bar: 100 µm). CTCF values were calculated and averaged for 10 cells. The mean CTCF value ± SEM per cell is indicated in the top right.

## **3.2. Effect of Different Cellular Phenotypes on Wound Closure**

### **3.2.1. Fibroblasts and Myofibroblasts decrease myoblast wound closure.**

To assess the effect of fibroblasts, protomyofibroblasts and myofibroblasts on myoblast wound closure, myoblasts were plated out in the presence or absence of these cells and wound closure assessed over 7 hours. In the absence of other cell types, myoblast wound closure increased from  $18.83\% \pm 3.28\%$  (3 hours), to  $30.97\% \pm 3.89\%$  (5 hours) and  $42.63\% \pm 3.73\%$  (7 hours) (Figure 21B). In the presence of fibroblasts, protomyofibroblasts and myofibroblasts, myoblast wound closure was reduced at 3 hours with wound closure at  $4.78\% \pm 0.63\%$  in the presence of fibroblasts,  $8.75\% \pm 0.92\%$  in the presence of protomyofibroblasts and  $7.82\% \pm 2.25\%$  in the presence of myofibroblasts.

By 5 hours, myoblast wound closure was  $16.56\% \pm 1.19\%$  (in the presence of fibroblasts),  $26.32\% \pm 1.65\%$  (in the presence of protomyofibroblasts) and  $18.69\% \pm 3.91\%$  (in the presence of myofibroblasts), compared with  $30.97\% \pm 3.89\%$  alone; while by 7 hours, myoblast wound closure was  $29.05\% \pm 2.67\%$  (in the presence of fibroblasts),  $39.05\% \pm 2.23\%$  (in the presence of protomyofibroblasts) and  $26.67\% \pm 4.43\%$  (in the presence of myofibroblasts), compared with  $42.63\% \pm 3.73\%$  alone (Figure 21C). This effect was significant at 5 hours when comparing fibroblasts and protomyofibroblasts ( $p < 0.02$ ); and 7 hours when comparing fibroblasts and protomyofibroblasts ( $p < 0.02$ ) and protomyofibroblasts and myofibroblasts ( $p < 0.003$ ). This data suggests that by 7 hours, fibroblasts and myofibroblasts caused a significant decrease in myoblast wound closure, while protomyofibroblasts did not.



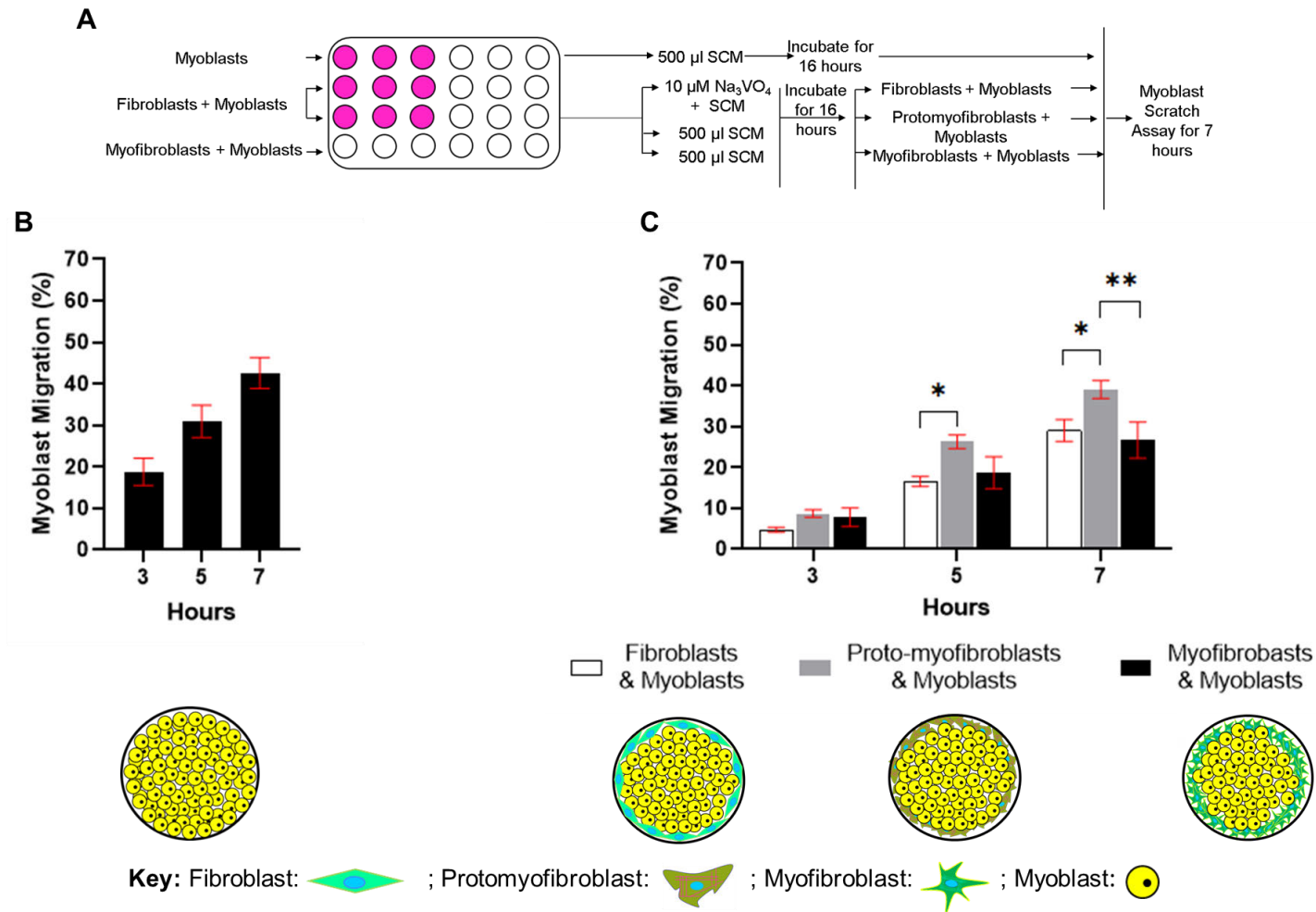


**Figure 21: Myoblast wound closure alone and when co-cultured with the different fibroblast phenotypes.** (A) Myoblasts or double co-cultures (containing myoblasts and the fibroblast phenotypes) were plated and treated, followed by an *in vitro* wound healing assay on the (B) Myoblasts cultures and the (C) Double co-cultures, and wound healing analysed at 3, 5 and 7 hours using the Olympus CKX41 microscope coupled to a Motic 3.0-megapixel camera (4x objective). Data are represented as Mean  $\pm$  Standard Error of the Mean (SEM). Statistical significance is indicated; n=6 (each n in triplicates). \*p<0.02. \*\*p<0.003.

Table 3 summarises the data shown in Figures 21B and 21C. We can see that there is a significant difference in myoblast wound closure when in the presence of fibroblasts and myofibroblasts at 3, 5 and 7 hours. When the myoblasts are co-cultured in the presence of the fibroblasts and myofibroblasts there is a significant decrease in their migration compared to monoculture conditions.

**Table 3: Summary of mean data showing differential significant effect of fibroblast and myofibroblast phenotypes on myoblast wound closure.**

	3 Hours	5 Hours	7 Hours
<b>Myoblasts Alone</b>	~19 %	~31 %	~43 %
<b>Myoblasts + Fibroblasts</b>	↓ ~5 % *	↓ ~17 % *	↓ ~29 % *
<b>Myoblasts + Myofibroblasts</b>	↓ ~8 % **	↓ ~19 % **	↓ ~27 % **

NB: \*p < 0.0114. \*\*p < 0.008 compared with myoblasts alone

The light microscope images show the myoblast wound closure when alone and in the presence of fibroblasts, protomyofibroblasts and myofibroblasts over 7 hours. Myoblast wound closure when cultured alone increased from 18.78% at 3 hours to 38.25% at 7 hours. When cultured in the presence of fibroblasts, protomyofibroblasts and myofibroblasts, myoblast wound closure increased from 4.84%, 8.47% and 5.71% at 3 hours to 37.84%, 36.91% and 25.45% at 7 hours, respectively.

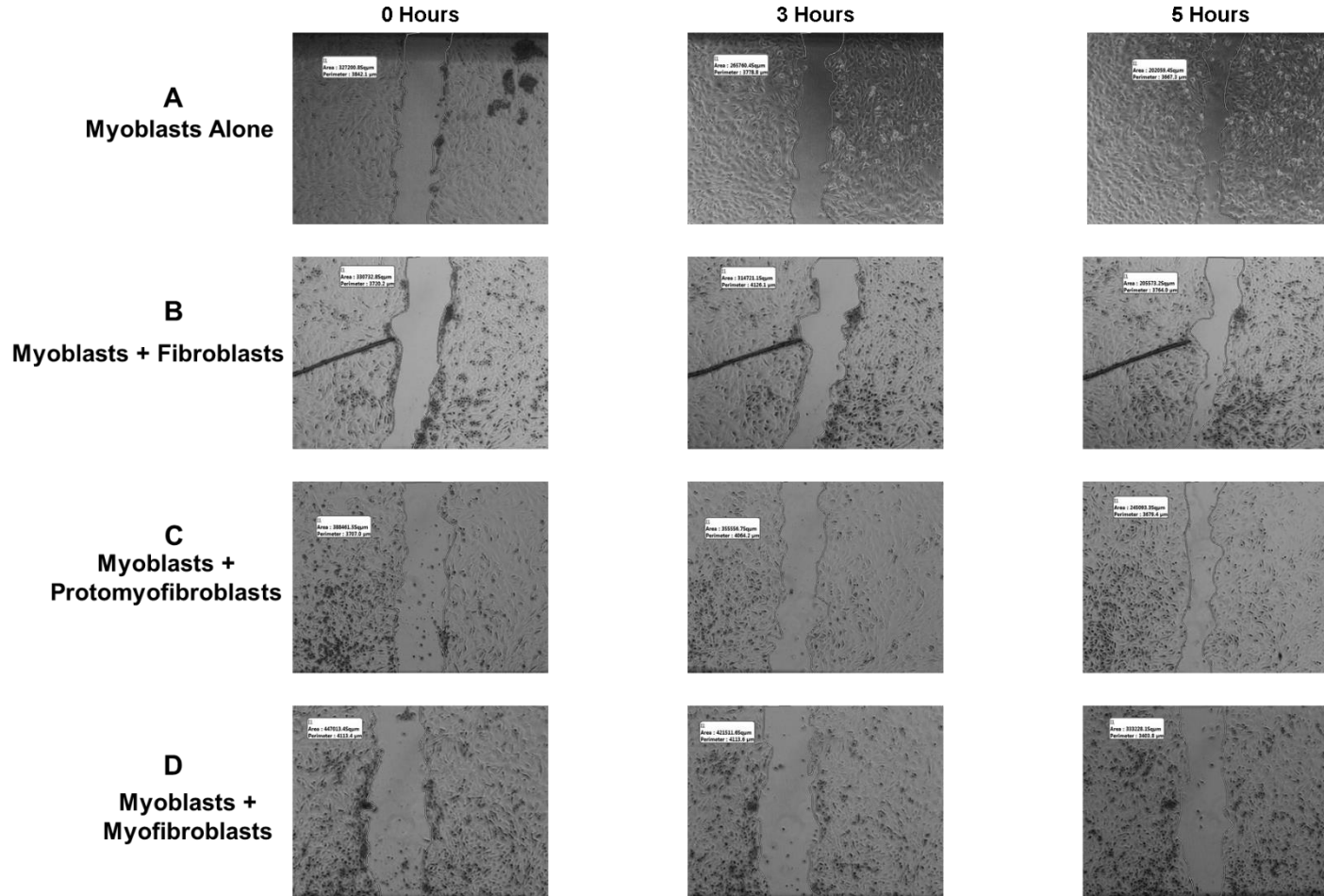


**Figure 22: Bright Field Light Microscopy Images of Myoblast Wound Closure over 7 hours** when cultured (A) alone, or in the presence of (B) fibroblasts, (C) protomyofibroblasts and (D) myofibroblasts. Images were captured using the Olympus CKX41 microscope using a 3.0-megapixel camera (4X objective lens used).

### **3.2.2. Myoblasts differentially affect myofibroblast vs fibroblast migration.**

Conversely, as a next step, the effect of myoblasts on migration of fibroblasts, proto-myofibroblasts and myofibroblasts was assessed (Figure 23). Fibroblasts, proto-myofibroblasts and myofibroblasts displayed similar wound closure when compared within each timepoint (3h, 5h, 7h) (Figure 23C and Table 4). When cells were co-cultured with myoblasts the wound closure of protomyofibroblasts decreased at all timepoints, from  $22.75\% \pm 2.94\%$  to  $17.43\% \pm 3.30\%$  at 3 hours,  $39.65\% \pm 5.09\%$  to  $31.80\% \pm 4.14\%$  at 5 hours and  $53.85\% \pm 6.05\%$  to  $43.45\% \pm 5.22\%$  at 7 hours (Figure 23D). Conversely, when co-cultured with myoblasts, myofibroblast wound closure at each timepoint was higher, increasing from  $18.53\% \pm 1.88\%$  to  $22.93\% \pm 3.72\%$  at 3 hours,  $33.71\% \pm 2.24\%$  to  $40.85\% \pm 5.32\%$  at 5 hours and  $50.22\% \pm 4.61\%$  to  $57.74\% \pm 6.11\%$  at 7 hours (Table 4 and Figure 23). Myoblasts did not have a significant effect on fibroblast wound closure. The effect was however significant ( $p < 0.05$ ) when comparing protomyofibroblast wound closure ( $43.45\% \pm 5.22\%$ ) with myofibroblast wound closure ( $57.74\% \pm 6.11\%$ ) in the presence of myoblasts at 7 hours. Contrastingly, this suggests that the presence of myoblasts significantly stimulates myofibroblast migration and inhibits motility of undifferentiated fibroblasts.

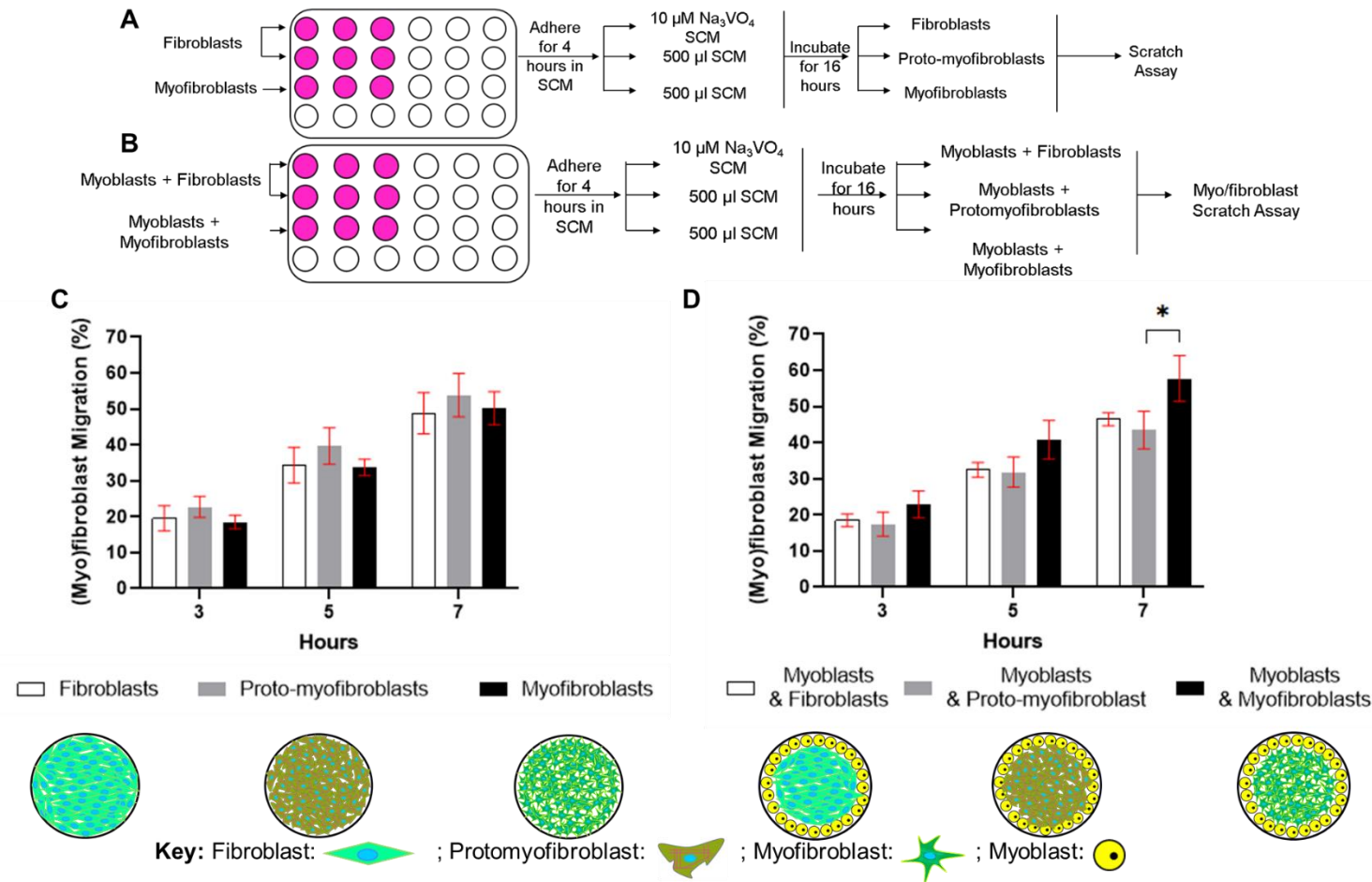


**Figure 23: Fibroblast, protomyofibroblast and myofibroblast migration.** Plate out of (A) fibroblasts and myofibroblasts alone; and (B) double co-cultures containing myoblasts and either fibroblasts or myofibroblasts (C) Fibroblasts and myofibroblasts migration over 7 hours. (D) Migration of fibroblasts or myofibroblasts co-cultured with myoblasts over 7 hours. Half of the wells plated with fibroblasts were incubated with vanadate for 16 hours to inhibit differentiation to myofibroblasts. Thereafter, an in vitro wound healing assay was performed, and wound healing analysed at 3, 5 and 7 hours using the Olympus CKX41 microscope coupled to a Motic 3.0-megapixel camera (4x objective). Data are represented as Mean  $\pm$  Standard Error of the Mean (SEM); n= 6 for C and n=7 for D (each n in triplicates). \* p<0.05.

A two-way ANOVA was performed on the mean migration averages of each fibroblast phenotype. The data shown in Table 2 indicated that the addition of myoblasts to the protomyofibroblasts significantly decreased migration whereas when added to myofibroblasts, it significantly increased migration, at 3, 5 and 7 hours.

**Table 4: Summary of mean data showing differential significant effect of myoblasts on fibroblasts, protomyofibroblast and myofibroblast migration**

Migration of:	3 hours			5 hours			7 hours		
	Myoblasts			Myoblasts			Myoblasts		
	-	+		-	+		-	+	
<b>Proto-Myofibroblasts</b>	~23 %	** ~17 %	↓	~40 %	** ~32 %	↓	~54 %	** ~43 %	↓
<b>Myofibroblasts</b>	~19 %	* ~23 %	↑	~34 %	* ~41 %	↑	~50 %	* ~58 %	↑

Myoblasts significantly decrease protomyofibroblast wound closure (red) and significantly increase myofibroblast wound closure (green). NB: \*p = 0.0311 and \*\*p = 0.0071 (comparing within a timepoint; in the presence or absence of myoblasts)

### 3.2.3. Effect of M1-LPS<sup>-</sup> and M1-LPS<sup>+</sup> macrophages on myoblast wound closure.

We previously established that the J774A.1 macrophages utilised in our study were already in part polarised to the M1 phenotype prior to LPS incubation; however, subsequent addition of LPS increased the CD86 expression suggesting additional polarisation. We therefore analysed the effect of LPS-untreated (termed M1-LPS<sup>-</sup> macrophages) and LPS-treated macrophages (termed M1-LPS<sup>+</sup> macrophages) on myoblast wound closure.

In the presence of M1-LPS<sup>-</sup> vs M1-LPS<sup>+</sup> macrophages, myoblast wound closure was 17.51% ± 1.49% and 9.48% ± 1.72% at 3 hours, 38.05% ± 2.59% and 22.94% ± 4.85% at 5 hours and 57.78% ± 3.23% and 35.13% ± 5.80% at 7 hours, respectively (Figure 24). This suggests that the presence of M1-LPS<sup>-</sup> macrophages result in faster myoblast wound closure than when cultured in the presence of M1-LPS<sup>+</sup> macrophages. This effect was significant at 7 hours (p<0.002) (Figure 24).

Moreover, it is important to note, that when incubating with LPS, myoblasts were present in the cultures. Therefore, the presence of LPS could have an effect on myoblast wound closure.

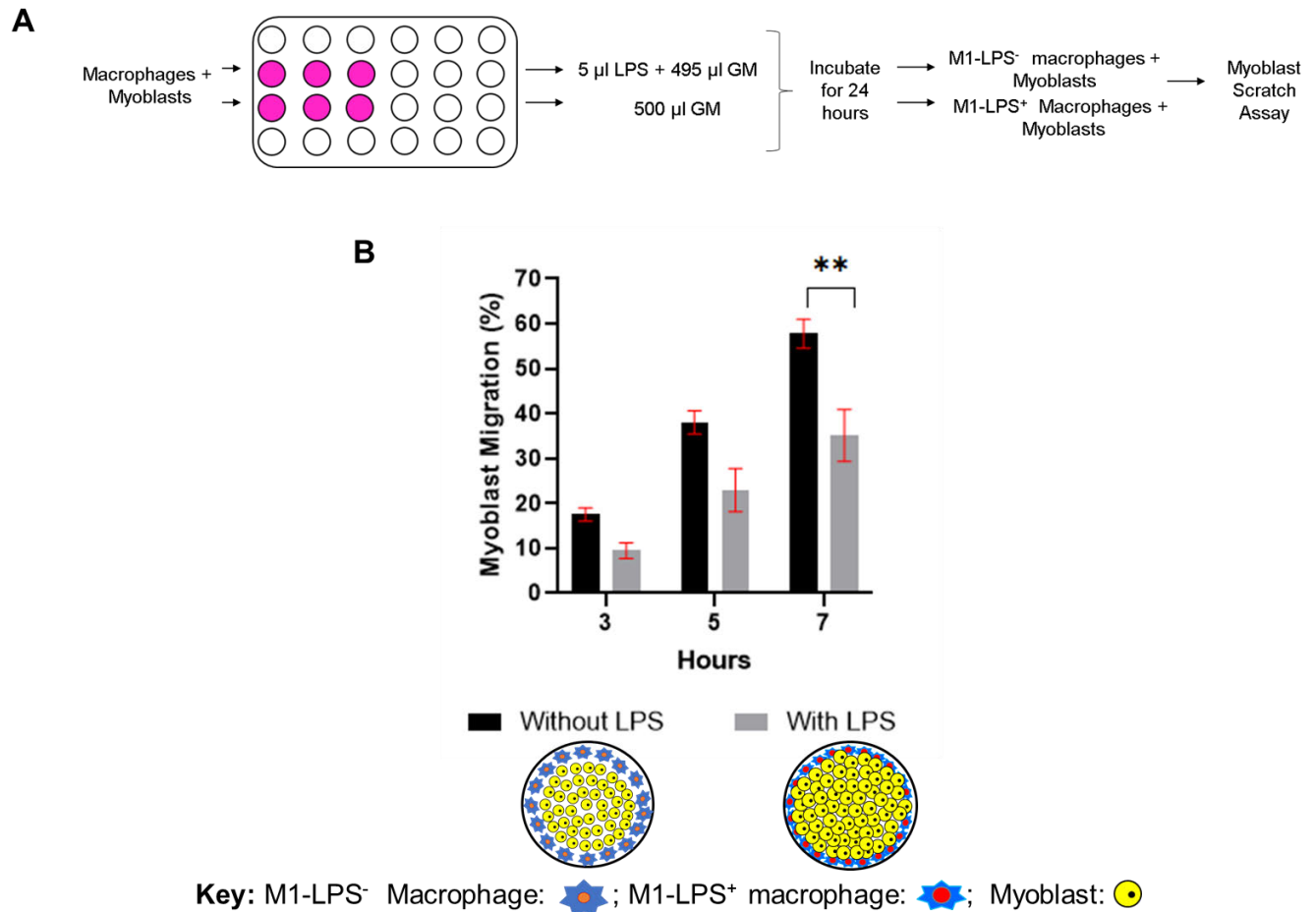


**Figure 24: Myoblast wound closure in the presence of M1-LPS<sup>-</sup> and M1-LPS<sup>+</sup> macrophages.** (A) Double co-cultures were plated and pre-treated, followed by (B) an in vitro wound healing assay and wound healing analysed at 3, 5 and 7 hours using the Olympus CKX41 microscope coupled to a Motic 3.0-megapixel camera (4x objective). Data are represented as Mean  $\pm$  Standard Error of the Mean (SEM). (6n, each ‘n’ done in triplicates).

#### 3.2.4. Effect of fibroblasts and myofibroblasts on myoblast wound closure when cultured in the presence of M1-LPS<sup>-</sup> and M1-LPS<sup>+</sup> macrophages.

The establishment of cell cultures that were either fibroblasts or myofibroblasts was imperative for the analysis of the presence of these phenotypes during wound healing in a triple co-culture, using myoblasts as the wound model. Vanadate was added to half of the wells containing fibroblasts to prevent the differentiation of fibroblasts to myofibroblasts whilst the myoblast

population reached confluence. M1-LPS<sup>+</sup> macrophages were pre-treated with LPS prior to triple co-cultures being plated-out.

The wound closure of myoblasts when cultured in the presence of M1-LPS<sup>-</sup> macrophages and fibroblasts, proto-myofibroblasts and myofibroblasts, at 3 hours was 11.02%  $\pm$  3.79% , 15.23%  $\pm$  2.42% and 14.51%  $\pm$  2.95%, at 5 hours was 19.77%  $\pm$  4.03%, 23.18%  $\pm$  4.15% and 22.02%  $\pm$  1.86% and at 7 hours was 41.52%  $\pm$  8.92%, 42.11%  $\pm$  3.95% and 38.78%  $\pm$  6.26%, respectively. This data is not statistically significant. This indicates that when M1-LPS<sup>-</sup> macrophages are added to the edge of the well (Figure 24B), the rate of myoblast wound closure is still the same as in the absence of M1-LPS<sup>-</sup> macrophages (Figure 25B).

When cultured in the presence of M1-LPS<sup>+</sup> macrophages, myoblasts wound closure; at 3 hours was 7.49%  $\pm$  1.63% , 8.78%  $\pm$  1.47% and 9.80%  $\pm$  1.21%; at 5 hours was 20.42%  $\pm$  1.71%, 20.07%  $\pm$  2.36% and 20.57%  $\pm$  1.28%; and at 7 hours was 34.10%  $\pm$  2.49%, 33.56%  $\pm$  1.79% and 34.82%  $\pm$  1.68%, when in the presence of fibroblasts, proto-myofibroblasts and myofibroblasts, respectively (Figure 25C). Myoblast wound closure in the presence of M1-LPS<sup>+</sup> macrophages and co-cultured with either fibroblasts, proto-myofibroblasts or myofibroblasts have the same rate of migration. This effect is not significant.

The overall motility of myoblasts decreases when in the presence of M1-LPS<sup>+</sup> macrophages compared with M1-LPS<sup>-</sup> macrophages, indicating that M1-LPS<sup>+</sup> macrophages negatively impact myoblast wound closure; however, there was no additional significant effect of the presence of fibroblast phenotypes.



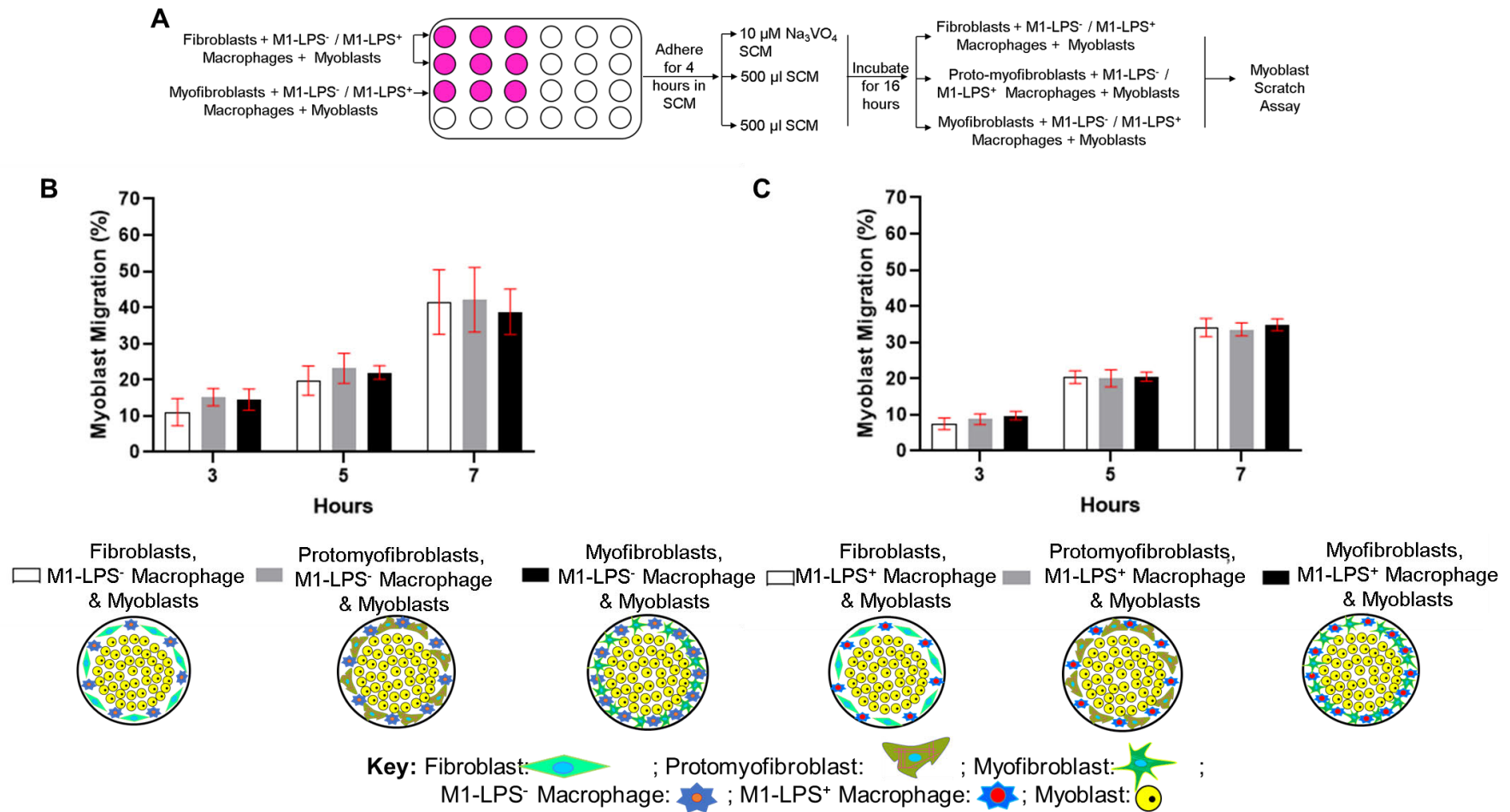


**Figure 25: The effect of the presence of fibroblasts, protomyofibroblasts and myofibroblasts during myoblasts wound healing in the presence of (B) M1-LPS<sup>-</sup> macrophages and (C) M1-LPS<sup>+</sup> macrophages. (A) Triple co-cultures were plated and treated, followed by (B/C) an *in vitro* wound healing assay, and wound closure analysed at 3, 5 and 7 hours using the Olympus CKX41 microscope coupled to a Motic 3.0-megapixel camera (4x objective). Data are represented as Mean  $\pm$  Standard Error of the Mean (SEM). n=6 (each n in triplicate).**

A two-way ANOVA was performed on the mean data of myoblast wound closure triple co-cultured with each of the fibroblast phenotypes and either M1-LPS<sup>-</sup> or M1-LPS<sup>+</sup> macrophages. This data showed no significant effect on myoblast wound closure whether in the presence of M1-LPS<sup>-</sup> or M1-LPS<sup>+</sup> macrophages.

#### 4. Discussion

Chronic non-healing wounds may arise due to pro-inflammatory diseases such as T2DM and are seen as a considerable financial and resource burden on health-care systems due to patients' loss of ability to move, decreased quality of life and extended hospitalisations (Chen, *et al.*, 2020). To provide novel approaches to address impaired and chronic wound healing, it is imperative to be cognizant of the intercellular communications that occurs between the many different cell types that play a vital role in successful wound repair. The intercellular communications that occur between macrophage phenotypes and fibroblast phenotypes are of importance, as the polarisation from M1 to M2 macrophages aid in the transition from the inflammatory stage to the proliferative stage while the migration of fibroblasts into the wound site to secrete ECM proteins (like type III collagen) and differentiate into myofibroblasts (that produce stronger type I collagen) to generate contractional forces that support wound closure.

To further understand the intercellular relationship between the above-mentioned cellular mediators of wound healing *in vitro*, it was first imperative to establish the fibroblast phenotypes in culture. This was on account that fibroblasts differentiate into myofibroblasts in the presence of serum (Pakshir, *et al.*, 2020). This was achieved by culturing L929 cells in SFM from which the results showed that 3 days post-culturing in SFM, protomyofibroblasts were generated and 6 days post-culturing in SFM, fibroblasts were generated. Although cost-effective, this method was also time-consuming and any subsequent assays needed to be carried out in a very short period as once exposed to serum for 24 hours, cells differentiate back to myofibroblasts.

Sodium orthovanadate blocks the expression of  $\alpha$ -SMA by inhibiting protein tyrosine phosphatases and the appearance of cytoplasmic stress fibres are suppressed (Maher, *et al.*, 1985; Mackay, *et al.*, 2003). Studies by Maher and colleagues (1985) indicated that phosphotyrosine containing proteins were concentrated in the cytoplasmic stress fibres and mature focal adhesions of myofibroblasts. They found that vanadate prevented the formation of cytoplasmic stress fibres and the expression of  $\alpha$ -SMA which are characteristics of myofibroblasts. Therefore, treatment with vanadate not only inhibited the expression of  $\alpha$ -SMA, but also inhibited the differentiation of fibroblasts to myofibroblasts. Hence, as seen by studies conducted by Ehrlich and colleagues (1999), vanadate was used in the current project to inhibit the expression of  $\alpha$ -SMA and fibroblast differentiation.

The expression of  $\alpha$ -SMA and the cell circularity studies of fibroblasts treated with vanadate showed that at the beginning of the wound healing assays fibroblasts are present, while by 16 and 24 hours the transient proto-myofibroblast and ultimately the myofibroblast transitions were underway. We therefore referred to the cells as either fibroblasts, proto-myofibroblasts or myofibroblasts, depending on the length of exposure time to SCM and vanadate. Vanadate could not be used throughout the wound healing assay as the addition of vanadate to the myoblasts resulted in cell death. This was specific to myoblasts, therefore if other cells are used as the wounding model, it might be possible to use vanadate throughout the assay, thereby keeping the fibroblast phenotype, as seen in the *in vivo* rat model studies conducted by Ehrlich and colleagues (1999).

Our results showed that the presence of myoblasts had a positive effect on the migration of myofibroblasts, migrating significantly faster than fibroblasts or protomyofibroblasts. There are not many studies that investigate the role of protomyofibroblasts within the wound healing environment, except to refer to their transient phase. Drawing from the results shown here, it could be of importance to gather more information on the paracrine effects and contractional forces produced by these transitional cells.

In 1981, a study by Harris and colleagues indicated that multiple fibroblasts exert a tractional force, same as that of a treadmill, on the collagen fibres across the wound matrix. Another study by Ehrlich and Rajaratnam (1990) demonstrated that wound contraction was caused by fibroblast locomotion. To a collagen lattice populated by fibroblasts, the addition and removal of myofibroblasts did not change the rate of wound closure or the collagen organisation. A subsequent study by Ehrlich *et al.*, (1999), in which he treated rats with vanadate, showed that the control and vanadate-treated rats had a similar degree of contraction. Moreover, vanadate altered the collagen fibres into “a more orderly arrangement”. Ehrlich *et al.*, (1999), concluded by saying that the myofibroblasts may contribute to wound contraction, but are not vital for wound closure to occur. This statement is synonymous with findings by Wrobel and colleagues (2002) in which they displayed that, similar forces are produced by both fibroblasts and myofibroblasts during wound repair and Ibrahim and colleagues (2015) who also stated that myofibroblasts are not required for wound contraction but contribute to it.

During normal wound healing, the polarisation of M1 to M2 macrophages marks the transition from the early inflammatory phase to the late inflammatory phase and the beginning of the proliferative phase. This is an important phenomenon as the transition from the inflammation

phase to the proliferation phase during chronic and impaired wound is either inhibited or prolonged in pro-inflammatory diseases such as T2DM.

From our results, it was demonstrated that the J774A.1 macrophages used were already partly polarised to the M1 macrophage phenotype as they expressed the CD86 surface marker; this was despite not having been previously exposed to LPS. However, Zhao *et al.*, (2017) indicated that CD86 is expressed by M0, M1 and M2 macrophages by varying degrees depending on their states of activation. The cells were then treated with LPS to further activate the M1 macrophage phenotype, which was successful. Activation of M2 macrophages via the alternative pathway using IL-4 proved however to be unsuccessful. It should also be noted that there was a lack of a positive M2 macrophage control. Hence, without this positive control, it is difficult to be sure of what positive arginase staining looks like. In *in vivo* assays conducted by Shahbazi, *et al.*, (2018), polarisation to M2 macrophage phenotype required large doses of IL-4 due poor access to target cells and IL-4 instability. Hence, they utilised high molecular weight hyaluronic acid attached to the IL-4 to target the CD44 receptors found on macrophages. They noticed a change in the activity of arginase 1, release of TNF- $\alpha$  and secretion of IL-10 which was thought to be due to the polarisation of the macrophages to the M2 phenotype. More recently, Lin and colleagues (2020) demonstrated that culturing macrophages in high doses of glucose contributes to the polarisation of macrophages to the M2 phenotype (Lin, *et al.*, 2020).

When co-cultured with LPS-activated M1 macrophages, myoblasts migrated significantly slower indicating that these activated M1 macrophage cells could delay wound healing. In chronic wounds, approximately 80% of the macrophages within the wound bed are M1 macrophages (Khanna, *et al.*, 2010). A study by Sindrilaru and colleagues (2011), in which they used macrophages with “an unrestrained pro-inflammatory M1 activation state”, showed that the polarisation to the M2-phenotype does not advance as it normally would. Furthermore, a study by Frost, *et al.*, (2003) stated that expression IL-6 (an important pro-inflammatory cytokine) by skeletal muscle cells (C2C12) was stimulated when cultured in the presence of LPS.

## 5. Limitations and Future Perspectives

Broadly, whilst *in vitro* studies provide the means to be able to control single parameters within a study, it does not accurately reflect in the physiological environment, hence, it may not be an absolute representation of what may occur within the host. Contrastingly, *in vivo* studies are more complex and are more difficult to decipher due to the many components involved in the various process.

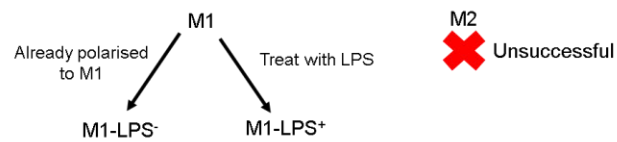
The plasticity of the fibroblast and macrophage phenotypes should be further studied to better understand the intercellular communication that occurs between these cell types during normal and chronic/impaired wound healing. It could be of importance to conduct BioPlex analysis, and or inhibitor studies, to gain further knowledge on the growth factors and cytokines released by these cell types and how they affect each other. Alternatively, study of the exosomes can be advantageous in the identification of unknown molecular and cellular intercellular communication that occurs during wound healing.

Furthermore, once an in-depth understanding of how the fibroblast population phenotypes and macrophage population phenotypes interact and stimulate each other and the wound environment, it would be important to assess the interactions of these cell types in an *in vivo* environment. This will then aid to provide future therapeutics to aid in eradicating impaired and chronic wounds.

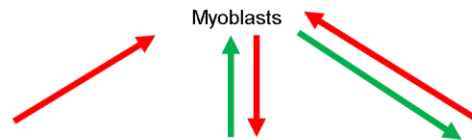
## 6. Conclusion

The different fibroblast phenotypes were successfully established and characterised within the different experimental parameters *in vitro*. When cultured in SFM for 6 days, L929 cells showed a decrease in cell circularity and appeared more elongated with a decrease in the expression of  $\alpha$ -SMA, indicative of the fibroblast phenotype. When cultured in SCM, the cells differentiated into myofibroblasts with an increase in cell circularity; cells appeared rounder with an increase in expression of  $\alpha$ -SMA. The macrophage population used was already polarised to the M1 phenotype prior to treatment with LPS (M1-LPS<sup>-</sup>). After treatment with LPS the M1 macrophage phenotype was further activated (M1-LPS<sup>+</sup>). However, the polarisation of the cells to the M2 phenotype was unsuccessful. Thereafter, the co-culture method was used to evaluate the intercellular interactions between the fibroblast phenotypes, macrophages phenotypes and myoblasts during wound healing. Double co-culture results showed that myofibroblasts migrated significantly faster when in the presence of myoblasts (Figure 26). Contrastingly, myoblasts migrate significantly faster when in the presence of proto-myofibroblasts (Figure 26). Myoblast wound closure was significantly slower in the presence of fibroblasts and myofibroblast than when cultured alone (Figure 26). This indicates that during the proliferative stage, the fibroblast phenotypes (i.e. fibroblasts and myofibroblasts) hinder the migration of the myoblasts within the wounded area. Finally, myoblasts migrate significantly faster in the presence of macrophages not treated with LPS. This underscores the importance of being specific on our description of the phenotypic stage of cells utilised *in vitro* when trying to understand the effect of the cellular role players on processes such as wound closure. It is therefore, imperative to then establish the M2 macrophage phenotype, to wholly understand the effect of each phenotype during the early and late stages myoblast wound closure. This will ultimately aid in understanding the difference between normal and impaired skeletal muscle wound healing, such as seen in diabetics, which will then assist in the establishment of specific therapeutic approaches to manage serve non-healing skeletal muscle injuries.

Macrophage Polarisation:



Wound closure model:



Established 3  
Fibroblast Phenotypes:

- Fibroblasts
- Loss of expression of  $\alpha$ -SMA
- Cells have a more elongated shape

- Protomyfibroblasts
- Transient phase

- Myofibroblasts
- Abundantly expresses  $\alpha$ -SMA
- Cells are rounder in shape

**Figure 26: Summary of study.** Arrow heads show the cells that have been affected. Green arrows indicate a positive effect of the cell causing a significant increase in wound closure, whilst red arrows indicate a negative effect of the cell causing a significant decrease in wound closure.



## 7. Conference

---

### **A Co-culture Model to Investigate the Effect of a Pro-Inflammatory Diabetic Microenvironment on Fibroblast Differentiation and Wound Healing *In Vitro*.**

**Ramklowan, D.S.H., van de Vyver, M. & Niesler, C.U.**

#### **Abstract**

Diabetes mellitus is a pro-inflammatory, chronic disease affecting 7% of the South African population. Non-healing foot ulcers are a common complication of diabetes. Fibroblasts differentiate to myofibroblasts and are critical for wound repair; their absence impairs normal tissue regeneration. Diabetic wounds show a distinct absence of myofibroblasts, which may underlie the impaired wound repair observed. The aim of the current study was to establish fibroblast and myofibroblast cultures in vitro in order to 1) analyse the effect of fibroblasts versus myofibroblasts on wound repair and 2) analyse the effect of a pro-inflammatory diabetic microenvironment on fibroblast differentiation and wound repair.

Detection of  $\alpha$ -smooth muscle actin ( $\alpha$ -SMA) using fluorescence microscopy and circularity was used to confirm the presence of myofibroblasts versus fibroblasts. Co-culture assays and the scratch assay were used to determine wound healing in vitro. Conditioned media was generated and analysed (Bioplex) following culture of mesenchymal stem cells from wildtype versus ob/ob diabetic mice.

Myofibroblasts dedifferentiated to fibroblasts when cultured in serum-free medium for six-days as confirmed by the loss of  $\alpha$ -SMA and the decrease in circularity of the cells. Myoblast wound closure was not significantly different in the presence of myofibroblasts vs. fibroblasts. Surprisingly, conditioned media representing a pro-inflammatory diabetic microenvironment resulted in an increased expression of  $\alpha$ -SMA, suggesting increased fibroblast differentiation. Myoblast wound closure however was not significantly altered in the presence of a diabetic pro-inflammatory microenvironment compared with control conditioned media.

Fibroblast and myofibroblast populations were successfully established and characterized using the detection of  $\alpha$ -SMA and circularity analysis. Myoblast wound closure occurred at the same rate in the presence of fibroblasts versus myofibroblasts. The presence of a diabetic pro-inflammatory microenvironment resulted in an increase in fibroblast differentiation, but no

significant effect on myoblast wound closure. This may suggest that the lack of myofibroblasts in diabetic wounds is not the sole cause of the observed impaired wound healing.

# A Co-culture Model to Investigate the Effect of a Pro-Inflammatory Diabetic Microenvironment on Fibroblast Differentiation and Wound Healing In Vitro.

Phyllis Thembuwa, Phyllis C. Mphahlele, Phyllis A. M. Mphahlele, Phyllis C. Mphahlele, Phyllis C. Mphahlele, Phyllis C. Mphahlele, Phyllis C. Mphahlele, Phyllis C. Mphahlele, Phyllis C. Mphahlele, Phyllis C. Mphahlele

Phyllis C. Mphahlele



## INTRODUCTION

Type 2 diabetes mellitus is a pro-inflammatory, metabolic disease characterised by high blood glucose levels that impairs the wound healing process.<sup>1</sup> South Africa is one of the sub-Saharan African countries with the highest rate of T2DM.<sup>2</sup> Evidence of experimental and clinical studies suggest diabetics suffer with impaired wound healing which results in diabetic foot ulcers (DFUs) that may lead to sepsis or gangrene, ultimately ending in lower limb amputations.<sup>3,4</sup> The DFUs occur as a result of hinderances to the stages of wound repair.<sup>5</sup> The hyperglycaemic environment affects skeletal muscle wound healing as it reduces blood flow to the area, hence many important cells (e.g. fibroblasts) cannot migrate to the site of injury.<sup>6</sup> Moreover, the hyperglycaemic disease has adverse effects on molecular and cellular physiology, slowing the maturation of wounds by decreasing the number of fibroblasts and has a negative impact on overall function of fibroblasts.<sup>6</sup>

Fibroblasts are spindle-shaped mesenchymal cells that characteristically express vimentin but not  $\alpha$ -SMA (contractile protein) or desmin (intermediate filament protein).<sup>7</sup> Fibroblasts synthesize extracellular matrix proteins (e.g. collagen) and secrete growth factors that aid in cell-to-cell communication during the wound healing process.<sup>8</sup> Therefore, any derangement to the functioning of the fibroblasts results in chronic, non-healing wounds.<sup>9</sup> Fibroblasts differentiate to myofibroblasts which are distinguishable from fibroblasts as they contain stress fibres which express  $\alpha$ -SMA and desmin but do not express vimentin.<sup>9</sup> Myofibroblasts have a principle role in the closure of wounds as they produce the contractile forces which allows the wound to close.<sup>7</sup>

When in serum, fibroblasts differentiate to myofibroblasts. Hence, the aim of the study included culturing L929 cells (myofibroblasts) in serum free medium (SFM) to generate a fibroblast population of cells in order to carry-out a triple co-culture assay to investigate the effect of fibroblasts versus myofibroblasts on myoblast wound closure. Subsequently, the effect of a diabetic microenvironment on the ability of fibroblasts to differentiate to myofibroblasts was examined.

## METHODS & RESULTS

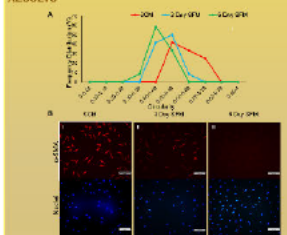
### Dedifferentiation of Myofibroblast cells

Serum contains cytokines and growth factors that promote the differentiation of fibroblasts to myofibroblasts. Hence, the removal of serum will allow for the establishment of a population that is phenotypically fibroblasts.

#### METHOD



#### RESULTS



**Panel A:** A shift in cell circularity when cultured in serum containing medium (SCM) as opposed to SFM. Cells cultured in SFM have a decreased cell circularity compared to cells cultured in SCM.  
**Panel B:** Loss of expression of  $\alpha$ -SMA when cells were cultured for 6 days in SFM as opposed to SCM.

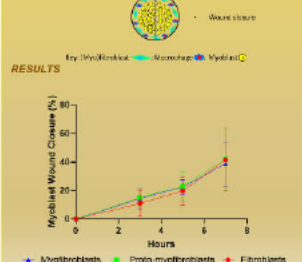
### Fibroblast vs Myofibroblast

Some studies suggest that the fibroblast phenotype can allow for faster wound closure as compared to the myofibroblast phenotype. A 'scratch assay' was performed on a triple co-culture containing (myofibroblasts (L929), macrophages (J774) and myoblasts (C2C12), as the wound model. The percentage wound closure was determined at 3, 6 and 7 hours.

#### METHOD



#### RESULTS

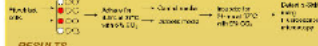


Wound healing occurs at the same rate when in the presence of either fibroblast or myofibroblast phenotype.

### Effect of Diabetic Conditioned Media

Conditioned media from bone marrow (of wild type (control) mice and diabetic obese mice (ob/ob)) were harvested. Bioplex analysis was conducted on the media. The effect of a diabetic microenvironment on the ability of fibroblasts to differentiate to myofibroblasts was determined by pre-incubating fibroblasts in diabetic conditioned media and detecting the presence of  $\alpha$ -SMA using Fluorescence microscopy.

#### METHOD

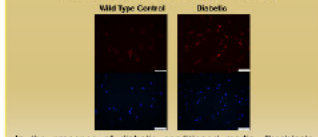


#### RESULTS

Table 1: BioPlex Analysis Data showing the concentrations of cytokines of Control Conditioned Media and Diabetic Conditioned Media

Media Type	IL-6	NC	MCP-1	MDP-1	RANTES
Wild Type Control	2.33	8.38	71.64	43.80	0
Diabetic	2.32	7.72	49.37	4.18	0

NC = no cytokine detected; MCP-1 = monocyte chemoattractant protein-1; MDP-1 = macrophage derived protein-1; RANTES = regulated on activation, normal T-cell expressed and secreted.



In the presence of diabetic conditioned media, fibroblasts differentiated to myofibroblasts. This was apparent by the high detection of  $\alpha$ -SMA within the diabetic microenvironments as compared to the wild type control.

## SUMMARY

**Aim:** Establish a fibroblast population *in vitro*.  
**Conclusion:** Myofibroblasts dedifferentiate to fibroblasts when cultured in SFM for 6 days. Fibroblasts lost expression of  $\alpha$ -SMA.

**Aim:** Compare the effect of fibroblasts versus myofibroblasts on myoblast wound closure *in vitro*.  
**Conclusion:** Regardless of the presence of fibroblasts or myofibroblasts, wound closure occurs at the same rate.

**Aim:** Determine the effect of a diabetic microenvironment on fibroblast differentiation.  
**Conclusion:** The diabetic microenvironment did not prevent the differentiation of fibroblasts to myofibroblasts.

## DISCUSSION & CONCLUSION

- Myofibroblast cells dedifferentiate to fibroblast when cultured in SFM for 6 days.
  - Cells with an elongated cell shape are fibroblasts, whilst cells with a rounder cell shape are myofibroblasts.
  - Myofibroblasts express  $\alpha$ -SMA which decreases in proto-myofibroblasts and is absent in fibroblasts.
- The effect of fibroblasts versus myofibroblasts on myoblast wound closure.
  - Regardless of presence of fibroblasts or myofibroblasts, wound closure occurs.
- The effect of a diabetic microenvironment on the ability of fibroblasts to differentiate into myofibroblasts.
  - Interestingly, the diabetic microenvironment did not prevent the differentiation of fibroblasts to myofibroblasts.
  - This was apparent by the high detection of  $\alpha$ -SMA within the diabetic microenvironments as compared to the wild type control.
  - There may be other factors involved (such as growth factors), which cause the dysfunction of the fibroblasts leading to impaired wound healing.

## REFERENCES

- Phyllis C. Mphahlele, et al. (2018). *BMC Open* 8, e201020.
- Gow T.T. & Ndlovu M. (2010). *African Journal of Primary Health Care and Family Medicine*, 8(1).
- Loomis et al. (1985). *The Journal of Investigative Dermatology*, 111(5), 550-557.
- Alonso A.G. et al. (2015). *Wound Repair and Regeneration*, 23(4), 528-533.
- Yu Q. et al. (2017). *Scientific Reports* 7, 11811.
- Broughton G. et al. (2008). *Plastic and Reconstructive Surgery* 117, 16-S - 326-S.
- Li S. and Wang J. (2015). *Journal of Biomedical Research*, 29, 105-120.
- Lerman D.P. et al. (2000). *American Journal of Pathology* 157, 305-312.
- Duffy J.A. et al. (2014). *Chronic Wounds and Wound Healing*, 2, 101-111.

## ACKNOWLEDGEMENTS

We are grateful to the HRC, NRF and Prof. T.H. Coetzee for funding this study and to the IMU (PMB, UKZN) for facilitating the Fluorescence microscopy work.

## 8. References

---

- Abbas, Z.G., Gill, G.V. & Archibald, L.K.** (2002). *The epidemiology of diabetic limb sepsis.: an African perspective*. Diabetic Medicine, 19(11): 895-899.
- Aitcheson, S.M., Frentiu, F.D., Hurn, S.E., Edwards, K. & Murray, R.Z.** (2021). *Skin Wound Healing: Normal Macrophage Function and Macrophage Dysfunction in Diabetic Wounds*. Molecules, 26: 4917.
- Alhajj, M., Bansal, P. & Goyal, A.** (2021). *Physiology, Granulation Tissue*. Treasure Island (FL): StatsPerals Publishing.
- Al-Shaibani, M.B.H., Wang, X., Lovat, P.E. & Dickinson, A.M.** (2016). *Cellular Therapy for Wounds: Applications of Mesenchymal Stem Cells in Wound Healing*. Wound Healing: New Insights into Ancient Challenges, Chapter 5: 99-131.
- Bainbridge, P.** (2013). *Wound healing and the role of fibroblasts*. Journal of Wound Care, 22(8): 407-412.
- Barrientos, S., Stojadinovic, O., Golinko, M.S., Brem, H. & Tomic-Canic, M.** (2008). *Growth factors and cytokines in wound healing*. Wound Repair & Regeneration, 16: 585-601.
- Berlanga-Acosta, J., Schultz, G.S., López-Mola, E., Guillen-Nieta, G., García-Siverio, M. & Herrera-Martínez, L.** (2013). *Glucose Toxic Effects on Granulation Tissue Productive Cells: The Diabetics' Impaired Healing*. BioMed Research International, 2013: 256043.
- Brancato, S.K. & Albina, J.E.** (2011). *Wound Macrophages as Key Regulators of Repair Origin, Phenotype and Function*. The American Journal of Pathology, 178: 19-25.
- Brem, H. & Tomic-Canic, M.** (2007). *Cellular and molecular basis of wound healing in diabetes*. Journal of Clinical Investigation, 117: 1219-1222.
- Broughton, G. & Janis, J.E.J.** (2006). *Wound Healing: An Overview*. Plastic and Reconstructive Surgery, 1eS-32eS.
- Broughton, G., Janis, J.E.J. & Attinger, C.E.** (2006). *The basic science of wound healing*. Plastic and Reconstructive Surgery, 117(7 suppl): 12S-34S.
- Caley, M.P., Martins, V.L.C. & O'Toole, E.A.** (2015). *Metalloproteinases and Wound Healing*. Advances in Wound Care, 4: 225-234.
- Chen, L., Cheng, L., Gao, W., Chen, D., Wang, C. & Ran, X.** (2020). *Telemedicine in Chronic Wound Management: Systematic Review and Meta-Analysis*. JMIR Mhealth Uhealth, 8(6): e15574.
- Chittun, R.T., Balasubramaniam, M., Parameswar, A., Kesavan, G., Haris, K.T.M. & Mohideen, K.** (2015). *The Role of Myofibroblasts in Wound Healing, Contraction and its Clinical Implications in Cleft Palate Repair*. Journal of International Oral Health, 7(3): 75-80.
- Cho, N.H., Whiting, D., et al.** (2015). *IDF Diabetes Atlas*. 7<sup>th</sup> Edition. Brussels: IDF.

- Cossu, G. & Biressi, S.** (2005). *Satellite cells, myoblasts and other occasional myogenic progenitors: Possible origin, phenotypic features and role in muscle regeneration*. *Seminars in Cell and Developmental Biology*, 16: 623-631.
- Crisco, J.J., Jokl, P., Heinen, G.T., Connell, M.D & Panjabi, M.M.** (1994). *A muscle contusion injury model: biomechanics, physiology, and histology*. *The American Journal of Sports Medicine* 22: 702-710.
- Danna, N.R., Beutel, B.G., Campbell, K.A. & Bosco, J.A.** (2014). *Therapeutic Approaches to Skeletal Muscle Repair and Healing*. *Sports Health*, 6(4): 348-355.
- Darby, I.A., Laverdet, B., Bonté, F. & Desmoulière, A.** (2014). *Fibroblasts and myofibroblasts in wound healing*. *Clinical, Cosmetic & Investigational Dermatology*, 7: 301-311.
- Delavary, B.M., van der Veer, W.M., van Egmond, M., Niessen, F.B. & Beelen, R.H.J.** (2011). *Macrophages in skin injury and repair*. *Immunology*, 216(7): 753-762.
- Desmoulière, A., Geinoz, A., Gabbiani, F. & Gabbiani, G.** (1993). *Transforming Growth Factor- $\beta$ 1 Induces  $\alpha$ -Smooth Muscle ACTIN Expression in Granulation Tissue Myofibroblasts and in Quiescent and Growing Cultured Fibroblasts*. *The Journal of Cell Biology*, 122(1): 103-111.
- Du, J.** (2018). *The research advancement of fibroblasts on diabetic non-healing skin wound*. *Journal of Community Medicine*, 1: 1005.
- Dumont, N.A., Bentzinger, C.F., Sincennes, M. & Rudnick, M.A.** (2015). *Satellite Cells and Skeletal Muscle Regeneration*. *Comprehensive Physiology*, 5: 1027-1059.
- Ehrlich, H.P. & Rajaratnam, J.B.M.** (1990). *Cell locomotion forces versus cell contraction forces for collagen lattice contraction: An in vitro model of wound contraction*. *Tissue and Cell*, 22(4): 407-417.
- Ehrlich, H.P., Keefer, K.A., Myers, R.L. & Passaniti, A.** (1999). *Vanadate and the Absence of Myofibroblasts in Wound Contraction*. *Archives of Surgery*, 134(5): 494-501.
- El-Sharkawey, A.E.** (2016). *Calculate the Corrected Total Cell Fluorescence (CTCF)*. Accessed from: [https://www.researchgate.net/publication/309350959\\_Calculate\\_the\\_Corrected\\_Total\\_Cell\\_Fluorescence\\_CTCF](https://www.researchgate.net/publication/309350959_Calculate_the_Corrected_Total_Cell_Fluorescence_CTCF).
- Eming, S.A., Werner, S., Bugnon, P., Wickenhauser, C., Siewe, L., Utermöhlen, O., Davidson, J.M., Krieg, T. & Roers, A.** (2007). *Accelerated Wound Closure in Mice Deficient for Interleukin-10*. *The American Journal of Pathology*, 170: 188-202.
- Fabrick, B.O., van Bruggen, R., Deng, D.M., Ligtenberg, A.J.M., Nazmi, K., Schornagel, K., Vloet, R.P.M., Dijkstra, C.D. & van den Berg, T.K.** (2009). *The macrophage scavenger receptor CD163 functions as an innate immune sensor for bacteria*. *Blood*, 113(4): 887-892.
- Feoktistova, M., Geserick, P. & Leverkus, M.** (2016). *Crystal violet assay for determining viability of cultured cells*. *Cold Spring Harbor Protocols*, 2016(4): pdb.prot087379.
- Frost, R.A., Nystrom, G.J. & Lang, C.H.** (2003). *Lipopolysacchride and proinflammatory cytokines stimulate IL-6 expression in C2C12 myoblasts: role of Jun NH<sub>2</sub>-terminal*

- kinase. *The American Journal of Physiology – Regulatory, Integrative and Comparative Physiology*, 285: R1153-R1164.
- Gabbiani, G.** (2003). *The myofibroblast in wound healing and fibrocontractive disease*. *The Journal of Pathology*, 200(4): 500-503.
- Garrett Jr, W.E., Seaber, A.V., Boswick, J., Urbaniak, J.R., and Goldner, J.L.** (1984). *Recovery of skeletal muscle after laceration and repair*. *The Journal of Hand Surgery*, 9: 683-692.
- Goie, T.T. & Naidoo, M.** (2016). *Awareness of diabetic foot disease amongst patients with type 2 diabetes mellitus attending chronic outpatient's department at a regional hospital in Durban, South Africa*. *African Journal of Primary Health Care & Family Medicine*, 8(1).
- Goetsch, K.P. & Niesler, C.U.** (2011). *Optimization of the scratch assay for in vitro skeletal muscle wound healing analysis*. *Analytical Biochemistry*, 411: 158-160.
- Goldber, M.T., Han, Y-P., Yan, C., Shaw, M.C. & Garner, W.L.** (2007). *TNF- $\alpha$  Suppresses  $\alpha$ -Smooth Muscle actin Expression in Human Dermal Fibroblasts: An Implication for Abnormal Wound Healing*. *Journal of Investigative Dermatology*, 127: 2645-2655.
- Greene, D.A., Sima, A.A.F., Pfeifer, M.A. & Albers, J.W.** (1990). *Diabetic Neuropathy*. *Annual Review of Medicine*, 41: 303-317
- Guo, S. & DiPietro, L.A.** (2010). *Factors Affecting Wound Healing*. *Journal of Dental Research*, 89(3): 219-229.
- Harris, A.K., Stopak, D. & Wild, P.** (1981). *Fibroblast traction as a mechanism for collagen morphogenesis*. *Nature*, 290(5803): 249-251.
- Hart, J.** (2002). *Inflammation 1: its role in the healing of acute wounds*. *Journal of Wound Care*, 11: 205-209.
- Hashimoto, D., Chow, A., Noizat, C., Teo, P., Beasley, M.B., Leboeuf, M., Becker, C.D., See, P., Price, J., Lucas, D., Greter, M., Mortha, A., Boyer, S.W., Forsberg, E.C., Tanaka, M., van Rooijen, N., García-Sastre, A., Stanely, E.R., Ginhoux, F., Frenette, P.S. & Merad, M.** (2013). *Tissue resident macrophages self-maintain locally throughout adult life with minimal contribution from circulating monocytes*. *Immunity*, 38(4): 792-804.
- Hesketh, M., Sahin, K.B., West, Z.E. & Murray, R.Z.** (2017). *Macrophage Phenotypes Regulate Scar Formation and Chronic Wound Healing*. *International Journal of Diabetes Complications*, 30(4): 746-752.
- Hinz, B.** (2007). *Formation and Function of the Myofibroblast during Tissue Repair*. *Journal of Investigative Dermatology*, 127(3): 526-537.
- Hinz, B., Phan, S.H., Thannickal, V.J., Galli, A., Bochaton-Piallat, M. & Gabbiani, G.** (2007). *The myofibroblast: One function, multiple origins*. *American Journal of Pathology*, 170: 1807-1815.
- Hunt, T.K., Hopf, H. & Hussain, Z.** (2000). *Physiology of wound healing*. *Advances in Skin and Wound Care*, 13: 6-11.

- Ibrahim, M.M., Chen, L., Bond, J.E., Medina, M.A., Ren, L., Kokosis, G., Selim, A.M. & Levinson, H.** (2015). *Myofibroblasts Contribute to but are not Necessary for Wound Contraction*. *Laboratory Investigation*, 95(12): 1429-1438.
- International Diabetes Federation.** (2015). *IDF Diabetes Atlas*. 7<sup>th</sup> edition.
- Ishida, Y., Kondo, T., Kimura, A., Matsushima, K. & Mukaida, N.** (2006). *Absence of IL-1 Receptor Antagonist Impaired Wound Healing along with Aberrant NF- $\kappa$ B Activation and a Reciprocal Suppression of TGF- $\beta$  Signal Pathway*. *Journal of Immunology*, 176: 5598-5606.
- Järvinen, T.A.H., Järvinen, T.L.N., Kääriäinen, M., Kalimo, H. & Järvinen, M.** (2005). *Muscle Injuries: Biology and Treatment*. *The American Journal of Sports Medicine*, 33(5): 745-764.
- Kawabe, T., Matsushima, M., Hashimoto, N., Imaizumi, K. & Hasegawa, Y.** (2011). *CD40/CD40 ligand interactions in immune responses and pulmonary immunity*. *Nagoya Journal of Medical Science*, 73:69-78.
- Kendall, R.T. & Feghali-Bostwick, C.A.** (2014). *Fibroblasts in fibrosis: novel roles and mediators*. *Frontiers in Pharmacology*, 5.
- Khanna, S., Biswas, S., Shang, Y., Collard, E., Azad, A., Kaoh, C., Bhasker, V., Gordillo, G.M., Sen, C.K. & Roy, S.** (2010). *Macrophage Dysfunction Impairs Resolution of Inflammation in the Wounds of Diabetic Mice*. *PLoS ONE*, 5(3): e9539.
- Kim, S.Y. & Nair, M.G.** (2019). *Macrophages in wound healing: activation and plasticity*. *Immunology & Cell Biology*, 97(3): 258-267.
- Kim, W., Mohan, R.R., Mohan, R.R. & Wilson, S.E.** (1999). *Effect of PDGF, IL-1 $\alpha$ , and BMP2/4 on Corneal Fibroblast Chemotaxis: Expression of the Platelet-Derived Growth Factor System in the Cornea*. *IOVS*, 40(7): 1364-1372.
- Ko, U.H., Choi, J., Choung, J., Moon, S. & Shin, J.H.** (2019). *Physiochemically Tuned Myofibroblasts for Wound Healing Strategy*. *Scientific Frontiers*, 9.
- Kwan, P., Desmoulière, A. & Tredget, E.E.** (2012). *Molecular and Cellular Basis of Hypertrophic Scarring in Total Burn Care* (5<sup>th</sup> ed.), pp: 455-465.
- Laumonier, T. & Menetrey, J.** (2016). *Muscle injuries and strategies for improving their repair*. *Journal of Experimental Orthopaedics*, 3:15.
- Lerman, O.Z., Galiano, R.D., Armour, M., Levine, J.P. & Gurtner, G.C.** (2003). *Cellular Dysfunction in the Diabetic Fibroblast: Impairment in Migration, Vascular Endothelial Growth Factor Production, and Response to Hypoxia*. *American Journal of Pathology*, 162: 303-312.
- Li, B. & Wang, J.H.C.** (2011). *Fibroblasts and Myofibroblasts in Wound Healing: Force Generation and Measurement*. *Journal of Tissue Viability*, 20(4): 108-120.
- Lin, J., Kong, Q., Hao, W. & Hu, W.** (2020). *High glucose contributes to the polarization of peritoneal macrophages to the M2 phenotype in vivo and in vitro*. *Molecular Medicine Reports*, 22: 127-134.

- Lin, L. & Hu, K.** (2019). *Tissue-type plasminogen activator modulates macrophage M2 to M1 phenotypic change through annexin A2-mediated NF- $\kappa$ B pathway*. *Oncotarget*, 8(50): 88094-88103.
- Lin, Z., Kondo, T., Ishida, Y., Takayasu, T. & Mukaida, N.** (2003). *Essential involvement of IL-6 in the skin wound-healing process as evidenced by delayed wound healing in IL-6 deficient mice*. *Journal of Leukocyte Biology*, 73:713-721.
- Liu, R., Bal, H.S., Desta, T., Behl, Y. & Graves, D.T.** (2006). *Tumor Necrosis Factor- $\alpha$  Mediates Diabetes-Enhanced Apoptosis of Matrix-Producing Cells and Impairs Diabetic Healing*. *American Journal of Pathology*, 168(3): 757-764.
- Liu, R., Desta, T., He, H. & Graves, D.T.** (2004). *Diabetes Alters the Response to Bacteria by Enhancing Fibroblast Apoptosis*. *Endocrinology*, 145(6): 2997-3003.
- Loots, M.A.M., Lamme, E.N., Zeegelaar, J., Mekkes, J.R., Bos, J.D. & Middlekoop, E.** (1998). *Difference in Cellular Infiltration and Extracellular Matrix of Chronic Diabetic and Venous Acute Wounds*. *Journal of Investigative Dermatology*, 111(5): 850-857.
- Louis, M., Zanou, N., Van Schoor, M. & Gailly, P.** (2011). *TRPC1 regulates skeletal myoblast migration and differentiation*. *Journal of Cell Science*, 121: 3951-3959.
- Mackay, D.J.D., Moyer, K.E., Sagers, G.C., Myers, R.L., Mackay, D.R. \* Ehrlich, H.P.** (2003). *Topical vanadate optimizes collagen organization within granulation tissue*. *Wound Repair & Regeneration*, 11(3): 204-212.
- Mackey, A.L., Magnan, M., Chazaud, B. & Kjaer, M.** (2017). *Human skeletal muscle fibroblasts stimulate in vitro myogenesis and in vivo muscle regeneration*. *Journal of Physiology*, 595.15: 5115-5127.
- Maher, P.A., Pasquale, E.B., Wang, J.Y.J. & Singer, S.J.** (1985). *Phosphotyrosine-containing proteins are concentrated in focal adhesions and intercellular junctions in normal cells*. *Proceedings of the National Academy of Sciences of the U.S.A.*, 82(19): 6576-6580.
- Mann, C.J., Perdiguero, E., Kharraz, Y., Aguilar, S., Pessina, P., Serrano, A.L. & Muñoz-Cánoves, P.** (2011). *Aberrant repair and fibrosis development in skeletal muscle*. *Skeletal Muscle*, 1:21.
- Martins, L., Gallo, C.C., Honda, T.S.B., Alves, P.T., Stilhano, R.S., Rosa, D.S., Koh, T.J. & Han, S.W.** (2020). *Skeletal muscle healing by M1-like macrophages produced by transient expression of exogenous GM-CSF*. *Stem Cell and Therapy*, 11:473.
- Mirza, R.E., Fang, M.M., Ennis, W.J. & Koh, T.J.** (2013). *Blocking Interleukin-1 $\beta$  Induces a Healing-Associated Wound Macrophage Phenotype and Improves Healing in Type 2 Diabetes*. *Diabetes*, 62: 2579-2587.
- Monaco, J.L. & Lawrence, W.T.** (2003). *Acute wound healing: An overview*. *Clinics in Plastic Surgery*, 30: 1-12.
- Nguyen, J.H., Chung, J.D., Lynch, G.S. & Ryall, J.G.** (2019). *The Microenvironment is a Critical Regulator of Muscle Stem Cell Activation and Proliferation*. *Frontiers in Cell and Developmental Biology*, 7:254.



- Nikolaou, P.K., Macdonald, B.L., Glisson, R.R., Seaber, A.V., and Garrett Jr, W.E.** (1987). *Biomechanical and histological evaluation of muscle after controlled strain injury*. The American Journal of Sports Medicine 15: 9-14.
- Orecchioni, M., Ghosheh, Y., Pramod, A.K. & Ley K.** (2019). *Macrophage Polarisation: Different Gene Signatures in M1(LPS+) vs. Classically and M2(LPS-) vs. Alternatively Activated Macrophages*. Frontiers in Immunology, 10:1084.
- Pakshir, P., Noskovicova, N., Lodyga, M., Son, D.O., Schuster, R., Goodwin, A., Karvonen, H. & Hinz, B.** (2020). *The myofibroblast at a glance*. Journal of Cell Science, 133: jcs227900.
- Pheiffer, C., Pillay-van Wyk, V., Joubert, J.D., Levitt, N., Nglazi, M.D. & Bradshaw, D.** (2018). *The prevalence of type 2 diabetes in South Africa: a systematic review protocol*. BMJ Open, 8: 021029.
- Pilling, D., Vakil, V., Cox, N. & Gomer, R.H.** (2015). *TNF- $\alpha$ -stimulated fibroblasts secrete lumican to promote fibrocyte differentiation*. Proceeding of the National Academy of Sciences of the United States of America, 112(38): 11929-11934.
- Porter, S.** (2007). *The role of the fibroblasts in wound contraction and healing*. Wounds UK, 3: 33-40.
- Powell, D.W., Mifflin, R.C., Valentich, J.D., Crowe, S.E., Saada, J.I. & West, A.B.** (1999). *Myofibroblasts. I. Paracrine cells important in health and disease*. American Journal of Physiology, 277(46): C1-C19.
- Richardson, M.** (2004). *Acute wounds: an overview of the physiological healing process*. Nursing Times, 100: 50-53
- Ritsu, M., Kawakami, K., Kanno, E., Tamno, H., Ishii, K., Imai, Y., Maruyama, R. & Tachi, M.** (2017). *Critical role of tumor necrosis factor- $\alpha$  in the early process of wound healing in skin*. Journal of Dermatology & Dermatology Surgery, 21: 14-19.
- Robson, M.C., Steed, D.L. & Franz, M.G.** (2001). *Wound Healing: Biologic Features and Approaches to Maximize Healing Trajectories*. Current Problems in Surgery, 38: 72-141.
- Roy, S.G., Nozaki, Y. & Phan, S.H.** (2001). *Regulation of alpha-smooth muscle actin gene expression in myofibroblast differentiation from rat lung fibroblasts*. The International Journal of Biochemistry & Cell Biology, 33: 723-734.
- Rozario, T. & DeSimone, D.W.** (2010). *The extracellular matrix in development and morphogenesis: A dynamic view*. Developmental Biology, 341: 126-140.
- Sahadew, N., Singaram, V.S. & Brown, S.** (2016). *Distribution, incidence, prevalence and default of patients with diabetes mellitus accessing public healthcare in the 11 districts of KwaZulu-Natal, South Africa*. South African Medical Journal, 106(4): 389-393.
- Said, G.** (2007). *Diabetic neuropathy – a review*. Nature Clinical Practice Neurology, 3(6): 331-340.
- Salazar, J.J., Ennis, W.J. & Koh, T.J.** (2016). *Diabetes Medications: Impact on Inflammation and Wound Healing*. Journal of Diabetes Complications, 30(4): 746-752.

- Schliefssteiner, C., Ibesich, S. & Wadsack, C.** (2020). *Placental Hofbauer Cell Polarization Resists Inflammatory Cues In Vitro*. International Journal of Molecular Science, 21(3): 736.
- Seitz, O., Schürmann, C., Hermes, N., Müller, E., Pfeilschifter, J., Frank, S. & Goren, I.** (2010). *Wound Healing in Mice with High-Fat Diet-or ob Gene-Induced Diabetes-Obesity Syndromes: A comparative Study*. Experimental Diabetes Research, 2010: 1-15.
- Shahbazi, M., Sedighi, M., Bauleth-Ramos, T., Kant, K., Correia, A., Poursina, N., Sarmiento, B., Hirvonen, J. & Santos, H.A.** (2018). *Targeted Reinforcement of Macrophage Reprogramming Toward M2 Polarisation by IL-4-Loaded Hyaluronic Acid Particles*. ACS Omega, 3: 18444-18455.
- Shakya, S., Wang, Y., Mack, J.A. & Maytin, E.V.** (2015). *Hyperglycaemia-Induced Changes in Hyaluronan Contribute to Impaired Skin Wound Healing in Diabetes: Review and Perspective*. International Journal of Cell Biology 2015: 1-11.
- Sibbald, R.G. & Woo, K.Y.** (2008). *The biology of chronic foot ulcers in persons with diabetes*. Diabetes/Metabolism Research & Reviews, 24(51): 525-530.
- Sindrilaru, A., Peters, T., Wieschalka, S., Baican, C., Baican, A., Peter, H., Hainzl, A., Schatz, S., Qi, Y., Schlecht, A., Weiss, J.M., Wlaschek, M., Sunderkötter, C. & Scharffetter-Kochanek, K.** (2011). *An unrestrained proinflammatory M1 macrophage population induced by iron impairs wound healing in humans and mice*. The Journal of Clinical Investigation, 121(3): 985–997.
- Singer, A.J. & Clark, R.A.** (1999). *Cutaneous wound healing*. The New England Journal of Medicine, 341: 738-746.
- Snijders, T., Nederveen, J.P., McKay, B.R., Joannis, S., Verdijk, L.B., van Loon, L.J.C. & Parise, G.** (2015). *Satellite cells in human skeletal muscle plasticity*. Frontiers in Physiology, 6:283.
- Stojadinovic, O., Brem, H., Vouthounis, C., Lee, B., Fallon, J., Stallcup, M., Merchant, A., Galiano, R.D. & Tomic-Canic, M.** (2005). *Molecular Pathogenesis of Chronic Wounds: The Role of  $\beta$ -catenin and c-myc in the inhibition of Epithelialisation and Wound Healing*. American Journal of Pathology, 167: 59-69.
- Suda, S., Williams, H., Medbury, H.J. & Holland, A.J.A.** (2015). *A Review of Monocytes and Monocyte-Derived Cells in Hypertrophic Scarring Post Burn*. Journal of Burn & Care Research, 37(5): 265-272.
- Suttles, J. & Stout, R.D.** (2009). *Macrophages CD40 signalling: A pivotal regulator of disease protection and pathogenesis*. Seminars in Immunology, 21: 257-264.
- Suzuki, Y., Shirai, M., Asada, K., Yasui, H., Karayama, M., Hozumi, H., Furuhashi, K., Enomoto, N., Fujisawa, T., Nakamura, Y., Inui, N., Shirai, T., Hayakawa, H. & Suda, T.** (2018). *Macrophages mannose receptor, CD206, predict prognosis in patients with pulmonary tuberculosis*. Scientific Reports, 8:13129.
- Tomasek, J.J., Gabbiani, G., Hinz, B., Chaponnier, C. & Brown, R.A.** (2002). *Myofibroblasts and mechanoregulation of connective tissue remodelling*. Nature Reviews Molecular Cell Biology, 3: 349-363.
- Valluru, M., Staton, C.A., Reed, M.W.R. & Brown, N.J.** (2011). *Transforming growth factor- $\beta$  and endoglin signalling orchestrate wound healing*. Frontiers in Physiology, 2.

- van Linthout, S., Miteva, K. & Tschöpe, C.** (2014). *Crosstalk between fibroblasts and inflammatory cells*. Cardiovascular Research, 102: 72-258-269.
- Velnar, T., Bailey, T. & Smrkolj, V.** (2009). *The Wound Healing Process: An Overview of the cellular and molecular mechanisms*. The Journal of International Medical Research, 37: 1528-1542.
- Venter, C. & Niesler, C.U.** (2018). *A triple co-culture method to investigate the effect of macrophages and fibroblasts on myoblast proliferation and migration*. BioTechniques, 64: 52-58.
- Venter, C. & Niesler, C.U.** (2019). *Rapid quantification of cellular proliferation and migration using ImageJ*. Biotechniques, 66(2): 99-102.
- Venter, C., Myburgh, K.H. & Niesler, C.U.** (2021). *Co-culture of pro-inflammatory macrophages and myofibroblasts: Evaluating morphological phenotypes and screening the effects of signalling pathway inhibitors*. Physiological Reports, 9(2): e14704.
- Wallace, H.A. & Zito, P.M.** (2021). *Wound Healing Phases*. Treasure Island (FL): StatsPearls Publishing Internet.
- Wan, R., Weissman, J.P., Grundman, L., Lang, L., Grybowski, D.J. & Galiano, R.D.** (2021). *Diabetes wound healing: The impact of diabetes on myofibroblast activity and its potential therapeutic treatments*. Wound Repair and Regeneration, 29: 573-581.
- Wen, Y., Gu, J., Li, S., Reddy, M.A., Natarajan, R. & Nadler, J.L.** (2006). *Elevated Glucose and Diabetes Promote Interleukin-12 Cytokine Gene Expression in Mouse Macrophages*. Endocrinology, 147(5): 2518-2525.
- Wrobel, L.K., Fray, T.R., Molloy, J.E., Adams, J.J., Armitage, M.P. & Sparrow, J.C.** (2002). *Contractility of Single Human Dermal Myofibroblasts and Fibroblasts*. Cell Motility and the Cytoskeleton, 52: 82-90.
- Yun, T.J. & Clark, E.A.** (1998). *Cooperation, mechanisms of cellular*. Encyclopaedia of Immunology. ISBN: 0-12-226765-6: (652-656).
- Zhao, Y., Tian, P., Han, F., Zheng, J. & Xia, X.** (2017). *Comparison of the characteristics of macrophages derived from murine spleen, peritoneal cavity, and bone marrow*. Journal of University-SCIENCE B (Biomedicine & Biotechnology), 18(12): 1055-1063.